

**INSTITUTO SUPERIOR DE ENGENHARIA DE LISBOA**  
**Área Departamental de Engenharia de Electrónica e**  
**Telecomunicações e de Computadores**

**Aumento de Capacidade em Sistemas MIMO**  
**Coordenados para Advanced LTE com Utilização de**  
**Repetidores Fixos**

**André Eduardo Ponciano Martins**  
(Licenciado)

Trabalho Final de Mestrado para Obtenção do Grau de Mestre em Engenharia de  
Electrónica e Telecomunicações

Orientador:

Doutor Pedro Manuel de Almeida Carvalho Vieira

Júri:

Presidente: Doutor Mário Pereira Véstias

Vogais:

Doutor António José Castelo Branco Rodrigues

Doutor Pedro Manuel de Almeida Carvalho Vieira

**Novembro de 2011**



# Abstract

With the aim of providing high data rates, the Long Term Evolution (LTE) standard makes use of relaying as one of the important techniques for new mobile networks. LTE will also make use of the Multiple-Input Multiple-Output (MIMO) technique, to improve the transmission's quality in hostile environments and to offer very high data rates.

The relay solution in mobile networks planning is a highly used technique in next LTE networks. This technique has the aim of increasing the network coverage and/or capacity and improves the cell edge throughput. The Relay Station (RS) performance depends on its position in the cell, the radio conditions to which the RS and the User Equipment (UE) are subjected, and the RS capability to receive process and forward the information.

The aim of this thesis is to conclude about the optimized position in which a RS (from types Amplify and Forward (AF)/ Selective Decode and Forward (SDF)) should be placed, with the aim of maximizing the UE throughput. Furthermore, to compare the performance of Transmit Diversity (TD) versus Open-Loop Spatial Multiplexing (OL-SM) MIMO in LTE, and under which conditions they should be used, in a network equipped with Fixed Relay Stations (FRSs).

**Key-words:** Wireless Communications, LTE, Relay, Amplify and Forward, Selective Decode and Forward, MIMO.



# Resumo

Com vista a revolucionar o sector das comunicações móveis, muito à custa dos elevados débitos prometidos, a tecnologia LTE recorre a uma técnica que se prevê que seja bastante utilizada nas futuras redes de comunicações móveis: *Relaying*. Juntamente com esta técnica, o LTE recorre à técnica MIMO, para melhorar a qualidade da transmissão em ambientes hostis e oferecer elevados ritmos de transmissão.

No planeamento das próximas redes LTE, o recurso à técnica *Relaying* é frequente. Esta técnica, tem como objectivo aumentar a cobertura e/ou capacidade da rede, e ainda melhorar o seu desempenho em condições de fronteira de célula. A performance de uma RS depende da sua localização, das condições de propagação do canal rádio a que tanto a RS como o UE estão sujeitos, e ainda da capacidade que a RS tem de receber, processar e reencaminhar a informação.

O objectivo da tese é estudar a relação existente entre o posicionamento de uma RS e o seu desempenho. Desta forma, pretende-se concluir qual a posição ideal de uma RS (tanto do tipo AF como SDF). Para além deste estudo, é apresentado um comparativo do desempenho dos modos MIMO TD e OL-SM, onde se conclui em que condições deverão ser utilizados, numa rede LTE equipada com FRSSs.

**Palavras-chave:** Comunicações sem fios, LTE, Repetidor, *Amplify and Forward*, *Selective Decode and Forward*, MIMO.



# Acknowledgments

First and foremost I want to thank my supervisor, Prof. Pedro Vieira. He has been far more than just a supervisor. He has been an exemplar teacher, in both the academic and the personal aspects. My special thanks go to him for all his immense knowledge, the motivation that he gave me, the critics, the praises, his professionalism and dedication. Also by the confidence that he entrusted me with by allowing me to be a part of this project.

Besides by supervisor, thanks also to the ISEL/ADEETC and the Instituto de Telecomunicações for the working conditions.

Thank you to my parents. Without them it would not be possible to do this. Thanks for all the given support, conditions, patience, incentive and advises.

A very special thanks to my brother João for all the availability. Especially in the final moments he was just an amazing person. Thanks for everything!

I would also like to thank my girlfriend Inês. Thank you for all the given support not only during, but also before. Thank you for all the motivation, orientation, help and comprehension moments!

Thank you my colleges Tiago, Márcio and Nuno for all the friendship and fellowship demonstrated throughout my academic career.

Last but not least, to those who are not mentioned here that directly or indirectly contributed, in some way, to my career so far.





*“Innovation distinguishes between a leader and a follower.”*

**Steve P. Jobs**



# Contents

<b>1</b>	<b>Introduction</b>	<b>1</b>
<b>2</b>	<b>State of The Art</b>	<b>5</b>
2.1	Changes to Traffic in Mobile Communications Networks . . . . .	5
2.2	Evolution of Mobile Communications Networks . . . . .	7
2.3	MIMO . . . . .	9
2.3.1	What is MIMO? . . . . .	9
2.3.2	Cooperative MIMO . . . . .	14
2.3.3	Types of Cooperative MIMO . . . . .	14
2.4	Long Term Evolution . . . . .	17
2.4.1	Introduction . . . . .	17
2.4.2	Targets for LTE . . . . .	19
2.4.3	LTE Overview . . . . .	20
2.4.4	Technologies for LTE . . . . .	23
2.5	LTE-Advanced . . . . .	31
2.5.1	Introduction . . . . .	31
2.5.2	LTE-A Overview . . . . .	31
2.5.3	LTE-Advanced Enhancements . . . . .	32
2.6	CO-MIMO Channel Models . . . . .	44
<b>3</b>	<b>System Model and Simulator Improvement</b>	<b>47</b>
<b>4</b>	<b>Simulation Results</b>	<b>57</b>
4.1	LoS Probability . . . . .	57
4.2	SNIR vs eNB-RS Distance . . . . .	60
4.3	Throughput Performance in the TD and OL-SM MIMO Modes . . . . .	65
4.4	Performance of AF and SDF Relay Station Types . . . . .	68

4.5	Relay Positioning Impact for TD and OL-SM MIMO Modes . . . . .	78
<b>5</b>	<b>Conclusions and Future Work</b>	<b>87</b>
5.1	Performed Work . . . . .	87
5.2	Future Work . . . . .	89

# List of Figures

2.1	Growth in data traffic. . . . .	5
2.2	Cisco forecasts 3.6 exabytes per month of mobile data traffic by 2014. . . . .	6
2.3	The traffic and revenue challenge. . . . .	7
2.4	Evolution of TDMA, CDMA, and OFDMA systems. . . . .	7
2.5	High rates of adoption of HSDPA. . . . .	8
2.6	HSPA observed performances. . . . .	9
2.7	Diversity Gain (Transmit Diversity). . . . .	10
2.8	Array Gain. . . . .	10
2.9	Spatial Multiplexing Gain. . . . .	11
2.10	SU-SISO scheme. . . . .	11
2.11	SU-SIMO scheme. . . . .	12
2.12	SU-MISO scheme. . . . .	12
2.13	SU-MIMO scheme. . . . .	13
2.14	MU-MIMO scheme. . . . .	13
2.15	Overview of MIMO schemes. . . . .	14
2.16	Coordinated multipoint transmission scheme. . . . .	15
2.17	Fixed-Relay scheme. . . . .	16
2.18	Mobile-Relay. . . . .	16
2.19	LTE milestones in 3GPP. . . . .	18
2.20	Relative adoption of technologies. . . . .	18
2.21	Screenshot of “www.ngconnect.org” site. . . . .	18
2.22	Screenshot of “www.alcatel-lucent.com” site. . . . .	19
2.23	Screenshot of “www.ericsson.com” site. . . . .	19
2.24	Main LTE performance targets. . . . .	20
2.25	TDD, FDD and HD-FDD schemes. . . . .	20
2.26	UMTS and LTE architectures. . . . .	22

2.27	OFDM and OFDMA subcarrier allocation. . . . .	24
2.28	Comparison of OFDMA and SC-FDMA transmitting a series of QPSK data symbols. . . . .	25
2.29	Signal processing for transmit diversity and spatial multiplexing. . . . .	26
2.30	Open-Loop Spatial Multiplexing with $N$ antennas and $M$ layers. . . . .	28
2.31	Closed-Loop Spatial Multiplexing with $N$ antennas and $M$ layers. . . . .	28
2.32	3GPP LTE-Advanced and ITU-R IMT-Advanced schedules. . . . .	31
2.33	LTE-Advanced maximum bandwidth in contiguous deployment. . . . .	32
2.34	Intraband Contiguous. . . . .	33
2.35	Intraband Non-Contiguous. . . . .	33
2.36	Interband Non-Contiguous. . . . .	34
2.37	Carrier Aggregation deployment first scenario. . . . .	34
2.38	Carrier Aggregation deployment second scenario. . . . .	34
2.39	Carrier Aggregation deployment third scenario. . . . .	35
2.40	Carrier Aggregation deployment fourth scenario. . . . .	35
2.41	Supported transmit layers in LTE and LTE-A. . . . .	36
2.42	Inter-Site and Intra-Site CoMP. . . . .	36
2.43	An illustration of Intra-eNB CoMP with a distributed eNB. . . . .	37
2.44	Example of CoMP in a distributed network architecture. . . . .	38
2.45	CoMP-SU-MIMO and CoMP-MU-MIMO schemes. . . . .	39
2.46	Downlink CoMP-MU-MIMO system structure. . . . .	40
2.47	Uplink CoMP-MU-MIMO system structure. . . . .	40
2.48	Non-cooperative system. . . . .	41
2.49	CoMP system with 3 sectors in different sites cooperation. . . . .	41
2.50	CoMP system with 21 sectors in the whole network. . . . .	42
2.51	Relays types. . . . .	43
2.52	Cost/benefit evaluation of LTE-Advanced features. . . . .	43
3.1	eNB's, RS's and UE's positions. . . . .	47
3.2	RS positioning. . . . .	48
3.3	Simulation flowchart. . . . .	50
3.4	Signal and Interference for the RS. . . . .	51
3.5	Geometry for $d_1$ and $d_2$ path-loss model. . . . .	52

3.6	RS Buffering when the used CQI in the eNB-RS link is lower than used CQI in the RS-UE link. . . . .	54
3.7	RS Buffering when used CQI in the eNB-RS link is higher than used CQI in the RS-UE link. . . . .	55
3.8	RS Buffering when the eNB has no more information for the UE. . . . .	55
4.1	eNB and RS in LoS situation. . . . .	57
4.2	eNB and RS in NLoS situation. . . . .	58
4.3	LoS Probability for the eNB-RS link. . . . .	58
4.4	LoS Probability for the RS-UE link. . . . .	59
4.5	LoS Probability for RS-UE link with $hRS=10\text{ m}$ . . . . .	60
4.6	RS SNIR in LoS and NLoS situation. . . . .	60
4.7	RS path-loss and path-loss for RS interference cells. . . . .	61
4.8	RS SNIR with LoS Probability Model. . . . .	62
4.9	UE SNIR in LoS and NLoS situation. . . . .	63
4.10	UE SNIR with LoS Probability Model. . . . .	63
4.11	UE path-loss and path-loss for UE interference cells. . . . .	64
4.12	eNB-RS and RS-UE path-Loss. . . . .	64
4.13	Throughput for the eNB-RS radio link in TD mode. . . . .	65
4.14	Throughput for the eNB-RS radio link in OL-SM mode. . . . .	66
4.15	Number of retransmissions for the eNB-RS link in TD mode. . . . .	67
4.16	Number of retransmissions for the eNB-RS link in OL-SM mode. . . . .	67
4.17	RS and UE SNIR in the first scenario. . . . .	68
4.18	RS and UE SNIR in the second scenario. . . . .	69
4.19	Used CQI for AF RS type in the first scenario. . . . .	69
4.20	Used CQI for AF RS type in the second scenario. . . . .	70
4.21	Used CQI for SDF RS type in the first scenario. . . . .	70
4.22	Used CQI for SDF RS type in the second scenario. . . . .	71
4.23	UE BER in the first scenario. . . . .	72
4.24	UE BER in the second scenario. . . . .	72
4.25	Normalized histogram for AF RS type in the first scenario. . . . .	73
4.26	Normalized histogram for SDF RS type in the first scenario. . . . .	74
4.27	Normalized histogram for AF RS type in the second scenario. . . . .	75
4.28	Normalized histogram for SDF RS type in the second scenario. . . . .	75

4.29	UE throughput in the first scenario. . . . .	76
4.30	UE throughput in the second scenario. . . . .	77
4.31	Used CQI in the eNB-RS link in the first scenario. . . . .	78
4.32	Used CQI in the RS-UE link in the first scenario. . . . .	79
4.33	Used CQI in the eNB-RS link in the second scenario. . . . .	80
4.34	Used CQI in the RS-UE link in the second scenario. . . . .	80
4.35	UE BER in the first scenario. . . . .	81
4.36	UE BER in the second scenario. . . . .	81
4.37	Normalized histogram for OL-SM in the first scenario. . . . .	82
4.38	Normalized histogram for TD mode in the first scenario. . . . .	83
4.39	Normalized histogram for OL-SM in the second scenario. . . . .	84
4.40	Normalized histogram for TD mode in the second scenario. . . . .	84
4.41	UE throughput in the first scenario. . . . .	85
4.42	UE throughput in the second scenario. . . . .	85



# List of Tables

2.1	Categories of LTE User Equipment. . . . .	21
2.2	Summary of key performance requirement targets for LTE. . . . .	23
2.3	Decision matrix for the main LTE MIMO modes. . . . .	30
2.4	LTE modulation techniques. . . . .	30
2.5	IMT-A Requirements and Anticipated LTE-A. . . . .	32
2.6	Comparison between Inter-Site and Intra-Site CoMP. . . . .	37
2.7	Possible approaches for CoMP schemes in different scenarios. . . . .	39
3.1	Matching between CQI value and modulation and ECR. . . . .	48
3.2	Simulation parameters. . . . .	49



# Acronyms

**1G** 1<sup>st</sup> Generation. 1

**2G** 2<sup>nd</sup> Generation. 1, 8

**3G** 3<sup>rd</sup> Generation. 1, 2, 8

**3GPP** 3<sup>rd</sup> Generation Partnership Project. 1, 17, 19, 21, 44

**4G** 4<sup>th</sup> Generation. 1, 2, 9, 14, 17, 18, 31, 32, 35

**AF** Amplify and Forward. iii, v, 54, 68–71, 73, 76–78, 87, 89

**BER** Bit Error Rate. 47, 56, 68, 70, 71, 73, 76, 79, 82, 85, 86, 89

**BLER** Block Error Rate. 48, 71

**BS** Base Station. 11, 12, 14–17, 21, 22, 52, 53

**CA** Carrier Aggregation. 33–35

**CC** Component Carriers. 33

**CDMA** Code Division Multiple Access. 17, 24, 25

**CL-SM** Closed-Loop Spatial Multiplexing. 28–30, 90

**CO-MIMO** Cooperative MIMO. 14–17, 40, 44, 45

**CoMP** Coordinated Multipoint Transmission. 2, 14, 15, 17, 36, 38–41, 44, 89

**CoMP-CBF** Coordinated Beamforming. 38, 39

**CoMP-CS** Coordinated Scheduling. 38, 39

**CoMP-JP** Joint Processing. 38, 39

**CoMP-JT** Joint Transmission. 38, 39

**CoMP-MU-MIMO** Coordinated Multipoint Transmission-MU-MIMO. 39, 40

**CoMP-SU-MIMO** Coordinated Multipoint Transmission-SU-MIMO. 39

**CP** Cyclic Prefix. 24

**CQI** Channel Quality Indicator. 27, 28, 37, 47, 48, 53, 54, 56, 65, 66, 68–71, 73, 74, 76–79, 82, 83, 85–89

**D-ICIC** Dynamic Interference Coordination. 38

**DF** Demodulation and Forward. 42

**ECR** Effective Code Rate. 48

**eNB** evolved NodeB. 22, 27–30, 34–40, 42, 45, 47, 48, 50–62, 64, 65, 68–71, 73, 74, 76–79, 82, 83, 86–89

**ETSI** European Telecommunications Standards Institute. 23

**F2F** Fixed-to-Fixed. 17

**F2M** Fixed-to-Mobile. 17

**FDD** Frequency-Division Duplexing. 20, 33

**FRS** Fixed Relay Station. iii, v, 15, 16, 47

**GGSN** Gateway GPRS Support Node. 22

**GPRS** General Packet Radio Service. 1

**GSM** Global System for Mobile Communications. 18, 21, 23, 25

**HARQ** Hybrid Automatic Repeat Request. 47, 54–56, 73, 74, 82, 87–89

**HD-FDD** Half-Duplex Frequency-Division Duplexing. 20

**HSDPA** High Speed Downlink Packet Access. 8, 44

**HSPA** High Speed Downlink Packet Access. 1, 5, 8, 17–19, 21, 22

**HSPA** + High Speed Packet Access Evolution. 8

**HSUPA** High Speed Uplink Packet Access. 8

**ICI** Inter-Cell Interference. 14, 15, 24, 25, 37, 41

**ICIC** Inter-Cell Interference Coordination. 38, 40

**IEEE** Institute of Electrical and Electronics Engineers. 2, 17

**IMT-Advanced** International Mobile Telecommunications-Advanced. 2, 31

**IP** Internet Protocol. 21

**ITU-R** ITU Radiocommunication Sector. 31

**LoS** Line-of-Sight. 13, 29, 45, 47, 51–53, 57–62, 64, 68, 69, 71, 73, 74, 77–79, 82, 86, 88, 89

**LTE** Long Term Evolution. iii, v, 1, 2, 9, 12, 17–23, 25–27, 29–32, 35, 42, 65, 86, 87, 89

**LTE-A** Long Term Evolution - Advanced. 2, 31, 32, 34, 35, 37–39, 42

**M2M** Mobile-to-Mobile. 17

**MAN** Metropolitan Area Network. 9

**MIMO** Multiple-Input Multiple-Output. iii, v, 2, 8–12, 14, 21, 24–27, 29, 31, 35, 39, 40, 43–45, 49, 65, 66, 78, 82, 83, 86–88, 90

**MISO** Multiple-Input Single-Output. 12, 27

**MME** Mobility Management Entity. 22

**MMSE** Minimum Mean Square Error. 41

**MRS** Mobile Relay Station. 16, 17, 89

**MS** Mobile Station. 10–12, 15–17, 20, 21, 52, 53

**MU-MIMO** Multi-User MIMO. 10–13, 26, 28

**NB** NodeB. 21, 22

**NLoS** Non-Line-of-Sight. 47, 51–53, 57, 60–62, 68, 77, 88

**OFDM** Orthogonal Frequency Division Multiplexing. 9, 23–25

**OFDMA** Orthogonal Frequency-Division Multiple Access. 20, 23–25

**OL-SM** Open-Loop Spatial Multiplexing. iii, v, 27–30, 49, 65, 66, 68, 78, 79, 82, 83, 85–89

**PAN** Personal Area Network. 9

**PAPR** Peak-to-Average Power Ratio. 20, 25

**PBCH** Physical Broadcast Channel. 27

**PCFICH** Physical Control Format Indicator Channel. 27

**PDCCH** Physical Downlink Control Channel. 27

**PDSCH** Physical Downlink Shared Channel. 27

**PHICH** Physical Hybrid ARQ Indicator Channel. 27

**PMI** Precoding Matrix Indicator. 27, 28

**QAM** Quadrature Amplitude Modulation. 8

**QoS** Quality of Service. 15

**QPSK** Quadrature Phase-Shift Keying. 25

**RF** Radio Frequency. 33, 42

**RI** Rank Indicator. 27–29

**RNC** Radio Network Controller. 21, 22

**RRU** Remote Radio Units. 35, 37

**RS** Relay Station. iii, v, 15, 17, 42–45, 47, 48, 50, 51, 53–62, 64, 65, 68–71, 73, 74, 76–79, 82, 83, 85–89

**S-GW** Serving Gateway. 22

**S-ICIC** Static Interference Coordination. 38

**SAE** System Architecture Evolution. 21

**SC** Single Carrier. 34

**SC-FDMA** Single-carrier Frequency-Division Multiple Access. 20, 25

**SCM** Spatial Channel Model. 44

**SDF** Selective Decode and Forward. iii, v, 48, 53, 54, 68, 70, 71, 73, 74, 76–78, 87, 89

**SFBC** Space-Frequency Block Codes. 27

**SGSN** Serving GPRS Support Node. 22

**SIMO** Single-Input Multiple-Output. 11, 26

**SISO** Single-Input Single-Output. 11, 26

**SM** Spatial Multiplexing. 29, 30

**SMS** Short Message Service. 1

**SNIR** Signal-to-Noise plus Interference. 10, 15, 29, 30, 48, 50, 53, 57, 60–62, 64–66, 68–71, 73, 74, 76, 77, 79, 82, 83, 85, 87–89

**SU-MIMO** Single-User MIMO. 11–13, 26

**SUI** Stanford University Interim. 45

**TB** Transport Block. 54

**TD** Transmit Diversity. iii, v, 27, 29, 30, 49, 65, 66, 68, 78, 79, 82, 83, 85–89

**TDD** Time-Division Duplexing. 20

**TDMA** Time Division Multiple Access. 23

**UE** User Equipment. iii, v, 21, 26–30, 33, 36–45, 47, 48, 50–57, 59, 60, 62, 64, 65, 68–71, 73, 74, 76–79, 82, 83, 85–89

**UMTS** Universal Mobile Telecommunications System. 5, 8, 17, 18, 21, 22, 24

**WAN** Wide Area Network. 9

**WCDMA** Wideband Code Division Multiple Access. 17, 21

**WiMAX** Worldwide Interoperability for Microwave Access. 1, 2, 17, 45





# Chapter 1

## Introduction

Over the past few years, mobile communications have suffered a great technological advancement. A few years ago an user was satisfied making a call, with a reasonable quality, to a given mobile terminal, but, in these days, most users' demand to see high-definition video, hosted in web services, on their mobile device. Due to this continued and increasing exigency from users, and also to offer new features with the aim of stimulating market, the mobile operators were forced to develop new techniques and technologies.

The 1<sup>st</sup> Generation (1G) cellular mobile network was deployed in 1981, where connections between terminals had a highly variable quality, due to interference, and where the confidence with which the data was transmitted was low.

In 1990 was launched the 2<sup>nd</sup> Generation (2G). Even to this day, it is the generation that has more percentage of users. It is defended by many as the generation that revolutionized the world of mobile communications and the truth is that his successor, failed to migrate as many users as it would be expected. Also note worthy, is that this generation introduced the Short Message Service (SMS), which continues to be highly used. This service again had a big boom when it was offered to users with lower price plans. This change is due to the introduction of General Packet Radio Service (GPRS) networks in the 2G.

When in 1998 it was launched the 3<sup>rd</sup> Generation (3G), the concept of mobile broadband had become part of users' everyday life. This generation has as its “buzzword” peak data rates in the order of 10 *Mbps* (considering the High Speed Downlink Packet Access (HSPA)). It is because of this generation, that making a video call or an Internet access with a very acceptable quality from a mobile device, has become a task within the reach of most users.

Towards the 4<sup>th</sup> Generation (4G) there were developed several telephony standards, that highlight the LTE, by the 3<sup>rd</sup> Generation Partnership Project (3GPP) Family, and Worldwide

Interoperability for Microwave Access (WiMAX) (IEEE 802.16e), developed by Institute of Electrical and Electronics Engineers (IEEE). Both technologies, were developed with the aim of fulfilling the requirements to be considered as a 4G technology. This term, while undefined, may also be applied to the forerunners of these technologies, LTE and WiMAX, and to other evolved 3G technologies providing a substantial level of improvement in performance and capabilities with respect to the initial third generation systems now deployed [1].

In the following, International Mobile Telecommunications-Advanced (IMT-Advanced) compliant versions of LTE are under development and call Long Term Evolution - Advanced (LTE-A). In order to fulfill the requirements, LTE-A adopted several improvements compared to LTE, such as Bandwidth Aggregation, Enhanced Multiple Antenna Technologies, Coordinated Multipoint Transmission (CoMP) and Relaying.

The aim of this thesis is to provide a better understanding of some of these improvements, specifically the differences between some of the various MIMO schemes used in LTE-A and Relaying.

The document is organized as follows. Chapter 2 presents an overview about the Mobile Communications Networks, the MIMO technique, LTE and LTE-A Technologies. In Chapter 3 is described the Simulation System Model and the Simulator Integration is explained. In Chapter 4, the Simulation Results and Analysis are presented. Finally, the Conclusions are drawn in Chapter 5.

## Publications

A part of the developed work on this thesis has been previously published elsewhere, as listed below:

- **Martins, A.**; Vieira, P.; Rodrigues, A.; “Throughput Enhancement using Fixed Relaying in LTE Networks”, Conference on Electronics, Telecommunications and Computers (CETC 2011), 24-25 November 2011, ISEL, Lisbon, Portugal [2].
- **Martins, A.**; Vieira, P.; Rodrigues, A.; “Transmit Diversity versus Open Loop Spatial Multiplexing MIMO Performance for LTE Fixed Relaying”, The 2012 IEEE 75th Vehicular Technology Conference, (VTC2012-Spring), 6-9 May 2012, Yokohama, Japan [3]. (*submitted*)
- **Martins, A.**; Vieira, P.; Rodrigues, A.; “Análise de Desempenho utilizando Diversidade de Transmissão e Multiplexagem Espacial em Malha Aberta para Redes LTE com

Repetidores Fixos”, 5º Congresso URSI/Anacom, 11 November 2011, Portugal [4].



## Chapter 2

# State of The Art

### 2.1 Changes to Traffic in Mobile Communications Networks

The traffic generated by mobile networks has suffered major changes over the recent years, both in the amount of data that these kind of networks started to generate, and also in the type of traffic. By mid-2007 the total traffic in this type of communications network was divided between voice and packet data. Since then, packet data has been increasing, whereas voice traffic remains stable. Figure 2.1 shows the rapid growth of data traffic compared to voice traffic, from January 2007 until May 2009, across multiple operators and based on one leading Universal Mobile Telecommunications System (UMTS)-HSPA infrastructure vendor's statistics.

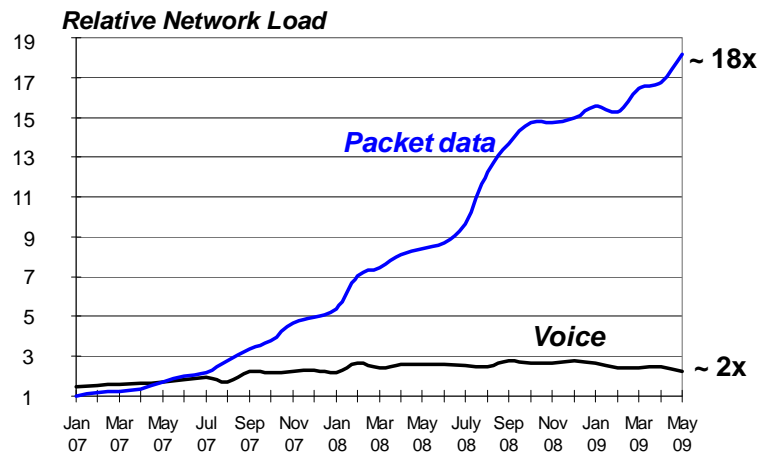


Figure 2.1: Growth in data traffic [5].

Please note that when the packet data traffic started to gain ground against the voice traffic, it corresponds precisely to the time that HSPA was released. It's interesting that

the two inflection points correspond to the release date for the iPhone<sup>®</sup> (July 2007) and iPhone3G<sup>®</sup> (July 2008).

According to [6], global mobile data traffic grew 2.6-fold in 2010, nearly tripling for the third year in a row. The 2010 mobile data traffic growth rate was higher than anticipated.

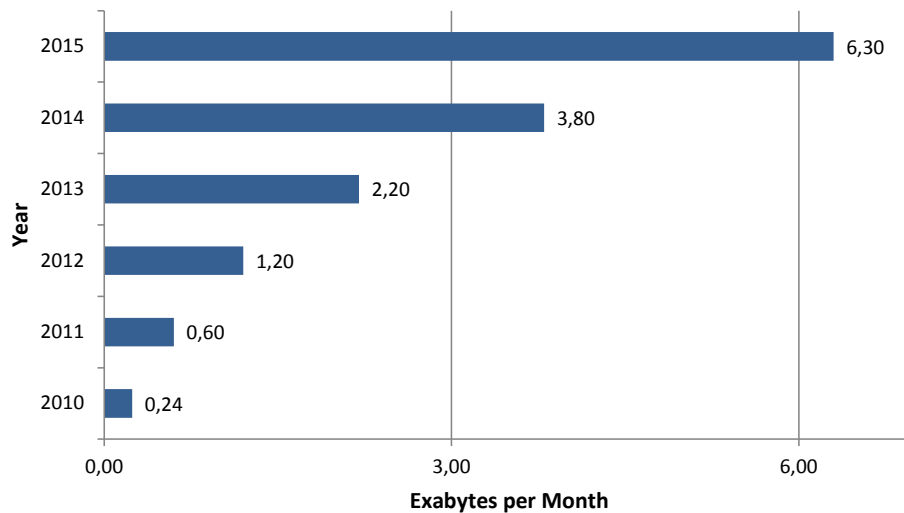


Figure 2.2: Cisco forecasts 3.6 exabytes per month of mobile data traffic by 2014 (adapted from [6]).

Besides that, the packet data traffic generated by users is very demanding in terms of the amount of required bandwidth. Services such as YouTube<sup>®</sup> gained prominence in recent years, and the proof is that, according to [7], almost 66% of the world's mobile packet data traffic will be video by 2014.

This means that operators must make new investments in order to strengthen their networks, and that mobile communications providers must develop new techniques to fulfill the users' requirements.

The video service, being a major provider of packet data traffic, can create a problem for operators. Unlike voice traffic, where investment is directly proportional to revenue, packet data traffic will not increase in this way with the investment. This happens because the bandwidth consumed by an user is not related to his payments of the service.

From Figure 2.3, it is seen that in the voice dominant area, the traffic/revenues lines have the same growing. But in the data dominant area, the traffic line has a much bigger growing compared to revenues.

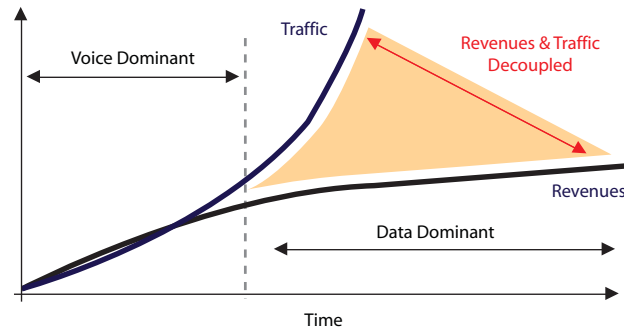
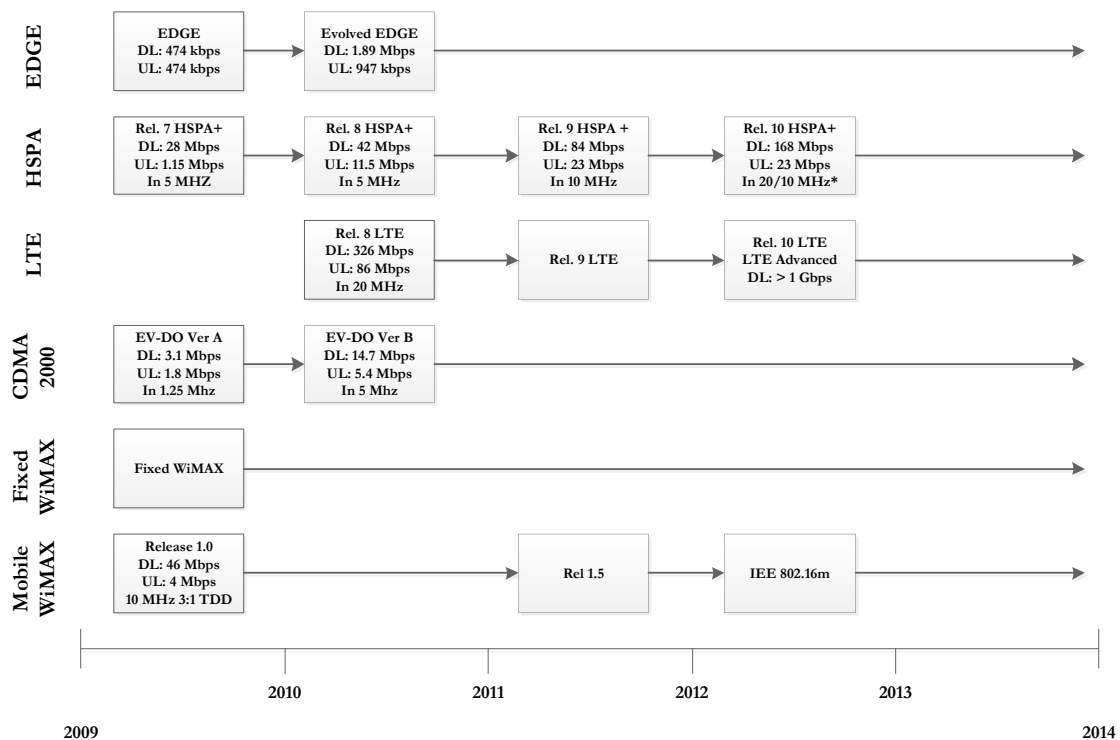


Figure 2.3: The traffic and revenue challenge [8].

## 2.2 Evolution of Mobile Communications Networks

In a time where the traffic generated by mobile communications networks has grown very significantly, a need arises to create a completely new technology that can fulfill both the needs of users and operators.

As it is illustrated in Figure 2.4, there has always been a degree of technology development in mobile communications networks.



Throughput rates are peak theoretical network rates. Radio channel bandwidths indicated. Dates refer to expected initial commercial network deployment except 2009, which shows available technologies that year. There are no public announcements of deployment of WiMAX Rel1.5.  
 \* 20/10 MHz indicates 20 MHz used on the downlink and 10 MHz used on the uplink.

Figure 2.4: Evolution of TDMA, CDMA, and OFDMA systems (adapted from [5]).

The UMTS mobile network was upgraded to HSPA with the goal of providing to users a greater speed and download capability. At this time, download speeds of 1.8 *Mbps* rose up to 14.4 *Mbps*. This change of speed is one of the features of Release 5.

In Figure 2.5 we can get an idea of the percentage of 2G, High Speed Downlink Packet Access (HSDPA) and 3G networks after being commercial.

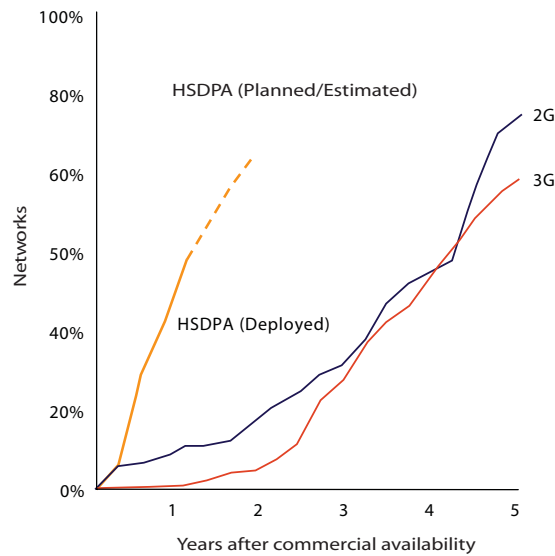


Figure 2.5: High rates of adoption of HSDPA [8].

In opposition to 2G and 3G, the percentage of HSDPA networks reached 50% in only one year after being commercially available, while the others have taken four years to the same percentage.

In 2005, with Release 6, the uplink was also subject to changes and performance improvement. This time, the uplink went from 0.4 *Mbps* to 1.4 *Mbps*, which was later upgraded to 5.8 *Mbps*. These improvements on the uplink performance, were the origin of High Speed Uplink Packet Access (HSUPA) and the combination of this with HSDPA is called HSPA.

In Figure 2.6 it is illustrated, the HSPA observed performances when comparing the latency and the downlink and uplink speed. It is emphasized that these figures relate to the date for initial HSPA (2007) implementations under typical load conditions, and devices limited to 3.6 *Mbps* in Downlink and 1.5 *Mbps* in uplink.

Still, the evolution of UMTS has continued with Release 7 and got to know another development, High Speed Packet Access Evolution (HSPA +). At this point, the downlink began offering 21 *Mbps* with 64 Quadrature Amplitude Modulation (QAM) or 28 *Mbps* using MIMO technique. The uplink increased by about 6 *Mbps*, to 11.4 *Mbps*.



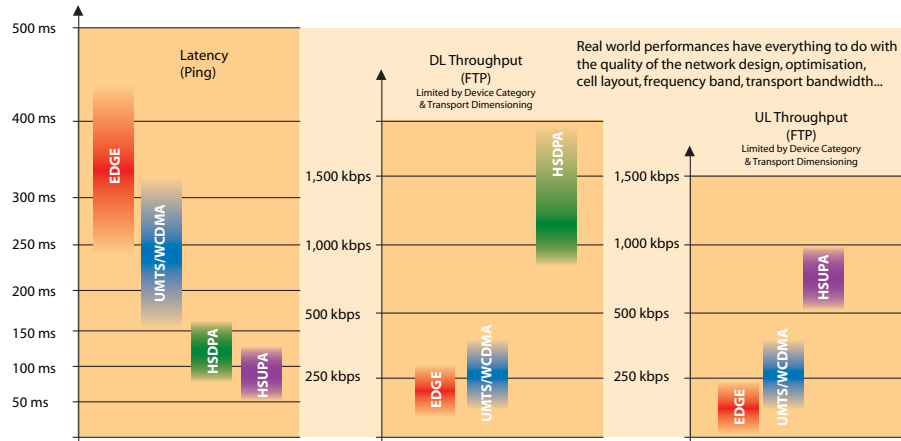


Figure 2.6: HSPA observed performances [8].

The Release 8 is where a revolution in the field of mobile communications networks started - the LTE [9].

## 2.3 MIMO

### 2.3.1 What is MIMO?

MIMO is an advanced technology that can effectively exploit the spatial domain of mobile fading channels to bring significant performance improvements to wireless communications systems [10].

According to [11], the MIMO technology is used in Personal Area Networks (PANs), Wide Area Networks (WANs) and Metropolitan Area Networks (MANs), which proves that this technology is really important in current Telecommunication Systems.

In [12], it is said that this technology has attracted attention in wireless communications, since it offers significant increases in data throughput and link range without additional bandwidth or transmit power. The Release 7 was the first release that featured MIMO. MIMO and Orthogonal Frequency Division Multiplexing (OFDM) are the core of 4G Technologies.

The advantages of MIMO technology are, according to [11]:

- Diversity Gain (see Figure 2.7);
- Array Gain (see Figure 2.8);
- Spatial Multiplexing Gain (see Figure 2.9).

The Diversity Gain is related to the fading effect of multipath, by reason of the fading

being sufficiently decorrelated in transmissions using multiple antennas. The Diversity Gain is present in two transmission techniques: Transmit Diversity and Reception Diversity. In the first case, the transmission is done using at least two antennas and, in the second case, the reception is made with at least two antennas. With this technique, the signal is sent/received by two independent sources. One consequence of this gain is an improvement in Signal-to-Noise plus Interference (SNIR).

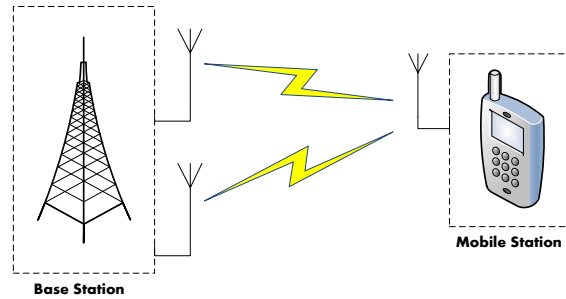


Figure 2.7: Divesity Gain (Transmit Diversity).

The Array Gain it is concentration of energy in one or more given directions via precoding or beamforming. As it is well known, using an Antenna Array, it is possible, controlling the antennas' phases and amplitude, to modulate the radiation pattern. With beamforming technique, the signal level in the Mobile Station (MS) target can be increase, and the interference level in the others MSs can be decreased.

This also allows multiple users located in different directions to be served simultaneously (so-called Multi-User MIMO (MU-MIMO)) [11].

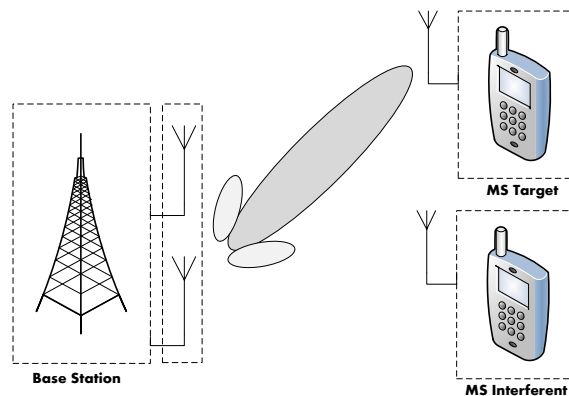


Figure 2.8: Array Gain.

Spatial Multiplexing Gain is related to the throughput improvements that a MS with good channel conditions can benefit. In this case, the MIMO technique is used with the aim

of increase the throughput, through multiple streams transmissions [13].

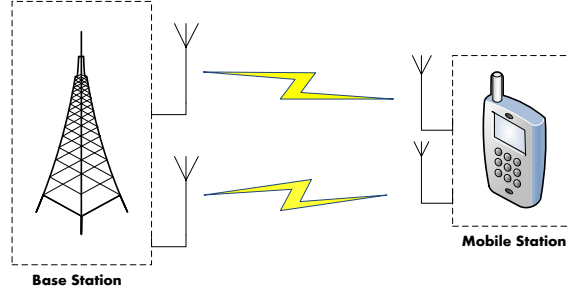


Figure 2.9: Spatial Multiplexing Gain.

There are currently two types of MIMO: Single-User MIMO (SU-MIMO) and MU-MIMO. The point-to-point multiple-antenna between Base Station (BS) and MS is designated SU-MIMO. The MU-MIMO situation occurs if several MSs are used simultaneously at the same frequency-domain and time-domain.

Figure 2.10 presents a typical situation of Single-Input Single-Output (SISO), in which the transmission and reception is done only with one antenna.

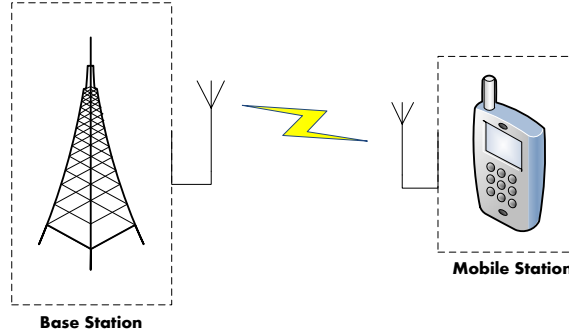


Figure 2.10: SU-SISO scheme.

While in SISO is only exploited the time-domain or frequency-domain for pre-processing and decoding of the transmitted and received data, respectively, with the use of MIMO an extra spatial dimension to signal detection and precoding is opened. The so-called space-time processing methods exploit this dimension with the aim of improving the link's performance in terms of one or more possible metrics, such as the error rate, communication data rate, coverage area and spectral efficiency ( $bps/Hz/cell$ ) [11].

These are the following types of multiple antenna configurations:

- Single-Input Multiple-Output (SIMO) – In this configuration, the transmission is made with one antenna and the reception with at least two antennas. This scheme is related

to the Diversity Gain, specifically Reception Diversity, since the signal reception is not only made by one antenna. This scheme is illustrated in Figure 2.11.

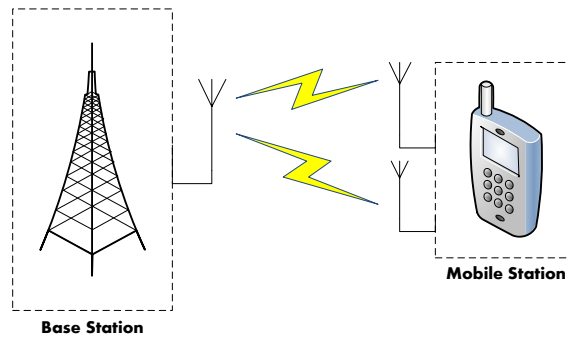


Figure 2.11: SU-SIMO scheme.

- Multiple-Input Single-Output (MISO) – The MISO scheme is the opposite of the previous situation: the signal is broadcasted in at least two antennas, while the reception is made by only one antenna. In this case, there is no receive diversity but there is transmit diversity. Figure 2.12 illustrates the MISO scheme.

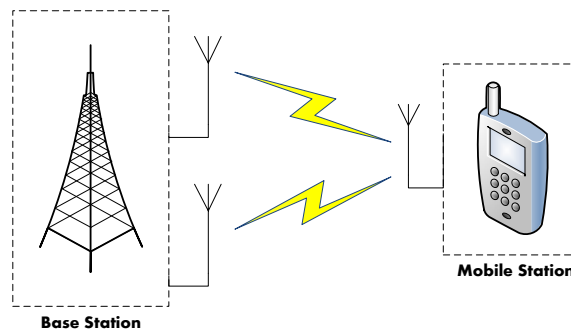


Figure 2.12: SU-MISO scheme.

- MIMO – In this case, the transmission and the reception are made with multiple antennas. In [13] is said that the multiple transmission antennas at the BS in combination with multiple receiver antennas at the MS, can be used to achieve higher peak data rates by enabling multiple data stream transmissions between the BS and the MS, by using MIMO spatial multiplexing. Therefore, in addition to larger bandwidths and high-order modulations, MIMO spatial multiplexing is used in the LTE system to achieve the peak data rate targets. Figure 2.13 and Figure 2.14 illustrates the SU-MIMO and the MU-MIMO scheme, respectively.

As can be seen, the BS and the MS have multiple antennas for transmission. In this case, the resources of BS are shared by two MSs.

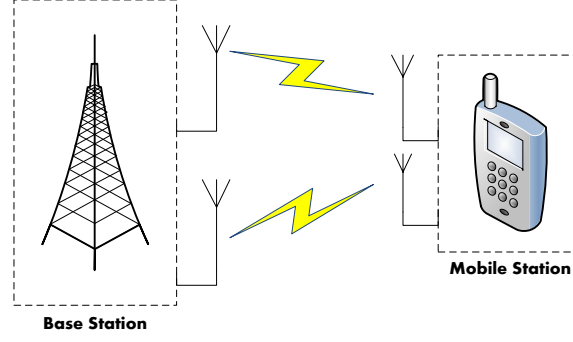


Figure 2.13: SU-MIMO scheme.

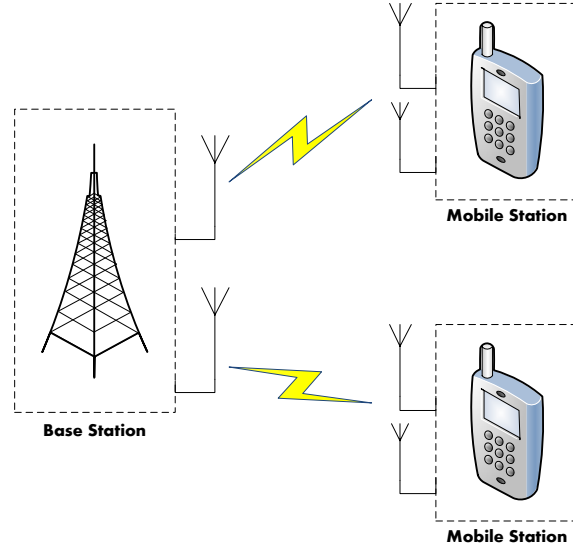


Figure 2.14: MU-MIMO scheme.

In [12] are presented the following advantages of MU-MIMO compared to SU-MIMO:

- MU-MIMO schemes allow for a direct gain in multiple access capacity (proportional to the number of BS antennas) thanks to the so called multiuser multiplexing schemes.
- MU-MIMO appears more immune to most of propagation limitations overcoming SU-MIMO communications such as channel rank loss or antenna correlation. Although increased correlation still affects per-user diversity, this may not be a major issue if multiuser diversity can be extracted by the scheduler instead. Additionally, Line-of-Sight (LoS) propagation, which causes severe degradation in single-user spatial multiplexing schemes, is no longer a problem in multiuser setting.
- MU-MIMO allows the spatial multiplexing gain at the BS to be obtained without the need for multiple antenna terminals, thereby allowing the development of small and

cheap terminals while complexity and cost is kept on the infrastructure side.

Finally, Figure 2.15 presents an overview of previously explained MIMO schemes.

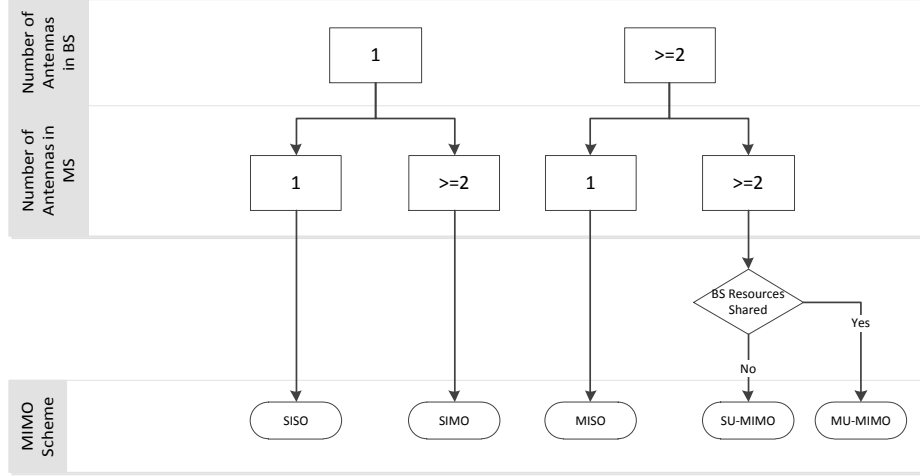


Figure 2.15: Overview of MIMO schemes.

### 2.3.2 Cooperative MIMO

Cooperative MIMO (CO-MIMO), also known as virtual or distributed MIMO, aims to succeed in creating a scenario at the expense of MIMO distributed antennas. The advantages of CO-MIMO are the cell's capacity, coverage and cell edge throughput improvements. With this technique, the terminals that are incapable of having multiple antennas, can exploit the analogous benefits of a MIMO system. With the introduction of new elements, or using existing elements in the network but with enhanced features, CO-MIMO has the disadvantage of increasing system complexity and also the large signalling overhead required for supporting device cooperation [10].

### 2.3.3 Types of Cooperative MIMO

As in [10], there are three schemes for CO-MIMO cellular systems: CoMP, Fixed-Relay and Mobile-Relay.

#### CoMP

The CoMP is a technique that has emerged with the aim of minimizing Inter-Cell Interference (ICI) and to improve cell edge performance. It is a strong candidate to be used in 4G. Within this scheme, there is cooperation between BSs by exchanging information in order to

coordinate their transmissions in the downlink, and jointly process the received signals from the MS in uplink.

The main goal is to use ICI in a constructive way, rather than a destructive one. The MS receives the signal from multiple sources, that can be harnessed in two ways. Either it sends the same signal from different sources, which means that there is redundancy information but increased SNIR, or it sends information separately, in order to increase the MS throughput.

The main advantage of this scheme is that it is able to make unwanted signals that would be useless, in true information, thus enabling to explore the diversity of the channel. However, this technique has a disadvantage: there must be a very fast exchange of information between BSs. Consequently, the core network must be prepared to provide conditions for such a requirement. In Figure 2.16, it is presented a basic CoMP scheme.

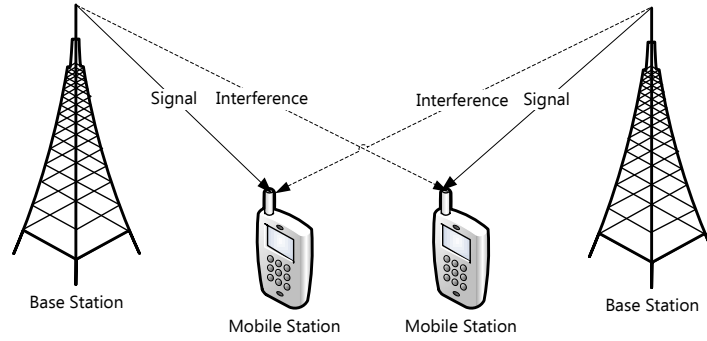


Figure 2.16: Coordinated multipoint transmission scheme.

From Figure 2.16, one can see that the MS can be exposed to two signal types: the signal with useful information and an unwanted signal from a neighbor BS. If a kind of cooperation exists between the BSs, the interference level can be reduced.

### Fixed-Relay

Another type of CO-MIMO is called Fixed-Relay. In this scheme, FRSs are used to send the signal to MS from the BS and vice versa. This type of CO-MIMO can be aimed also to increase the coverage and network capacity in a specific area, and to improve the Quality of Service (QoS).

On one hand, this type of scheme is very appealing because it can not only exploit the spatial diversity gain, but also to increase network performance or even expand the coverage area, at a low-cost. On the other hand, using this type of equipment introduces an additional delay in the network, and can create interference problems reusing the spectrum in the RS.

A simply BS-FRS-MS link, is illustrated in Figure 2.17.

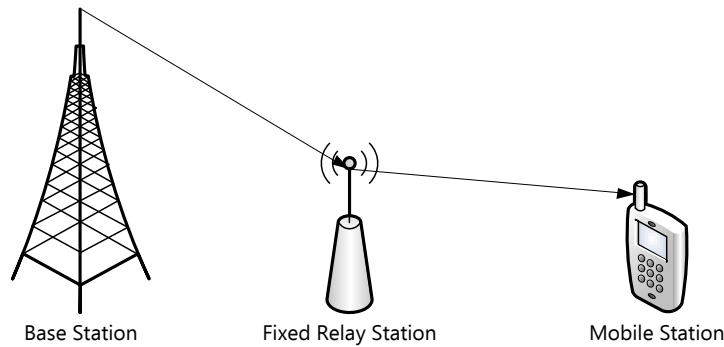


Figure 2.17: Fixed-Relay scheme.

### Mobile-Relay

Although this type of CO-MIMO has the same objective as the Fixed-Relay scheme, several problems exist since the relay instead of being a strategically placed element, it is a relay in motion. As such, the relay propagation conditions strongly vary, when compared with the previous case.

If a MS is supported by another MS, propagation conditions are being changed much faster at the expense of both movements, so it can create conditions for the Mobile Relay Station (MRS) to increase the signal level, or increase the throughput of this terminal at his expense. The advantage that exists in the fixed-relay scheme, continues to exist but, in this case, it is a cheaper solution for operators to achieve the same objectives.

The fact that these MRSs are not owned by operators may bring some problems. They have less control in its operation, in comparison to the previous two schemes. In addition, the relays are not as reliable, resulting in a very fickle network topology.

Figure 2.18 illustrates two typical situations of this kind of CO-MIMO: Moving Networks and Mobile User Relays.

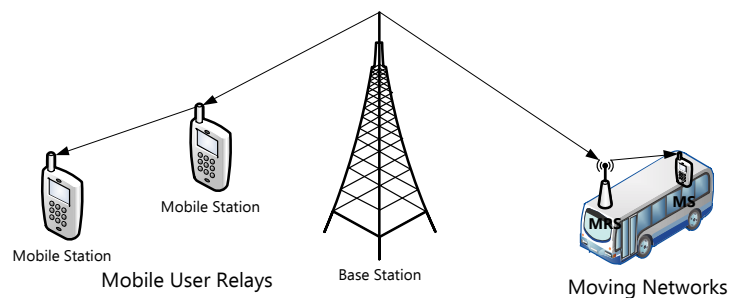


Figure 2.18: Mobile-Relay.



In the first case, it is used a dedicated RS to route information from the BS to the MS and vice versa. In the illustrated case, the MRS is a RS located on a bus, in order to improve the traveling passengers coverage. The Mobile User Relaying, is a technique that uses MSs as repeaters, enabling them to behave either as a relay or as a terminal, trying to create an ad-hoc network.

This particularly exposes the problem related to the autonomy of MSs. There are times when MSs are used as MRS consuming battery, without any given use by the owner. This type of CO-MIMO is supported by the WiMAX, and it is also intended to be adopted in 4G technology.

Considering the three types of CO-MIMO scheme, Fixed-Relaying is the more mature, and it has been already incorporated by the IEEE 802.16j to improve performance in WiMAX. Unlike CoMP, it is a scheme that has different links, which are: BS-RS, RS-MS, BS-MS and RS-RS. Thus, there are not only links of type Fixed-to-Mobile (F2M) but also the type Fixed-to-Fixed (F2F) which is the case of BS-RS and RS-RS.

On one hand, the Mobile User Relay implies the BS-MS and MS-MS links, that are links of type F2M and Mobile-to-Mobile (M2M), respectively. On the other hand, Moving Networks imply BS-MS, BS-RS and RS-MS. The first two links are links of type F2M, and the RS-MS link is a link of type F2F or F2M.

## 2.4 Long Term Evolution

### 2.4.1 Introduction

Despite of the induction of several network improvements such as HSPA and HSPA+, Nokia Siemens Networks<sup>®</sup> and UMTS Forum argue that data traffic in existing Wideband Code Division Multiple Access (WCDMA)/HSPA and Code Division Multiple Access (CDMA) networks is growing dramatically year by year. This causes a need for mobile operators to update their existing networks to match growing data needs [14].

The goal of LTE is to provide a high data-rate, low-latency and packet-optimized radio-access technology supporting flexible bandwidth deployments [13].

The LTE standardization process was launched at a workshop in Toronto in November 2004. Following the workshop, 3GPP approved the start of the study for LTE in December 2004. Figure 2.19 shows the phases that LTE suffered from its inception until the Protocol Freezing in early 2009.

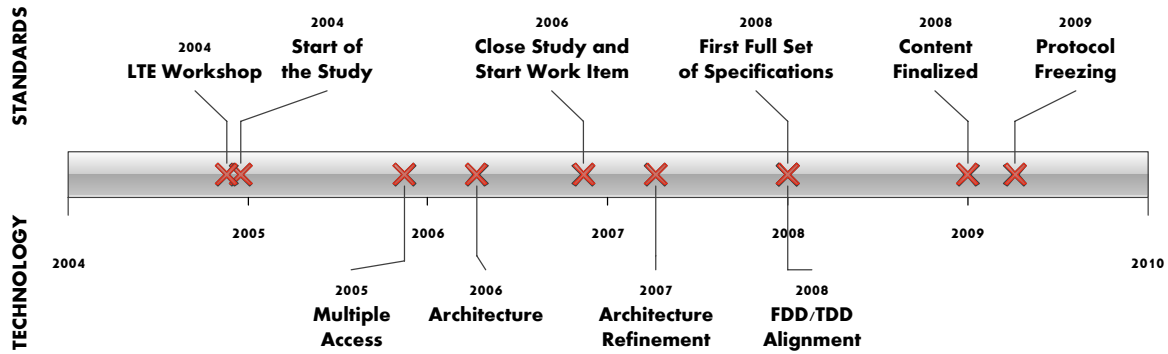


Figure 2.19: LTE milestones in 3GPP (adapted from [15]).

The relative adoption of this technology, in comparison to Global System for Mobile Communications (GSM)/EDGE and UMTS/HSPA levels, is visible in Figure 2.20.

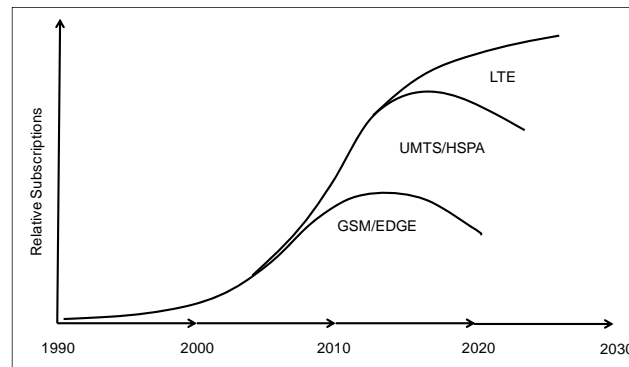


Figure 2.20: Relative adoption of technologies [5].

From the following figures, one can see that the LTE has been treated as a 4G Technology. (see Figure 2.21, Figure 2.22 and Figure 2.23).

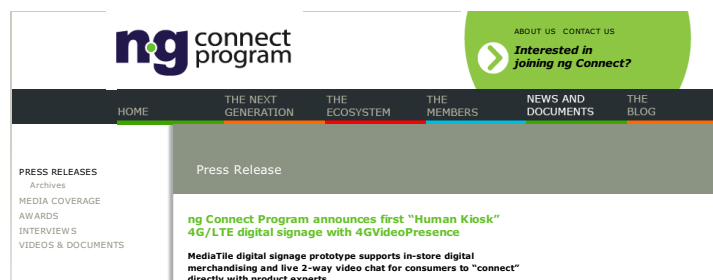


Figure 2.21: Screenshot of "www.ngconnect.org" site.

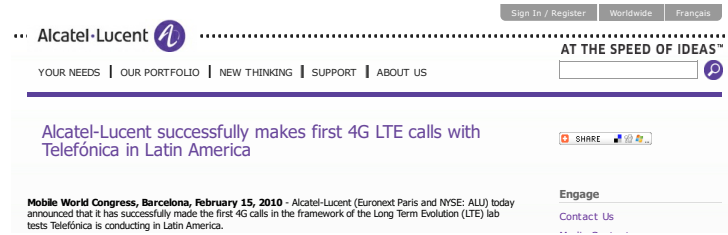


Figure 2.22: Screenshot of “www.alcatel-lucent.com” site.

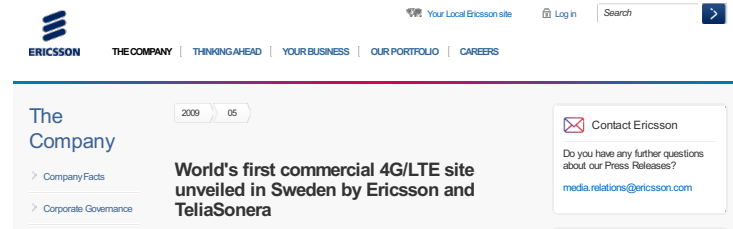


Figure 2.23: Screenshot of “www.ericsson.com” site.

### 2.4.2 Targets for LTE

The LTE’s goal is to reach a far superior performance then existing 3GPP networks based on HSPA technology. For the LTE it was established that [15]:

- Spectral efficiency should be two to four times more than with HSPA Release 6;
- Peak rates must exceed 100 *Mbps* in downlink and 50 *Mbps* in uplink;
- Round trip time less than 10 *ms*;
- Packet switched optimized;
- High level of mobility and security;
- Optimized terminal power efficiency;
- Frequency flexibility with from below 1.5 *MHz* up to 20 *MHz* allocations.

The main targets of LTE compared with Release 6 are shown in Figure 2.24. One can see that the Peak User Throughput had a 10-fold increase, the Latency decreased 2;3-fold, and the Spectral Efficiency had a 2;4-fold increase.

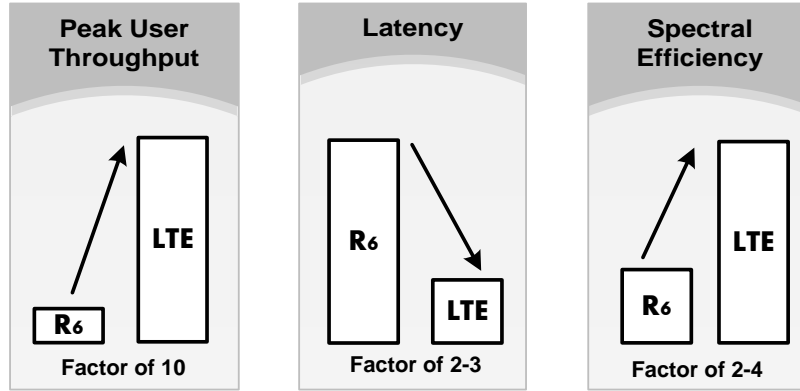


Figure 2.24: Main LTE performance targets (adapted from [15]).

### 2.4.3 LTE Overview

LTE uses Orthogonal Frequency-Division Multiple Access (OFDMA) in downlink and Single-carrier Frequency-Division Multiple Access (SC-FDMA) in the uplink, access schemes that make it possible to support flexible bandwidths. These multiple access schemes provide orthogonality between the users, reducing the interference and improving the network capacity.

LTE enables spectrum flexibility where the transmission bandwidth can be selected between 1.4 and 20 MHz, depending on the available spectrum.

In addition to the Frequency-Division Duplexing (FDD) and Time-Division Duplexing (TDD), LTE supports Half-Duplex Frequency-Division Duplexing (HD-FDD). As in this mode, the MS separates the transmission in time and frequency domain, the duplex-filter is less complex than in the FDD mode. Consequently, the MS complexity and its costs are reduced. The previous modes are shown in Figure 2.25

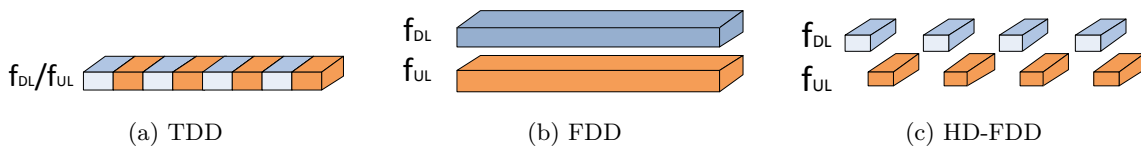


Figure 2.25: TDD, FDD and HD-FDD schemes.

Although the system is optimized for low speeds up to 15 km/h, the system displays a specification limit of 350 km/h, with a performance degradation.

Downlink access is done using the OFDMA, but uplink access is based on SC-FDMA that promises to increase uplink coverage due to low Peak-to-Average Power Ratio (PAPR) relative to OFDMA.

For the throughput, LTE supports downlink peak data rates of 326 *Mbps* using the MIMO technology. This throughput is a value that refers to a situation of MIMO 4×4 within a 20 *MHz* bandwidth. In a situation of MIMO 2×2, LTE can provide up to 150 *Mbps*. The uplink has the lowest values since the uplink MIMO is not employed in the first released of LTE standard. Thus, peak data rates are limited to 86 *Mbps* within a 20 *MHz* bandwidth. These speeds are also dependent on MS characteristics. It is important to underline that, in LTE, the MSs are designated by UEs. In Table 2.1 a summary is made for the five UE existing categories.

Table 2.1: Categories of LTE User Equipment (adapted from [11]).

	UE Category				
	1	2	3	4	5
Maximum Downlink Data Rate ( <i>Mbps</i> )	10	50	100	150	300
Maximum Uplink Data Rate ( <i>Mbps</i> )	5	25	50	50	75
Number of Receive Antennas Required	2	2	2	2	4
Number of Downlink MIMO Streams Supported	1	2	2	2	4
Support for 64QAM Modulation in Downlink	✓	✓	✓	✓	✓
Support for 64QAM Modulation in Uplink	✗	✗	✗	✗	✓

LTE aims for a higher spectral efficiency, about 2–4 more times than compared with Release 6 HSPA.

One of the strengths of LTE is also its low latency where, according to [13], the LTE radio-interface and network provides capabilities for less than 10 *ms* latency for downlink packet the transmission.

This decrease is due to the efforts made at the time of developing a new architecture for Release 8. In addition to LTE, the 3GPP is also defining an Internet Protocol (IP)-based, flat network architecture. This architecture is defined as part of the System Architecture Evolution (SAE) effort. The LTE–SAE architecture and concepts have been designed for efficient support of an IP-based service, considering the mass market usage. The architecture is based on an evolution of the existing GSM/WCDMA core network, with simplified operations and smooth cost-efficient deployment [16]. Its main difference from the previous architectures, is the number of network nodes, which was substantially decreased.

In UMTS, the BS are designated NodeB (NB), being linked to the Radio Network Con-

troller (RNC) by Iub interface. In turn, the RNCs are linked together by the Iur interface, communicating with the Gateway GPRS Support Node (GGSN) and the Serving GPRS Support Node (SGSN) via the Iu interface.

In the LTE architecture, there was a change in the names of the network nodes, some nodes were extinguish and new internodes links in the network were created. From Figure 2.26, one can see that the RNC element is no longer part of the architecture, with BSs, now known as evolved NodeB (eNB), directly connected to the network core, where there is Mobility Management Entity (MME) and Serving Gateway (S-GW).

Figure 2.26b shows also two interfaces: S1 and X2. The S1 interface connects the eNB to MME and S-GW and the X2 interface connects the eNB between each other, which is a big change from the architecture of UMTS where the NB were not interconnected.

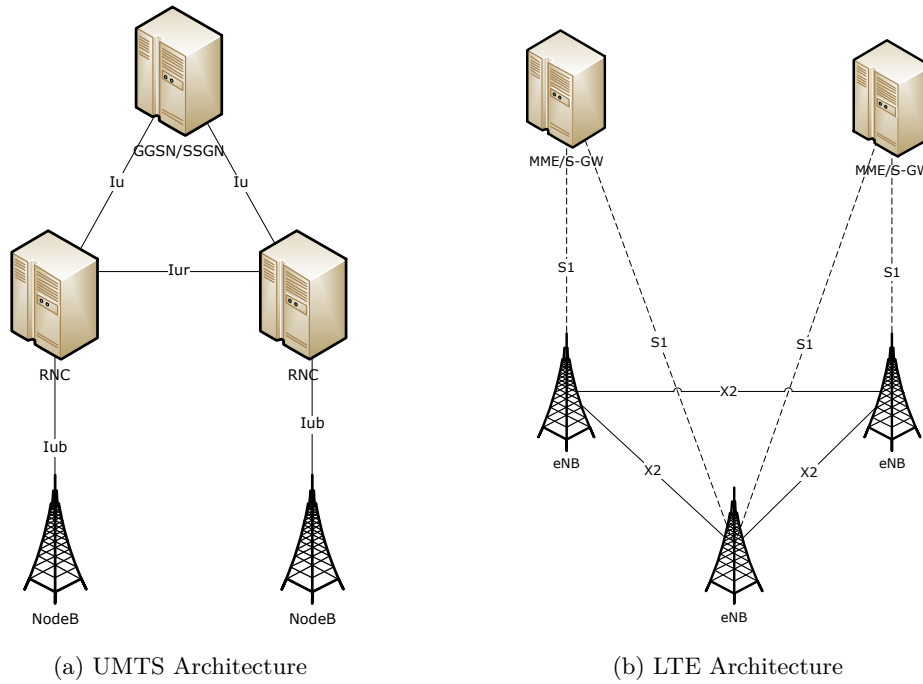


Figure 2.26: UMTS and LTE architectures.

Table 2.2 shows a comparison between the LTE and Release 6 HSPA, at radio link (uplink and downlink) and system level.

Table 2.2: Summary of key performance requirement targets for LTE (adapted from [11]).

		Absolute Requirement	Comparison to Release 6
Downlink	Peak Throughput Rate	$>100 \text{ Mbps}$	$7 \times 14,4 \text{ Mbps}$
	Peak Spectral Efficiency	$>5 \text{ bps/Hz}$	$3 \text{ bps/Hz}$
Uplink	Peak Throughput Rate	$>50 \text{ Mbps}$	$5 \times 11 \text{ Mbps}$
	Peak Spectral Efficiency	$>2,5 \text{ bps/Hz}$	$2 \text{ bps/Hz}$
System	User Plane Latency	$<10 \text{ ms}$	One Fifth
	Connection set-up latency	$<100 \text{ ms}$	
	Operating Bandwidth	$1,4 \text{ MHz} - 20 \text{ MHz}$	$5 \text{ MHz}$

#### 2.4.4 Technologies for LTE

This subsection presents the main technologies for LTE.

##### Orthogonal Frequency-Division Multiple Access (OFDMA)

In the downlink, LTE uses OFDMA. OFDMA is a variant of OFDM technology, the digital multi-carrier modulation scheme that is widely used in wireless systems, but relatively new to cellular. The European Telecommunications Standards Institute (ETSI) first looked at OFDM for GSM back in the late 1980s [17].

OFDMA, unlike OFDM, allows the subcarriers subsets to be allocated dynamically among the different users of the channel, since it incorporates variants of Time Division Multiple Access (TDMA). This property also leads to a more robust system with a greater capacity and a greater ability to combat the radio channel irregularities. It is possible to assign more slots to an user in terms of frequency and time, taking into account the radio propagation conditions that it is subjected.

OFDMA has been used in LTE and other systems due to the following properties [15]:

- Good performance in frequency selective fading channels;
- Low complexity of base-band receiver;
- Good spectral properties and handling of multiple bandwidths;
- Link adaptation and frequency domain scheduling;

- Compatibility with advanced receiver and antenna technologies.

Figure 2.27 shows the difference between the use of OFDM and OFDMA.

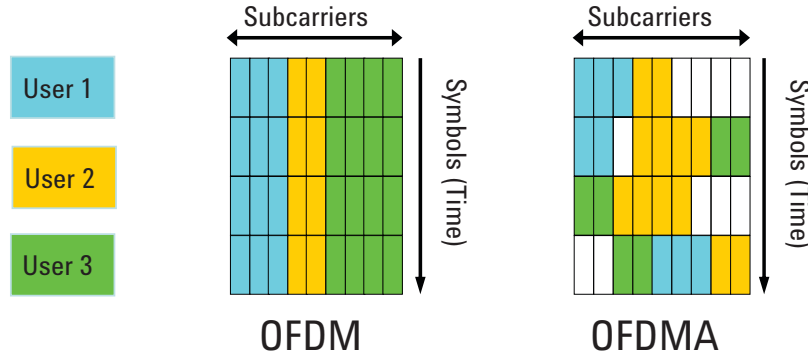


Figure 2.27: OFDM and OFDMA subcarrier allocation [17].

In the following, some advantages of OFDMA are presented, when compared with CDMA based UMTS [17]:

- OFDM can easily be scaled up to wide channels that are more resistant to fading;
- OFDM channel equalizers are much simpler to implement than CDMA equalizers, as the OFDM signal is represented in the frequency domain rather than the time domain;
- OFDM can be made completely resistant to multi-path delay spread. This is possible because the long symbols used for OFDM can be separated by a guard interval known as the Cyclic Prefix (CP). The CP is a copy of the end of a symbol inserted at the beginning. By sampling the received signal at the optimum time, the receiver can remove the time domain interference between adjacent symbols caused by multi-path delay spread in the radio channel;
- OFDM is better suited to MIMO. The frequency domain representation of the signal enables easy precoding to match the signal to the frequency and phase characteristics of the multi-path radio channel.

Although having advantages over CDMA, with the use of OFDM new problems arise: the OFDM system is sensitive to frequency errors and phase noise because the subcarriers may not be sufficiently spaced. This point is also associated with the Doppler effect that can cause interference between the subcarriers. This can cause problems at the edge of the cells. Unlike the CDMA scrambling codes which are used to avoid ICI, the OFDM's codes are not.



Thus, it is sometimes necessary to have a frequency reuse plan in order to avoid the ICI at the cell edges.

### Single-Carrier Frequency-Division Multiple Access

The main reason why this technology was adopted in detriment to the OFDMA in the uplink is the high PAPR that the previous one. The lower the PAPR, the higher the average power transmitted to the power amplifier. Hence, when single carrier transmission is used the amplifier has a greater efficiency, which is also reflected in an increased coverage. This scheme has characteristics of a single-carrier system, *e.g.*, GSM and CDMA, as is the case in low PAPR value but, like OFDM, frequency allocation is flexible and resistive to multipath.

Figure 2.28 makes a comparison between the use of OFDMA and SC-FDMA for the same sequence of Quadrature Phase-Shift Keying (QPSK) data symbols. As shown, in OFDMA, symbols are modulated only in phase with the constant amplitude. This is the main reason why this type of access has a high PAPR.

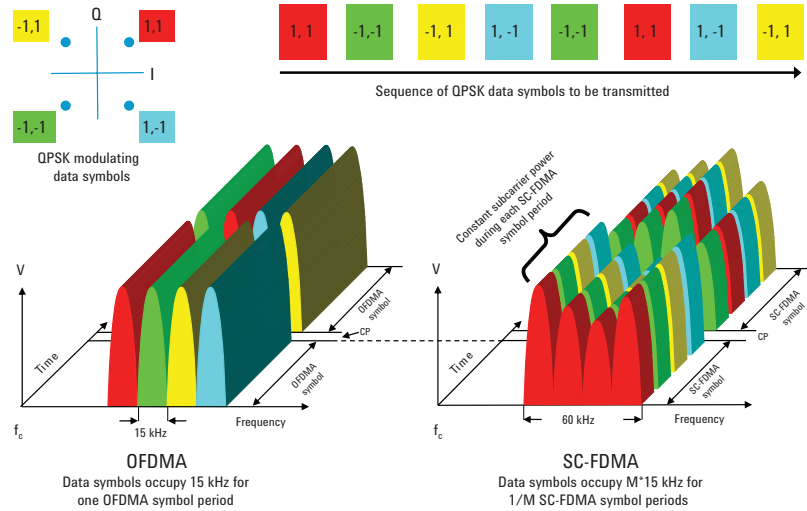


Figure 2.28: Comparison of OFDMA and SC-FDMA transmitting a series of QPSK data symbols [17].

### MIMO

This subsection lists various ways that LTE uses to explore the MIMO technique. Before exposing the seven modes of MIMO in LTE, it is important to introduce three concepts that are used specifically for LTE.

- Codeword – A codeword represents the data before being formatted prior to the trans-

mission. Two codewords can be used, for each UE, depending on the radio channel conditions and the utilized scheme. In the case of SU-MIMO, two codewords are sent to the UE and in the case of MU-MIMO each UE has a codeword.

- Layer – A layer corresponds to a data stream. That is, if two layers are used to transmit data, they are being used in the pattern of independent transmission. For spatial multiplexing are used at least two layers, with the maximum use of four layers. Note that the number of layers that can be used is always less or equal than to the number of antennas available.
- Precoding – As explained below, the conditions on which the transfer is made may vary in order to fit the radio channel. Two layers may have very different propagation conditions, meaning that one is more appropriate than the other depending on the conditions. The precoding operation modifies the layer signals before the transmission. The precoding may be done for diversity, beamforming or spatial multiplexing.

Figure 2.29 shows the processing steps to which the terms refer.

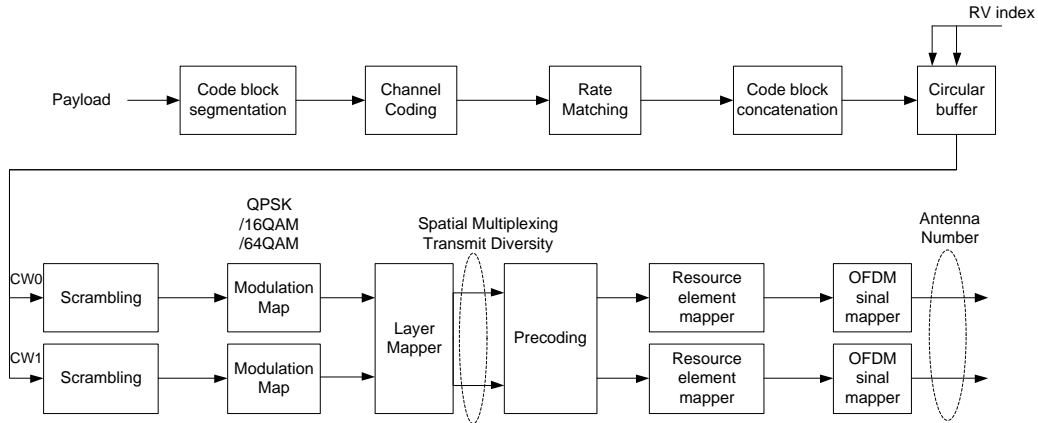


Figure 2.29: Signal processing for transmit diversity and spatial multiplexing (adapted from [17]).

According to [18], there are seven modes of MIMO in LTE, which are:

- Mode 1 – Single-Antenna port; Port 0: It is considered the most basic mode of transmission. This mode uses just one antenna for transmission while two can be used for reception. So, this is a traditional SISO or SIMO (in the case of using two antennas for reception). In the second case, there is more diversity in the reception. This mode provides little gain in good conditions but the users' throughput does not increase.

- Mode 2 – Transmit Diversity (TD): In this mode, the same information is sent via different layers. The information stream is coded using Space-Frequency Block Codes (SFBC), that repeats the information in multiple subcarriers on different antennas. This mode does not improve the peak data rate, since only one layer is used to convey the same information. Instead, there is an improvement in the robustness of the channel, which causes less errors in the decoded step.

TD can be applied to all physical channels as well as to Physical Downlink Shared Channel (PDSCH), Physical Broadcast Channel (PBCH), Physical Control Format Indicator Channel (PCFICH), Physical Downlink Control Channel (PDCCH) and Physical Hybrid ARQ Indicator Channel (PHICH), while the others MIMO schemes are only applicable to PDSCH [19]. The TD is not applied to the primary and secondary synchronization channels. It is through these channels that the UE will know the number of antennas that are being used for broadcasting. Depending on the number of antennas used for transmission, a specific TD scheme is used.

- Mode 3 – Open-Loop Spatial Multiplexing (OL-SM): Unlike the previous mode, two streams are used to transmit different information and, in the case of LTE, it can use up to four streams. In this case, there is already an increase in throughput, which was not the case in TD, since the received information by the UE is not the same.

The OL-SM is appropriate when the eNB does not have the Precoding Matrix Indicator (PMI) from the UE. This could be due to the fact that the UE has a very low transmission speed or when the feedback of the uplink channel is not reliable. Therefore, the conditions in which the broadcast is made is driven only by Rank Indicator (RI) and Channel Quality Indicator (CQI). The RI indicates to the eNB what is the maximum number of layers that the channel supports. It is based on this factor, in the traffic pattern and in the available power that eNB decides the number of layers. The CQI feedback indicates to the eNB what is the modulation scheme and channel coding that should be used, for a block error probability not exceeding 10%. In theory, the throughput for the OL-SM would be the double of a MISO scheme, for example. In practice, this does not happen because the channels are not independent and suffer from variable propagation conditions.

In short, these previous two modes can be understood in the following way: while the TD tends to increase the cell's capacity, the OL-SM has the main objective to increase the users' throughput.

The OL-SM with  $M$  layers and  $N$  transmit antennas ( $N \geq M$ ) is illustrated in Figure 2.30.

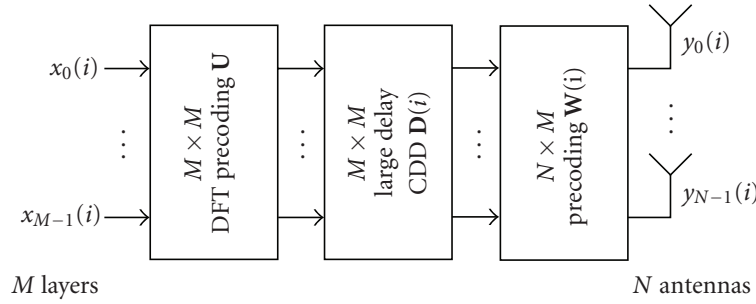


Figure 2.30: Open-Loop Spatial Multiplexing with  $N$  antennas and  $M$  layers [19].

- Mode 4 – Closed-Loop Spatial Multiplexing (CL-SM): In [19] is described that this mode of operation, unlike the previous one, involves feedback from to the UE to the eNB. Hence, the conditions under which the transmission is done, depend of the exchange of informations between UE and eNB. The conditions in which the broadcast is made are variable, with the aim to counteract the fluctuations in terms of propagation that the radio channel is subjected. The eNB applies the precoding spatial domain on the transmitted signal according to the PMI which was previously indicated by the UE. In this mode, the eNB also takes into account the RI and CQI. The Closed-Loop Spatial Multiplexing (CL-SM) with  $M$  layers and  $N$  transmit antennas ( $N = M$ ) is illustrated in Figure 2.31.

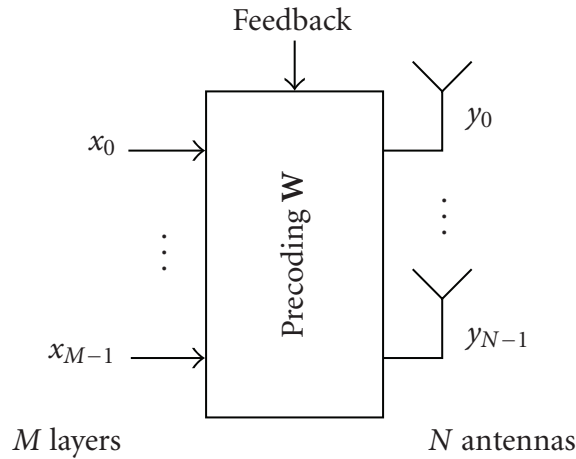


Figure 2.31: Closed-Loop Spatial Multiplexing with  $N$  antennas and  $M$  layers [19].

According to [18] this is the mode that will perform best.

- Mode 5 – MU-MIMO: According to [17], this mode is a special case of mode 3, in which

the codewords are designed for different UEs, *i.e.*, the information transmitted for each UEs is different. In this way, although the throughput of each user remains unchanged, the overall network data rate is improved because the UEs share the same resources. The mode 5 may have problems if the layers used for each UE are not completely orthogonal to each other, making the users to cause interference in each other.

- Mode 6 – Closed Loop Rank 1 with pre-coding: This mode is the fall-back scenario when mode 4 reports RI equal to 1. In this mode, beamforming is enabled, and its intention is to focus the signal power in a particular direction.
- Mode 7 – Single-Antenna port; Port 5: The seventh mode is the beamforming mode. Similarly to the mode one, the information is transmitted over a single layer. therefore, from a UE perspective, the mode one and seven are identical. According to [18], linear antenna arrays are expected to be used for this mode.

The performance of MIMO systems depends on several factors such as signal quality, the radio channel conditions, the speed of the UE and the correlation of the received signals at the receiver antennas.

Thus, an effort is made to use the best MIMO scheme suitable for each scenario. In the following paragraphs an analysis will be made to the presented LTE modes, indicating in what situations should one be used instead of another.

OL-SM and CL-SM mode should be applied when the received signal quality is at its highest. According to [18], the benefits of the Spatial Multiplexing (SM) schemes starts in at about  $SNIR = 15dB$  or higher and when the correlation is low. In a situation where the UE is close to the cell edge, the Closed-Loop Rank 1 or TD should be used. The TD can achieve better results than the OL-SM and CL-SM in rural environment, where signal scattering is low.

Another factor that influences the choice of schemes is the speed of the UE. Although the CL-SM obtains better results than the OL-SM, because it can adapt to radio channel conditions more efficiently, in a situation where the UE moves quickly, it is advisable that you use the OL-SM. The CL-SM mode can not keep up with changes in the radio channel. In [18] it is stated that TD is also robust to speed while it is performing in a low scattering environment and high SNIR and does not degrade as much as OL-SM. The following example is presented: for a vehicle moving at high speed along a highway with a clear LoS to the eNB, TD would provide the better spectral efficiency, while OL-SM would be preferred when the

UE is moving at high speed in a rich multipath environment and high SNIR.

SM schemes performs best when the signals have a low correlation coefficient. A high correlation signal will be the worst performance of these systems. The correlation signal is related to the scattering environment of the eNB and the UE. The performance is maximized by a high scattering signal. In urban areas, where the scattering is greater, it is appropriate to use a scheme of this type.

Beamforming techniques should be used in rural environments where there is a high correlation environment, and where the signal comes with a low angular spread.

Table 2.3 summarizes the conditions under which each scheme should be used. Note that the schemes can be adapted dynamically according to the UE position in the cell and the radio channel conditions.

Table 2.3: Decision matrix for the main LTE MIMO modes (adapted from [18]).

MIMO Mode	SNIR	Scattering	Speed	Dynamic Adaption
TD	Low	Low	High	None
OL-SM	High	High	High	TD
CL-SM	High	High	Low	TD or CL Rank=1
Closed-Loop Rank=1	Low	Low	Low	TD

## Higher-Order Modulations

To achieve the debits to which it proposes, LTE uses the following modulation techniques, presented in Table 2.4:

Table 2.4: LTE modulation techniques (adapted from [14]).

Modulation	Downlink	Uplink
QPSK	✓	✓
16 QAM	✓	✓
64 QAM	✓	✗
BPSK (pi/2-shift)	✗	✓
8PSK	✗	✓

## 2.5 LTE-Advanced

### 2.5.1 Introduction

With the aim to improve the LTE performance are in study several proposals. This series of changes, new features and functionalities gave rise to a new technology that underlies this thesis: LTE-A. The inauguration LTE-A workshop was held in Shenzhen, China, in April 2008.

Figure 2.32 shows what has been the evolution of LTE-A in terms of study and development.

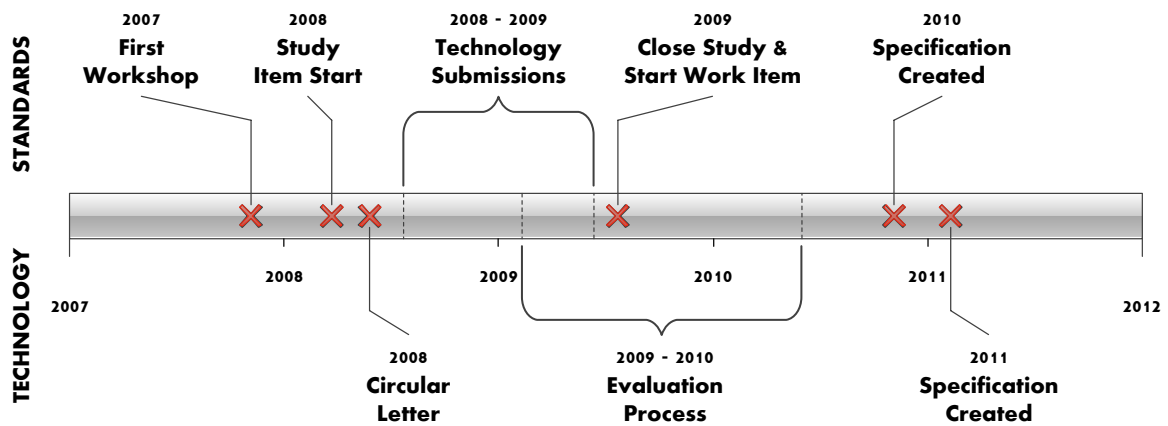


Figure 2.32: 3GPP LTE-Advanced and ITU-R IMT-Advanced schedules (adapted from [15]).

### 2.5.2 LTE-A Overview

An objective of the LTE-A is offering peak data rates of up to approximately 100 *Mbps* for high mobility and up to 1 *Gbps* for low mobility.

As previously mentioned, despite being LTE a 4G technology, this designation can only be applied to networks that meet the requirements of IMT-Advanced articulated that are in Report ITU Radiocommunication Sector (ITU-R) M.2134. In [5] are some aspects of these requirements:

- Support for scalable bandwidth up to and including 40 *MHz*;
- Encouragement to support wider bandwidths (*e.g.*, 100 *MHz*);
- Minimum downlink peak spectral efficiency of 15 *bps/Hz* (assumes MIMO 4×4);
- Minimum uplink peak spectral efficiency of 6.75 *bps/Hz* (assumes MIMO 2×4).

Also in Table 2.5 an overview is made concerning some of the requirements and characteristics of the LTE-A.

Table 2.5: IMT-A Requirements and Anticipated LTE-A (adapted from [5]).

Item	IMT-A Requirement	LTE-A Project Capability
Peak Data Rate Downlink		1 Gbps
Peak Data Rate Uplink		500 Mbps
Spectrum Allocation	Up to 40 MHz	Up to 100 MHz
Latency User Plane	10 ms	10 ms
Latency Control Plane	100 ms	50 ms
Peak Spectral Efficiency DL	15 bps/Hz	30 bps/Hz
Peak Spectral Efficiency UL	6,75 bps/Hz	15 bps/Hz
Average Spectral Efficiency DL	2,2 bps/Hz	2,6 bps/Hz
Average Spectral Efficiency UL	1,4 bps/Hz	2 bps/Hz
Cell-Edge Spectral Efficiency DL	0,06 bps/Hz	0,09 bps/Hz
Cell-Edge Spectral Efficiency UL	0,03 bps/Hz	0,07 bps/Hz

From Table 2.5, one can also see that the LTE-A meets all the presented requirements to be designated as a 4G technology.

### 2.5.3 LTE-Advanced Enhancements

This subsection presents the main aspects associated with the LTE-A, in order to fulfill it's objectives.

#### Bandwidth Aggregation

The idea of this technique is to make an aggregation of multiple LTE carriers. The Bandwidth Aggregation Technique is shown in Figure 2.33.

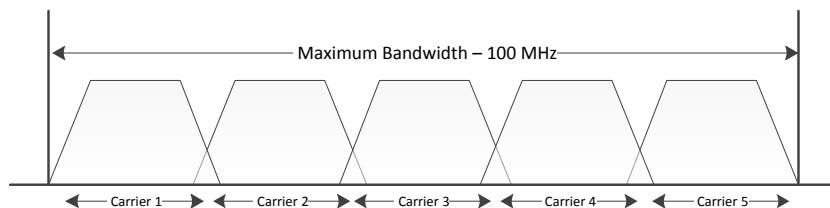


Figure 2.33: LTE-Advanced maximum bandwidth in contiguous deployment.



The aim is to achieve bandwidth aggregation of 100  $MHz$  of spectrum needed to support 1  $Gbps$  peak data rates. This solution has one huge drawback that can make its use not feasible: this requirement increases the complexity of UEs and their associated cost. According to [20], there will be a viable contiguous aggregation of two 20  $MHz$  channels. It is for this reason that Release 10 bandwidth will be limited to 40  $MHz$  for FDD.

Carrier Aggregation (CA) may be used in three different spectrum scenarios:

- Intraband Contiguous CA – This is where a contiguous bandwidth wider than 20  $MHz$  is used for CA. Because there is sufficient spectrum today to make CA high bandwidth, this becomes an unlikely scenario. Still, there is a solution to be adopted when new spectrum bands like 3.5  $GHz$  will be allocated in various parts of the world. Figure 2.34 illustrates this scenario.

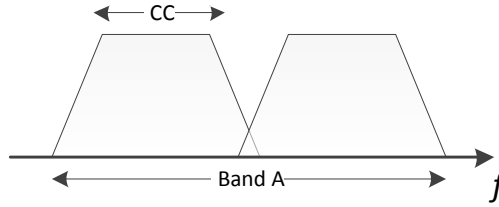


Figure 2.34: Intraband Contiguous.

- Intraband Non-Contiguous CA – In this case, the aggregation Component Carriers (CC) is made of a non-continuous bands. This type of CA can be used in countries where spectrum allocations is non-contiguous within a single-band, when the middle carriers are loaded with other users, or when network sharing is considered. This scenario is depicted in Figure 2.35.

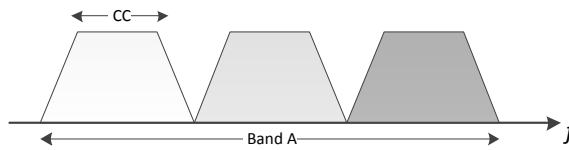


Figure 2.35: Intraband Non-Contiguous.

- Interband Non-Contiguous CA – In this situation the CC does not belong to the same band, *e.g.*, 800  $MHz$  and 2  $GHz$ . With this type of aggregation, mobility robustness can potentially be improved by exploiting different radio propagation characteristics of different bands [21]. This type of CA requires a higher level of complexity due to difficulties in meeting Radio Frequency (RF) requirements. Because of this factor, in

LTE-A the uplink is focused in the Intraband CA, while for the downlink the Interband CA and the Intraband CA are both viable solutions. Figure 2.36 presents this scenario.

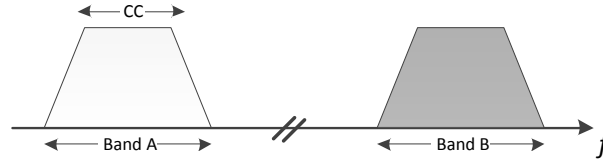


Figure 2.36: Interband Non-Contiguous.

In [22] are presented four CA deployment scenarios.

The first scenario (see Figure 2.37) is a scenario where the operator has eNBs co-located with the same level of coverage for the same zone. Although not completely contiguous bands assigned in this case the Single Carrier (SC) are separated with a little frequency separation.

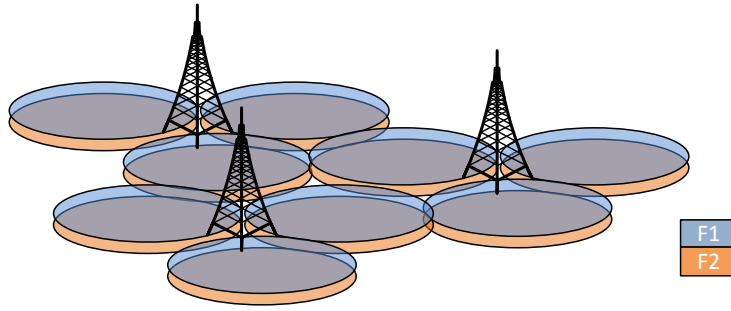


Figure 2.37: Carrier Aggregation deployment first scenario (adapted from [22]).

In the second case (see Figure 2.38) the frequencies should already belong to different bands, e.g. 800 MHz or 2 GHz and 3 GHz. In this situation, cells F1 and F2 are co-located and F1 has wider coverage. CA is used here to provide greater throughput to users who are covered by F2.

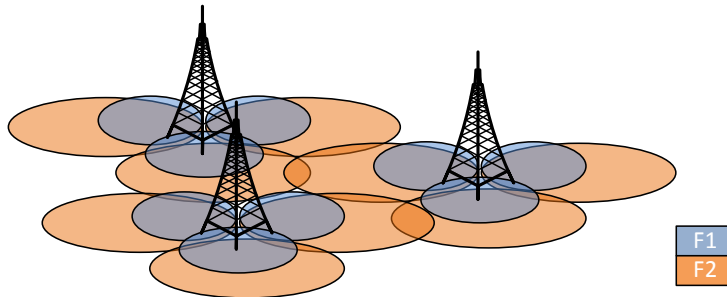


Figure 2.38: Carrier Aggregation deployment second scenario (adapted from [22]).

In the third case (see Figure 2.39), although the eNBs are co-located, these have different radiation patterns. In this situation the F2 cell aims to cover the cell edge of F1. Therefore, CA may be used for users to have a more uniform level of coverage. This scenario, like previous ones, is intended for situations where F1 and F2 are operating on different bands.

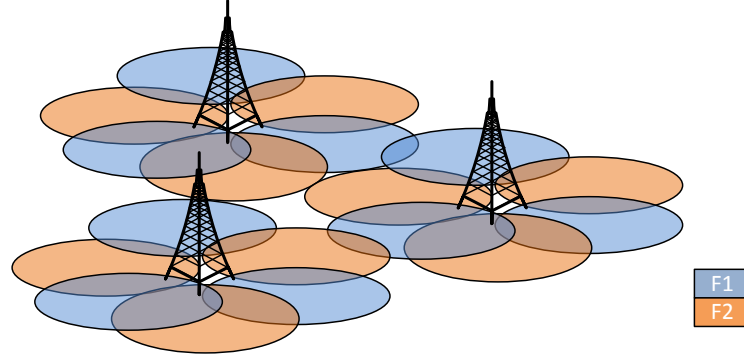


Figure 2.39: Carrier Aggregation deployment third scenario (adapted from [22]).

In the last presented scenario (see Figure 2.40), the cell F1 aims to enable coverage and F2 Remote Radio Unitss (RRUs) offers users of a given area a higher throughput, thereby giving rise to so-called hotspots. In this scenario, the F1 and F2 are also operating in different bands.

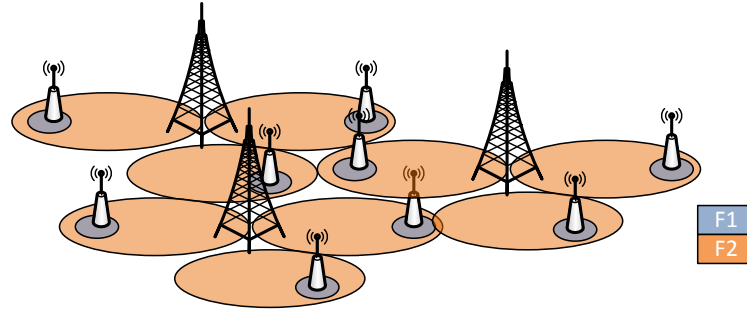


Figure 2.40: Carrier Aggregation deployment fourth scenario. (adapted from [22]).

### Enhanced Multiple Antenna Technologies

To comply with the 4G requirements, MIMO schemes have been improved. The most discussed has been the  $8 \times 8$  scheme, *i.e.*, 8 antennas used for transmit and 8 receiving antennas, are used to for the downlink, and in the uplink  $4 \times 4$ .

In Figure 2.41 a comparison is made with the number of layers used in LTE and LTE-A.

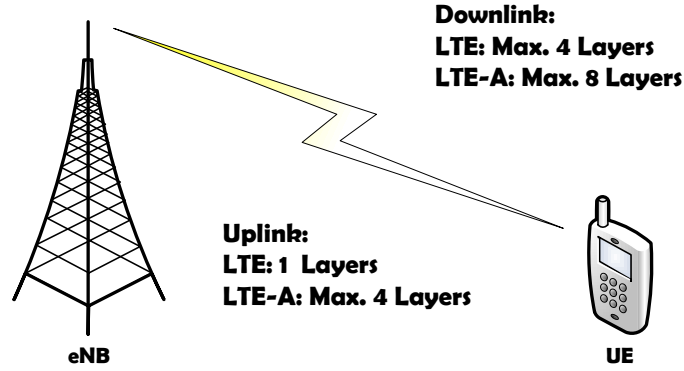


Figure 2.41: Supported transmit layers in LTE and LTE-A (adapted from [20]).

Using more antennas in the eNB makes new problems to arise:

- Increase in consumed power by the eNB;
- Radio towers with support for sets of eight antennas;
- Trade-off between the number of antennas per sector and number of sectors per cell. It may be preferable to have six sectors of four antennas instead of having three sectors with eight antennas.

Already, in the UE, are also emerging problems. In addition to the energy needed to process the data, there must exist enough space to place eight antennas, in order to exploit spatial beamforming.

## CoMP

As in [23], CoMP communications can occur in two different situations: Intra-Site or Inter-Site (see Figure 2.42).

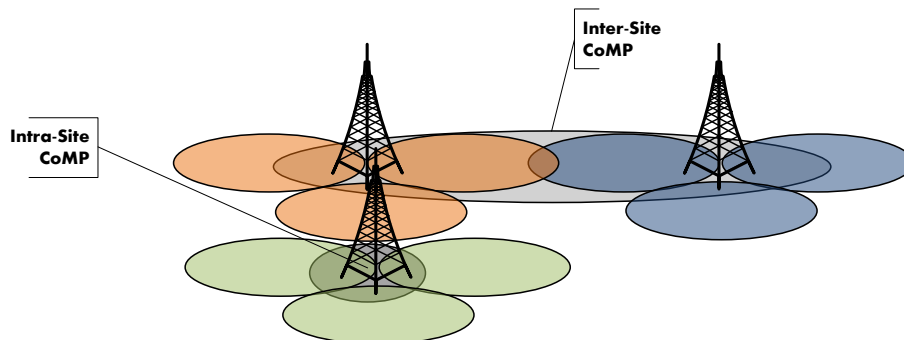


Figure 2.42: Inter-Site and Intra-Site CoMP.

Each type has advantages and disadvantages, and a comparison between different types of architectures is presented in Table 2.6.

Table 2.6: Comparison between Inter-Site and Intra-Site CoMP (adapted from [5]).

	Intra-eNB, Intra-Site	Intra-eNB, Inter-Site	Inter-eNB, Inter-Site (1)	Inter-eNB, Inter-Site (2)
Information shared between sites	Vendor Internal Interface	CQI, Scheduling Info	CQI, Scheduling Info	Traffic + CQI, Scheduling Info
Backhaul Properties	Baseband Interface over small distances provides very small latencies and ample bandwidth	Fiber-connector RRU provides small latencies and ample bandwidth	Requires small latencies only	Requires small latencies. Bandwidth dominated by traffic.

It is seen that the main advantage of Intra-Site compared to the Inter-Site configuration is that it does not require an exchange of information in the backhaul (connections between eNB), not saturating the network.

Also in [23] is presented an interesting architecture (see Figure 2.43) that despite involving only one eNB, can be considered as an Inter-Site architecture. This is because the RRUs that are associated with a particular eNB, are separated geographically, and the UE can receive signal from two distinct sources.

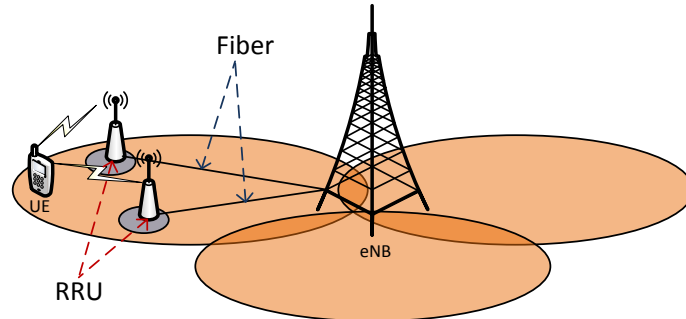


Figure 2.43: An illustration of Intra-eNB CoMP with a distributed eNB (adapted from [23]).

With regard to how the ICI will be minimized in LTE-A, there are two mechanisms in

study. According to [23], the Inter-Cell Interference Coordination (ICIC) can be classified as a Dynamic Interference Coordination (D-ICIC) or Static Interference Coordination (S-ICIC).

In the case of the D-ICIC, the eNBs are responsible for managing the reuse of frequencies, transmission powers and spatial resource (beam pattern). Thus, it is a very flexible and adaptable solution, making it possible, for example, load balancing between eNBs.

In what concerns S-ICIC, both static and semi-static spatial resource coordination among eNBs are being considered.

According to [23], the downlink CoMP has two different approaches, under consideration for LTE-A: Coordinated Scheduling (CoMP-CS) or Coordinated Beamforming (CoMP-CBF), and Joint Processing (CoMP-JP)/Joint Transmission (CoMP-JT). In the first case, the UE receives an eNB signal just as if it was not CoMP, but taking advantage of the existing cooperation between the eNBs, the UE will be served only by the eNB that presents itself in a better position to make the radio connection. Thus, it is possible to cause the desired signal level by the user and reduce the interference caused other users.

In the second case, the CoMP-JP/CoMP-JT, the UE is served by several eNBs geographically separated, thus allowing a better performance than the previous situation, because diversity gain and spatial multiplexing can be set. Nevertheless, in this case there is the disadvantage mentioned above: the exchange of information between eNBs, increase the core network traffic.

Figure 2.44 illustrates the two different approaches.

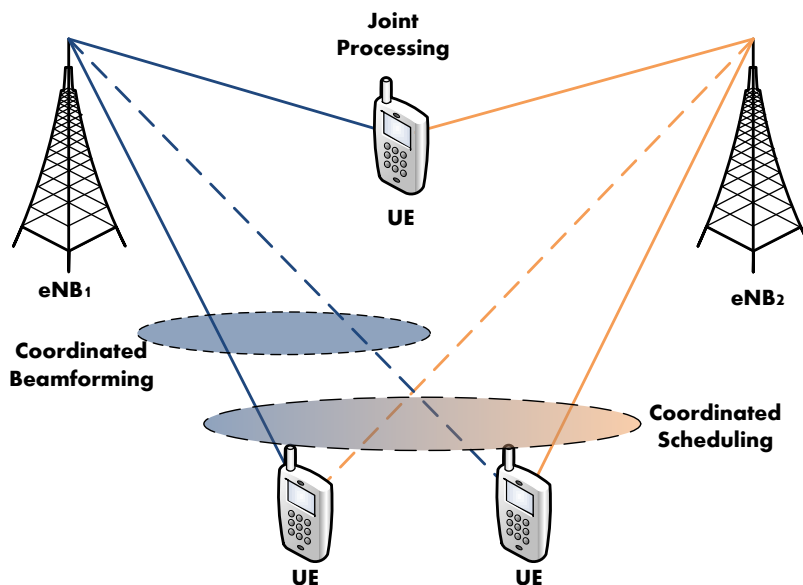


Figure 2.44: Example of CoMP in a distributed network architecture (adapted from [20]).

The possible approaches for CoMP schemes, in different scenarios, are presented in Table 2.7.

Table 2.7: Possible approaches for CoMP schemes in different scenarios (adapted from [5]).

	Intra-eNB, Intra-Site	Intra-eNB, Inter-Site	Inter-eNB, Inter-Site (1)	Inter-eNB, Inter-Site (2)
CoMP	CoMP-CS,	CoMP-CS,	CoMP-CS,	CoMP-CS,
Algorithms	CoMP-CBF,	CoMP-CBF,	CoMP-CBF	CoMP-CBF,
	CoMP-JP	CoMP-JP		CoMP-JP

In [24], are presented several scenarios for the use of CoMP for LTE-A.

In the case of CoMP-JP/CoMP-JT, there are two possibilities: Coordinated Multipoint Transmission-SU-MIMO (CoMP-SU-MIMO) and Coordinated Multipoint Transmission-MU-MIMO (CoMP-MU-MIMO). In the first case the points are for a specific UE, while in CoMP-MU-MIMO the transmission/reception is aimed at a group of UEs. These schemes are represented in Figure 2.45.

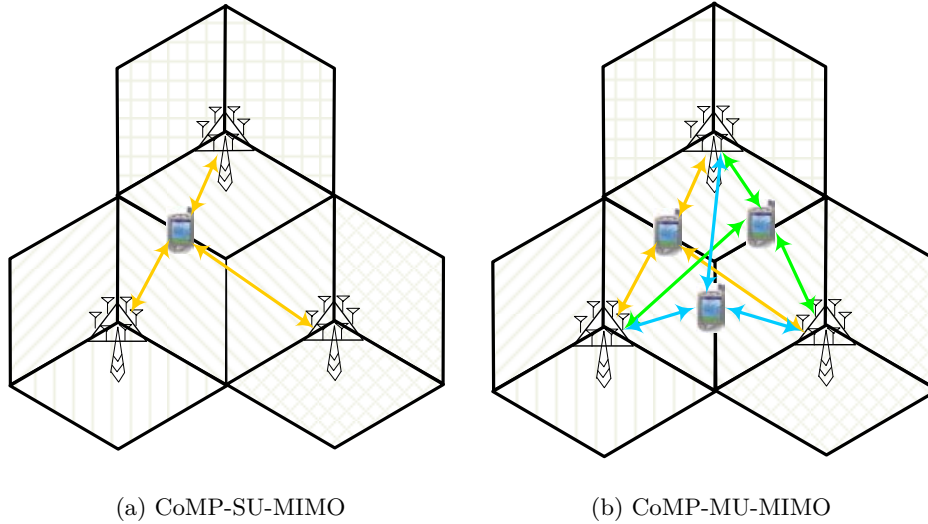


Figure 2.45: CoMP-SU-MIMO and CoMP-MU-MIMO schemes [24].

Also in [24], it is presented a system model for the downlink CoMP-MU-MIMO. Assuming that there are  $nt$  transmit antennas at each relay point and  $nr$  antennas in each UE, the cooperative  $M$  transmission points and  $M$  UEs form a  $(Mnt \times Mnr)$  virtual MIMO system. This scheme is illustrated in Figure 2.46.

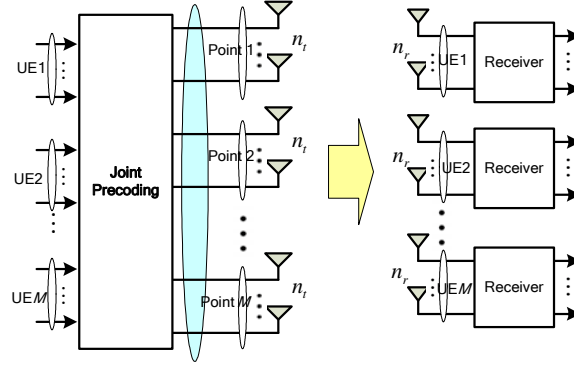


Figure 2.46: Downlink CoMP-MU-MIMO system structure [25].

As can be seen from the mentioned Figure, the information for each UE joint precoding is being sent and then shared by all UEs. These transmission points are serving at the same time and same frequency.

In the case of uplink, the system model is shown in Figure 2.47.

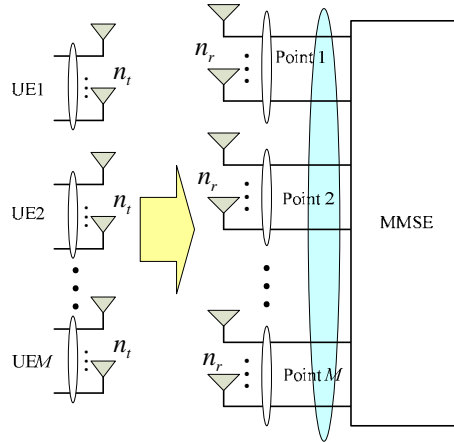


Figure 2.47: Uplink CoMP-MU-MIMO system structure [24].

In a situation of a non-cooperative planning system it may look identical to the one presented in Figure 2.48, where there is no cooperation between eNBs, thus ruling out the possibility of using the value of the factor ICIC.

The configurations for the use of CoMP-MU-MIMO can be different. In [24], are presented two settings for this type of CO-MIMO: 3-sector CoMP and 21-sector CoMP. In the first configuration, the CoMP system may have three different sites in sectors cooperation. In this case, for each cluster there are three reception points. If at each point there are two antennas and three UEs in different cells, they form a virtual  $3 \times 6$  MIMO system. The 3-sector CoMP scheme is depicted in Figure 2.49.



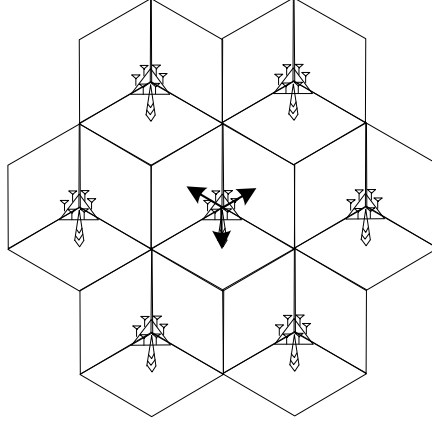


Figure 2.48: Non-cooperative system [24].

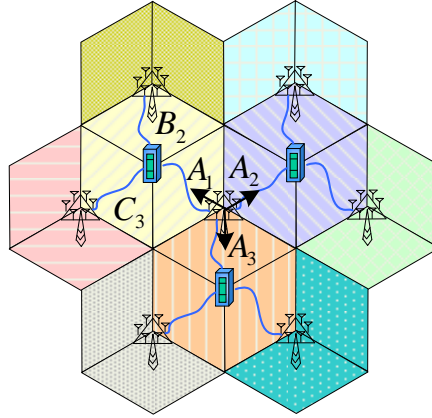


Figure 2.49: CoMP system with 3 sectors in different sites cooperation [24].

Using the A1 sector has an example, it is considered that the ICI in the sector is mainly B2 and C3, except the areas A2 and A3 due to the sector antenna direction. With this type of coordination, the three sectors in the different sites (A1, B2 and C3) can make the signal reception in a joint and coordinated way. As seen in Figure 2.49, the received signals from the UE within each CoMP reception are jointly processed with a linear Minimum Mean Square Error (MMSE) receiver.

Another presented configuration is the CoMP system with 21 sectors cooperation (21-sector CoMP), which is a much more complex setting than the one previously mentioned. In this case, there are 21 sectors in cooperation with each other, which makes it even a more efficient transmission/reception process. Figure 2.50 illustrates this scheme.

In this case, it is also important to underline the level of complexity required for the UE in relation to the required timing advance because the information must reach the receptions points at about the same time.

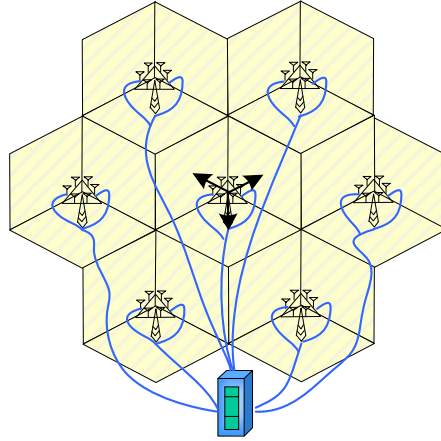


Figure 2.50: CoMP system with 21 sectors in the whole network [24].

## Relaying

Relaying is a technique to improve network performance, both in terms of coverage and user throughput. According to 2.5.3, there are three types of RSs:

- **Amplify and Forward (AF)** – This type of RS has the function to amplify the RF signal it receives and send it to the next hop. The problem with this RS type is that by amplifying the signal, noise and interference are also amplified;
- **Selective Decode and Forward (SDF)** – The second type of RS performs functions decode and forward, having more freedom to optimize the network's performance. It extracts the received data packets, processes, regenerates and delivers them to the next hop. Its processing delay is quite long;
- **Demodulation and Forward (DF)** – Another name for this type of RS is self-backhauling. In this situation, the RS acts like an eNB. It has therefore better results compared to the other two types, but it is a more expensive and complex solution.

The types of relay can be classified according to the function they perform as network nodes.

From the viewpoint of the UEs, the RSs are classified into two types:

- **Type I** – For the UE, a relay Type I, currently in standards development for LTE-A (Release 10) [26], is treated like an eNB. Thus, the RS creates its own cell, *i.e.*, transmits its own identity number, reference signals and synchronization channels. One of the requirements of LTE relay solutions, was that the RSs should be transparent for the UE.

Hence, it is ensured that the Release 8/9 terminals, may be served by relays introduced in Release 10.

- **Type II** – Using relay Type II, the UE is unable to RS, because the RS does not have its own cell id. This type of relay is still being discussed and has not been approved so far, in standardization bodies.

Figure 2.51 present the two types of RSs.

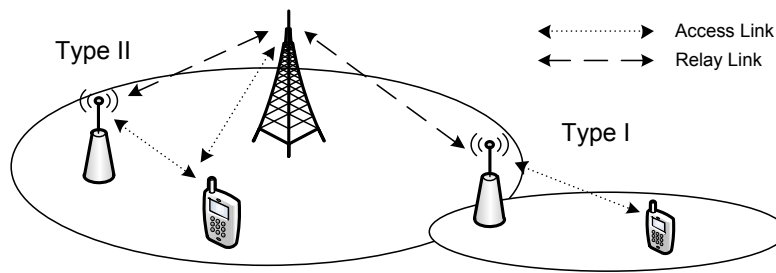


Figure 2.51: Relays types.

## Final Comments

Figure 2.52 shows the impact of the various improvements described for the peak data rate, spectral efficiency, cell edge performance, coverage, network cost and UE cost.

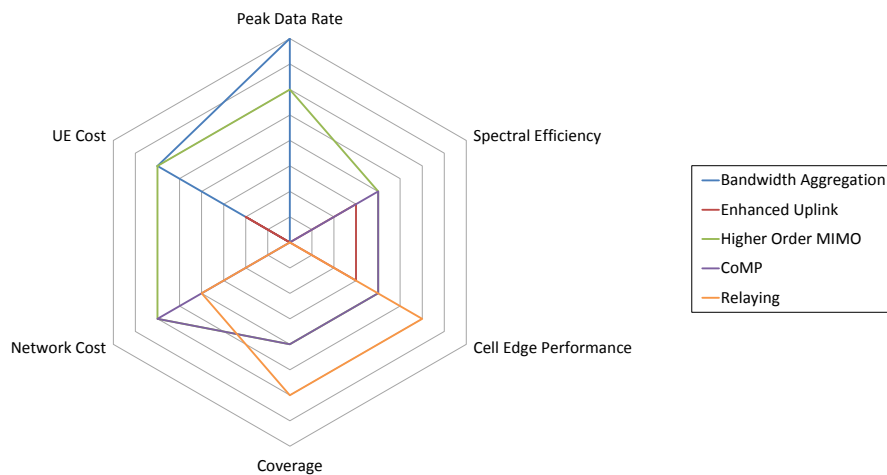


Figure 2.52: Cost/benefit evaluation of LTE-Advanced features (adapted from [20]).

Using high order MIMO schemes up to  $8 \times 8$ , it is possible increase significantly the peak data rate, spectral efficiency, cell edge performance and coverage. The disadvantage of these improvements is a greater complexity in the UE, making it the most expensive equipment.

Furthermore, using high order MIMO schemes, have impact in the network side, because it is necessary install new antennas.

Analyzing the impact of bandwidth aggregation technique, it has no impact in the core of network. With this technique, it is possible to significantly increase the peak data rate, only with greater complexity in the UEs.

The enhanced uplink does not leads to very significant improvements, with only small improvements in spectral efficiency and cell edge performance. Moreover, the requirements are also reduced, since it only requires a little more complexity in the UE.

The CoMP technique can improve spectral efficiency, the cell edge performance and coverage, with a more complex network and, therefore, with additional costs for providers.

Finally, the use of RSs also have an impact on the network side, without any gains in respect to spectral efficiency, but with better results on the cell edge performance and coverage, compared to technique CoMP.

## 2.6 CO-MIMO Channel Models

To test performance improvement of CO-MIMO, specific channel models must be used in order to simulate the radio channel.

According to [10], standardized channel models are developed for different purposes, based on which we can classify them into two types: system simulation models and calibration models. System simulation models are intended for accurate performance assessments of different algorithms and systems. They seek to represent the real-world channels as realistically as possible, with reasonable computational complexity. Calibration channel models, on the other hand, are simplified channel models developed for conformance testing of different products and technologies. Conformance testing specifies a required level of system performance when using the calibration channel model and indicates whether a tested system fulfills this requirement.

There are currently three main CO-MIMO channels models, which are [10]:

- The Spatial Channel Model (SCM) [27], which is a cellular MIMO channel model developed by the 3GPP in 2003 for the evaluation of different MIMO schemes in HSDPA systems. The SCM uses a center frequency of 2 *GHz* and a system bandwidth of 5 *MHz*.
- The WINNER II channel model [28], was developed by the IST-WINNER II project

in 2007 and represents the state of the art in wireless channel modeling. It supports a center frequency range from 2 to 6  $GHz$  and a system bandwidth up to 100  $MHz$ .

- The IEEE 802.16j channel model, which is based on the Stanford University Interim (SUI) model and was extended in 2007 to cover relay scenarios in IEEE 802.16j WiMAX systems. It supports a center frequency of 5  $GHz$  and a maximum system bandwidth of 20  $MHz$ .

The utilization of CO-MIMO introduces a new problem to simulate the radio channel: there are different types of links in a single connection. Because the eNBs, RSs, and UEs have different heights, densities, moving speeds, and transmission ranges, different links in a cooperative MIMO system can have distinct statistical properties in terms of the path loss, shadowing standard deviation, delay spread, Doppler spread, LoS probability, and so on. In other words, a high degree of link heterogeneity is expected in CO-MIMO systems [10].

According to [10], providing a pool of 13 scenarios, the WINNER II channel model is obviously the best existing channel model to use. Therefore, it is chosen for this dissertation. The WINNER II channel model is the subject of more detailed explanation in Chapter 3.



## Chapter 3

# System Model and Simulator Improvement

The present results in Chapter 4 were obtained utilizing a Link Level Simulator [29], which was adapted in order to support the existence of FRSs in the network. To calculate the impact on Type I relay usage, simulations were made for eNB-RS-UE links. In the following, the UE throughput, the UE Bit Error Rate (BER), the used CQI in two links and the performance of Hybrid Automatic Repeat Request (HARQ) mechanisms were calculated for several distances in which the RS is placed.

The simulation is based on snapshots where the UE is positioned at the cell edge, *i.e.*, considering the worst case. The RS's position ranged from 25 to 725 *m*. In Figure 3.1 is illustrated the locked position of the eNB and the UE, and the RS shifting position.

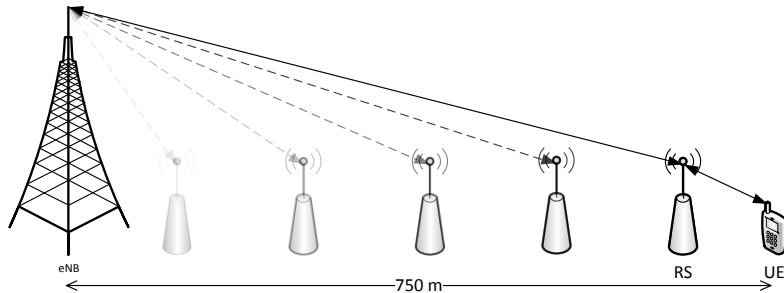


Figure 3.1: eNB's, RS's and UE's positions.

Depending on the distance, the RS may be in a LoS or in a Non-Line-of-Sight (NLoS) situation relatively to the eNB. The same happens for the RS-UE link. As can be seen in Section 4.1, it is one of the most important factors of concern about the quality's link. The

simulations consider that the RS is positioned below rooftops, as illustrated in Figure 3.2.

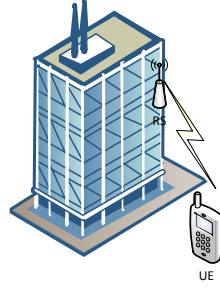


Figure 3.2: RS positioning.

In the eNB-RS link, the transmission is done with the CQI that better suits the RS SNIR, for the distance it is placed. Because a SDF RS type performance is being simulated, in the RS-UE link the used CQI value is the one that assures the highest throughput and a Block Error Rate (BLER) less than 10%, when it is possible. The matching between CQI value and modulation and Effective Code Rate (ECR) is shown in Table 3.1.

Table 3.1: Matching between CQI value and modulation and ECR [29].

CQI	Modulation	ECR
1	4QAM	0,0762
2	4QAM	0,1172
3	4QAM	0,1885
4	4QAM	0,3008
5	4QAM	0,4385
6	4QAM	0,5879
7	16QAM	0,3691
8	16QAM	0,4785
9	16QAM	0,6016
10	64QAM	0,4551
11	64QAM	0,5537
12	64QAM	0,6504
13	64QAM	0,7539
14	64QAM	0,8525
15	64QAM	0,9258



The transmission is made utilizing the TD and OL-SM MIMO modes. In the first mode, the same data is sent in different streams, and, in the second mode, different data is sent in each stream.

The simulations were implemented according to the parameters presented in Table 3.2.

Table 3.2: Simulation parameters.

<b>General</b>	
Bandwidth	20 <i>MHz</i>
Frequency	2.6 <i>GHz</i>
Cell Radius	750 <i>m</i>
Channel Model	Winner II
	Scenario B1 Los/NLoS [30]
Scheduling	Round Robin
Max. HARQ retransmissions	3
Background Noise	-174 <i>dBm/Hz</i>
Transmission Mode	TD and OL-SM
CQI	[1:15]
Height of roofs	15 <i>m</i>
Antenna Configuration	4 × 2 (eNB-RS link)
	2 × 2 (RS-UE link)
<b>eNodeB (eNB)</b>	
Height	25 <i>m</i>
Transmit Power	37 <i>dBm</i>
<b>Relay Station (RS)</b>	
Height	10 <i>m</i>
Transmit Power	30 <i>dBm</i>
Distance from eNB	[25 : 725] <i>m</i>
Types	Type I / AF and SDF
<b>User Equipment (UE)</b>	
Height	1,5 <i>m</i>
Distance from eNB	750 <i>m</i>

In order to simulate a network with an eNB, RS and UE, it has been necessary to make some improvements on the used simulator. Figure 3.3 illustrates the developed flowchart.

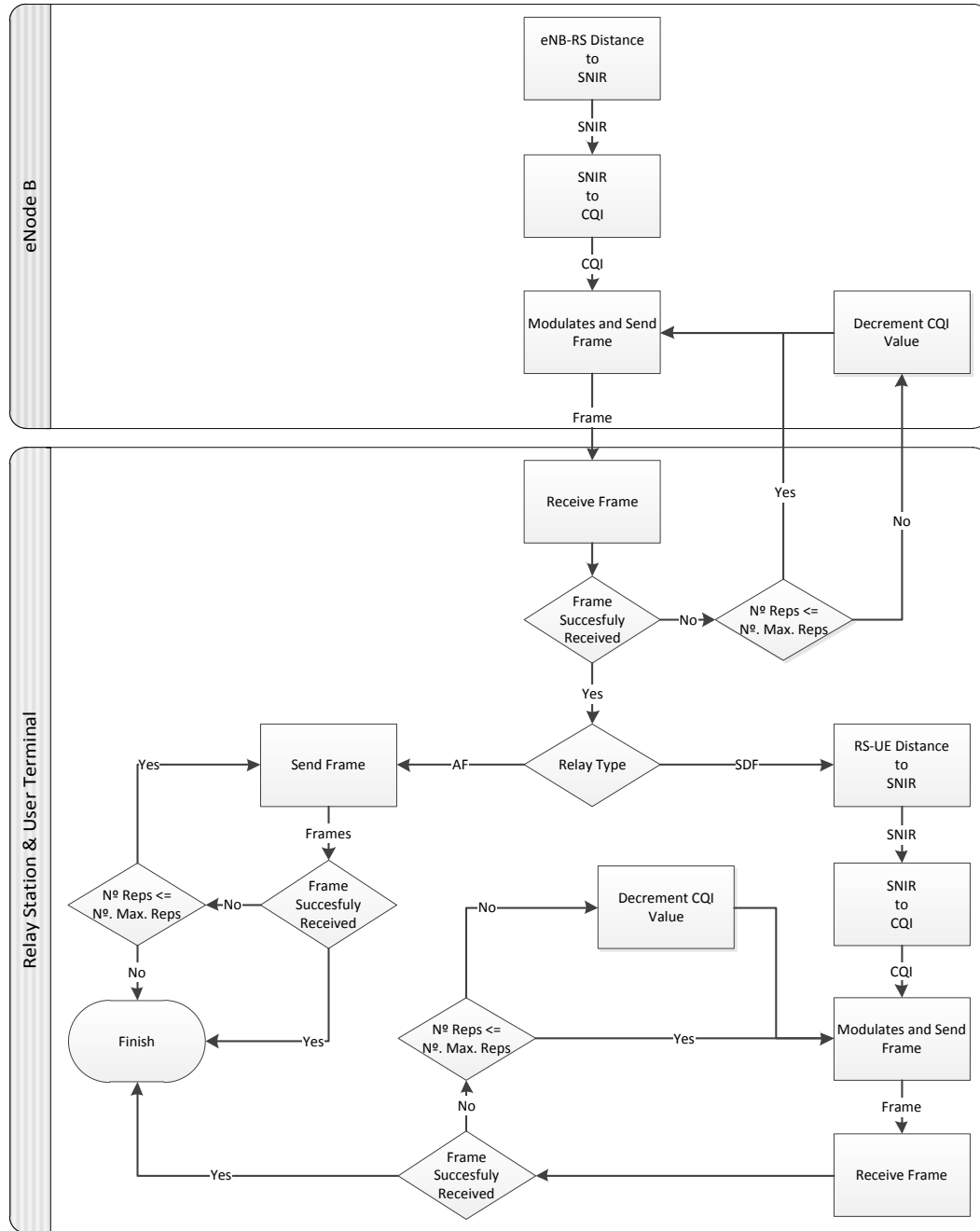


Figure 3.3: Simulation flowchart.

The used simulator calculates the UE throughput as a function of UE SNIR. So, in order to achieve the results as a function of the distance, as shown in Chapter 4, it was necessary to relate SNIR with the distance. Figure 3.4 presents a elementary scheme about the interference that the RS is subjected.

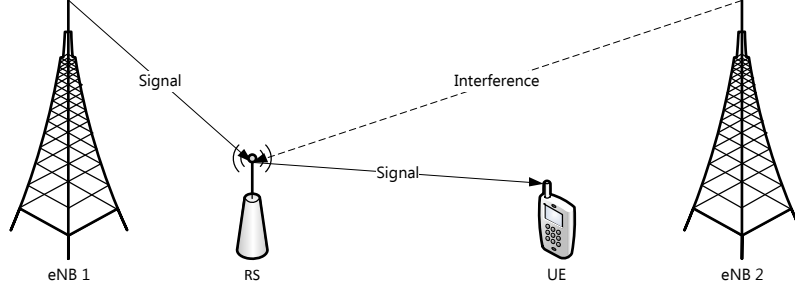


Figure 3.4: Signal and Interference for the RS.

According to [13],

$$SNIR = \frac{P(10^{\frac{PL_s}{10}})}{N_0W + \sum P_i(10^{\frac{PL_i}{10}})} \quad (3.1)$$

where  $P$  is the transmit power for the eNB or the RS, in the eNB-RS and the RS-UE links, respectively.  $PL_s$  corresponds to path-loss for the eNB-RS, RS-UE or eNB-UE links, and  $PL_i$  to path-loss for the RS six interference. Finally,  $N_0W$  is the thermal background noise (the expression is calculated in linear values).

It was used an implementation for the B1 Scenario (LoS/NLoS) using the Winner II Channel Model [30], to determine the path-loss:

- *LoS*

$$PL = 40\log_{10}(d_1) + 9.45 - 17.3\log_{10}(h'_{BS}) - 17.3\log_{10}(h'_{MS}) + 2.7\log_{10}\left(\frac{f_c}{5.0}\right) \quad (3.2)$$

- *NLoS*

$$PL = \min(PL(d_1, d_2), PL(d_2, d_1)) \quad (3.3)$$

where,

$$PL(d_k, d_l) = PL_{LOS}(d_k) + 20 - 12.5n_j + 10n_j\log_{10}(d_l) + 3\log_{10}\left(\frac{f_c}{5.0}\right) \quad (3.4)$$

and,  $n_j = \max(2.8 - 0.0024d_k, 1.84)$ ,  $PL_{LOS}$  is the path-loss of B1 LoS scenario and  $k, l \in \{1, 2\}$

Considerations:

1.  $f_c$  is the centre frequency in  $Hz$ ;

2.  $h'_{BS}$  and  $h'_{MS}$  represents the effective antenna heights at the eNB and the UE, respectively. These heights have been computed as follows:  $h'_{BS} = h_{BS} - 1.0m$ ,  $h'_{MS} = h_{MS} - 1.0m$ , where  $h_{BS}$  and  $h_{MS}$  are the actual antenna heights, and the effective environment height in urban environments is assumed to be equal to 1.0 m;
3. The NLoS path loss model for scenario B1 is dependent on two distances,  $d_1$  and  $d_2$ . As illustrated in Figure 3.5, these distances are defined according to a rectangular street grid, where the MS moves along a street perpendicular compared to the street where the BS is located.  $d_1$  is calculated by the distance from the BS to the center of the perpendicular street. In the same way,  $d_2$  is determined by the distance of the MS location in the perpendicular street to the middle point of the LoS street.

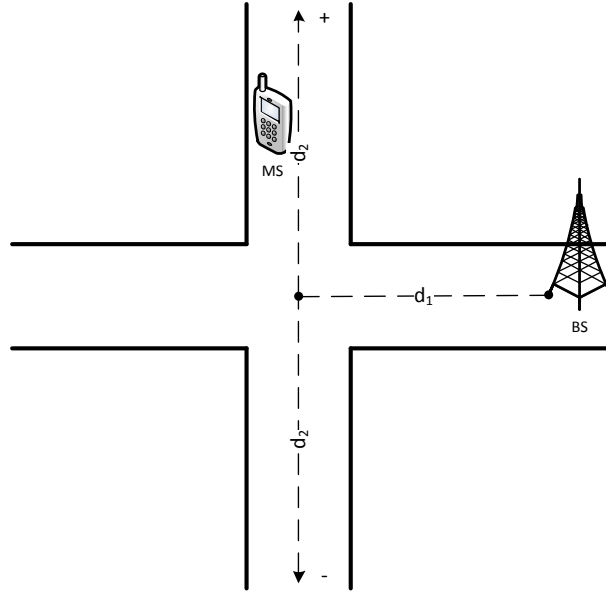


Figure 3.5: Geometry for  $d_1$  and  $d_2$  path-loss model.

As known, the transmission's quality depends heavily on the propagation conditions presented by a certain scenario. It is extremely important the transmitter's and receiver's location, whether or not in LoS situation. In the relay case, it can be strategically placed, in a position where it is in LoS with the eNB, in a way that maximizes its performance. In the following, the UE's radio conditions constantly change due to its mobility.

In order to increase simulation realism, a LoS model was implemented as it is described in [31]. The B1 scenario associated probability of LoS existence is given by (adapted from

[31]),

$$P_{LoS}(d) = \min\left(\frac{18}{d}, 1\right) \cdot [1 - P_{LoS,2}(d)] + P_{LoS,2}(d) \quad (3.5)$$

in which,

$$P_{LoS,2}(d) = \exp\left(-\frac{d(-d_0)}{L}\right) \quad (3.6)$$

is the LoS probability associated with other areas than the LoS streets.

In the following,  $d_0$  is given by,

$$d_0 = \max\left[d \cdot \frac{h_{BS} - h_{RT}}{h_{BS} - h_{MS}}, 0\right] \quad (3.7)$$

where  $d$  is the distance between the eNB and the RS, or between the RS and the UE.  $h_{BS}$ ,  $h_{RT}$  and  $h_{MS}$  corresponds to the height of the eNB, the average rooftop level and the UE, respectively.  $L$  denotes the mean unobstructed path length associated with propagation paths below the average rooftop level.

It is important to underline that the adjacent cells of the RS, have been always considered to be in NLoS situation.

After knowing the RS/UE SNIR, it was necessary to adapt the CQI value. To do this, a study was made in order to survey the throughput for CQI values ranging from 1 to 15, for a wide range of SNIR values.

The matching between the SNIR and CQI values is made in the following way: for a given SNIR value, it is chosen the CQI value with the highest throughput. The simulation will make the transmission with a range of CQI values which includes that value, plus the previous and posterior values to the CQI value with the highest throughput.

With this methodology, it is ensured that the transmission is guaranteed to be made with the better CQI value for the conditions that the radio channel presents in that moment, therefore the simulation is, thus, not restricted to a single CQI value. This technique is always utilized in the eNB-RS link, being that in the RS-UE link it is only used when the relay is a SDF type.

The used Link Level Simulator only implements a eNB to UE direct link [29]. In order to insert one RS in the BS-MS chain, it was necessary to develop a new RS module that was

added to the existing simulator.

This module works starting from the physical layer (L1) and considers two relay approaches, SDF and AF, already presented in section 2.5.3.

In what concerns AF implementation, the task was simpler when compared with the SDF approach, since it was only necessary to split the simulator way of implementation in the number of radio links connecting the different network nodes.

Regarding the SDF approach, extensive simulation work was set. A SDF relay implements CQI adaptation, in parallel with fast L1 HARQ, Transport Block (TB) segmentation and decoding/coding procedures, between the incoming and outgoing signals.

When this type of RS is utilized, the used CQI in the eNB-RS and RS-UE links may be different. Consequently, the size of the frames in the two links may also be different. Thus, it becomes necessary for the RS to have a buffering mechanism, in a way that makes it possible to do the management of the data received by the eNB that will be sent to the UE. Figure 3.6 schematizes the resource to the RS's buffer in the case where the CQI used in the eNB-RS link is lower than the used CQI in the RS-UE link.

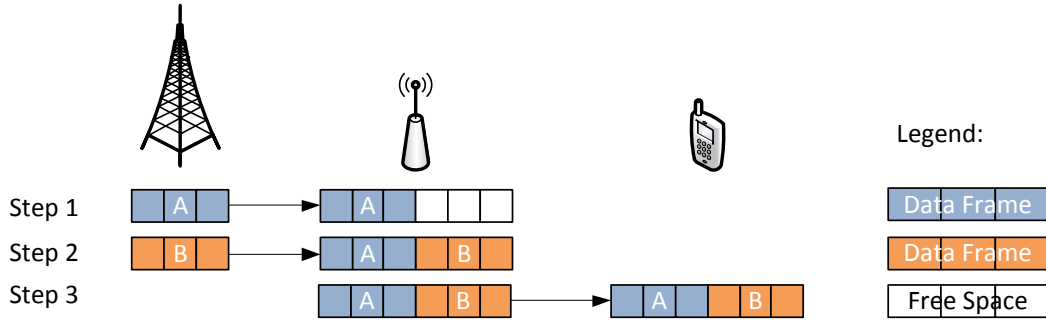


Figure 3.6: RS Buffering when the used CQI in the eNB-RS link is lower than used CQI in the RS-UE link.

The RS only sends a frame to the UE when the number of bits used is equal to the size of the frame that will be used in the RS-UE link. Hence, in the case where the used CQI in the eNB-RS link is lower than the one used in the RS-UE link, the RS utilizes its buffer to store the received frames from the eNB. When the frame which will be sent is completed, or the eNB no longer has more data to send, the frame is sent to the UE by the RS.

Figure 3.7 shows the buffer resource when the used CQI in the eNB-RS link is higher than the used CQI in the RS-UE link.

If the CQI used in the eNB-RS link is higher, the RS must split the received data. Therefore, knowing the amount of data received by the RS and the CQI which will be used

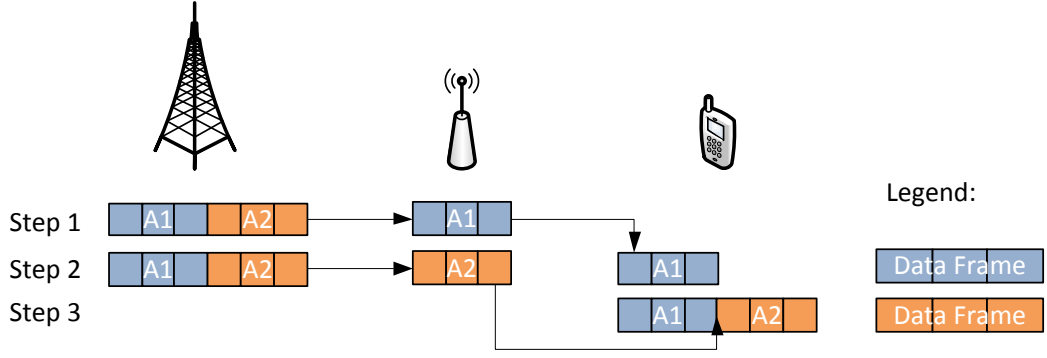


Figure 3.7: RS Buffering when used CQI in the eNB-RS link is higher than used CQI in the RS-UE link.

in the RS-RS link, the number of necessary frames to send the received data from the eNB to the UE is calculated. In this scenario, the RS receives the frame sent by the eNB, splits it in many smaller frames and sends all frames to the UE. It is only after sending all the data that composes the frame sent by the eNB, that the RS receives new data.

The last case is illustrated in Figure 3.8.

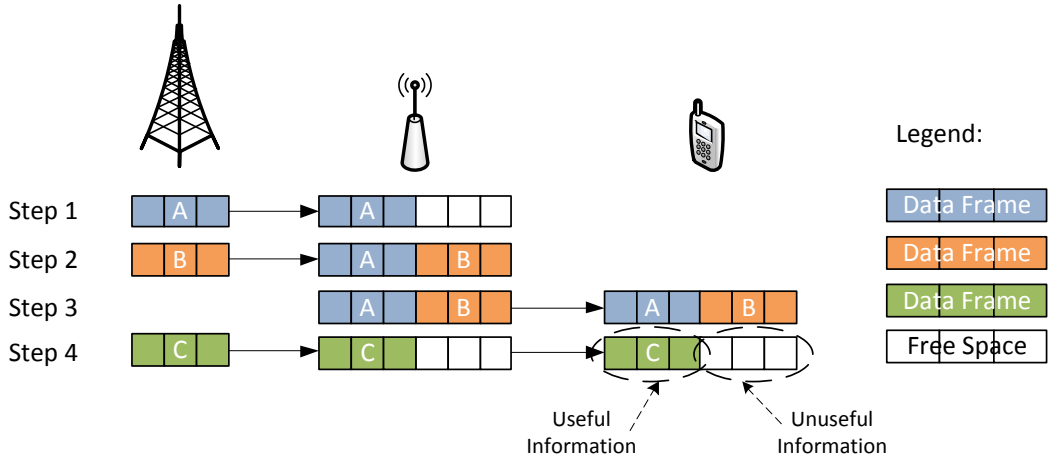


Figure 3.8: RS Buffering when the eNB has no more information for the UE.

One can see that, unlike the scenario in previous figures, the RS forwards the data to the UE even if the buffer is not full. This occurs when the eNB has no more information for the UE. As it will be possible to see, this phenomenon affects the UE throughput. Despite of the frame sent to the UE having the same length of the previous frames, the useful information percentage is less or equal than in these frames. Consequently, the useful throughput is lower.

Finally, the HARQ mechanism is utilized when a frame is not successfully received. If a frame is not correctly received by the RS, it will be sent repeatedly until a maximum of 3

retransmissions occurs. If, after these retransmissions, the frame is not correctly received, it is used a lower CQI value, ensuring that all the data sent by the eNB is well received by the RS. Thus, it is ensured that in the eNB-RS link there is not data loss. Interestingly, in the UE, it may happen that even with the HARQ mechanism and with lower CQI values, the data is not totally received, affecting the values of BER and throughput.



## Chapter 4

# Simulation Results

### 4.1 LoS Probability

The transmission's quality depends heavily on the radio propagation conditions. The SNIR value is directly related to the fact that the receiver is in LoS or NLoS with the transmitter. Hence, the RS positioning is one of the most important issues in the eNB-RS and the RS-UE links quality. The RS positioning can be separated in two features: the eNB-RS distance and the height that the RS is placed.

This section shows the effect of the RS's height and the distance that separates it from the eNB, in the probability of the RS and the UE being in a LoS situation with the eNB and the RS, respectively.

The height of RS follows two approaches: either the RS is located some meters above the roof-top (see Figure 4.1) or it is placed some meters below the roof-top (see Figure 4.2). As described in Table 3.2, the RS's height is 10 *m* and the roof-top height is 15 *m*. Thus, the simulation scenario is equivalent to the one presented in Figure 4.2.

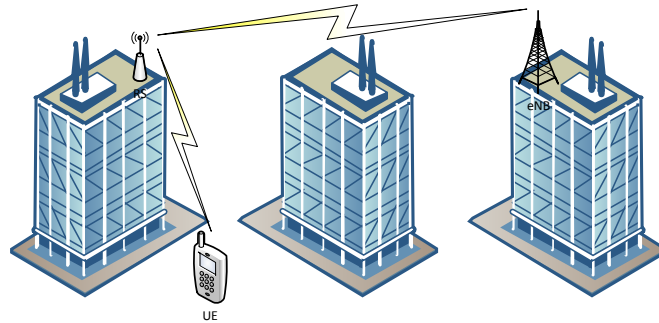


Figure 4.1: eNB and RS in LoS situation.

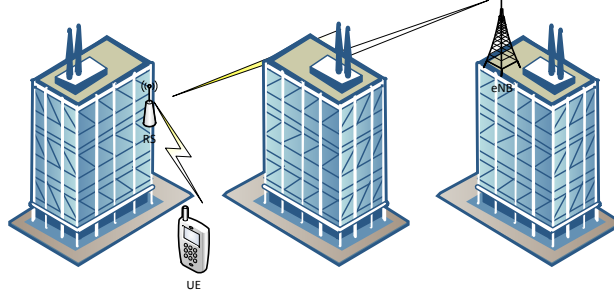


Figure 4.2: eNB and RS in NLoS situation.

Figure 4.3 shows the probability of the RS being in LoS situation with the eNB, for RS's heights ranging from 5 m to 15 m, and for eNB-RS distance values ranging from 25 m to 725 m.

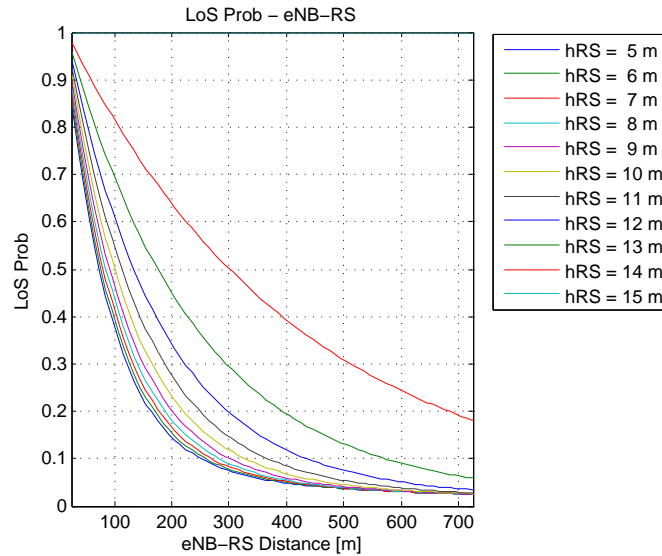


Figure 4.3: LoS Probability for the eNB-RS link.

For a RS's height equal to 15 m, the LoS probability is 100%, since there are no obstacles of greater height between each other. Therefore, for this height, the LoS probability is independent of the eNB-RS distance. This situation corresponds to illustrated scenario in Figure 4.1.

Analyzing the RS's heights lower than the roof-top, the LoS probability is dependent on the eNB-RS distance and the RS's height. As it can be seen, the lower the RS's height, the minor the LoS probability for the eNB-RS link. This is justified by an increase of the obstacles number between the eNB and the RS. The same behavior occurs if the eNB-RS distance is increased. Analyzing the Figure 4.3, it is demonstrated that a greater distance between the RS and the eNB decreases the probability of these being in a LoS situation.

From Figure 4.3, one can also see that for any RS's height less than the height of roof-top, for an eNB-RS distance of one half of the cell's radius, the LoS probability is at most 40%. By examining RS's height just less than 2 m from the height of roof-tops, this probability is between 5% and 20%. For the considered scenario, the probability of the RS being in LoS with the eNB is 50% since they are separated from 100 m, and for eNB-RS distance of one half of the cell's radius it is approximately 5%.

Figure 4.4 represents the LoS probability concerning the RS-UE link.

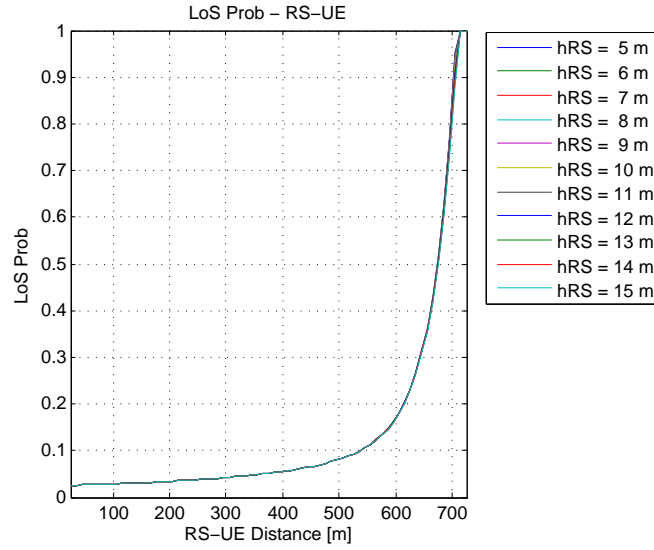


Figure 4.4: LoS Probability for the RS-UE link.

Unlike the previous analysis, the probability of the UE being in a LoS situation with the RS is almost independent of the height of RS. Observing the behavior of the curves in the Figure 4.4, is seen that when the RS moves away from the eNB, the RS-UE LoS probability increases. This is due to the fact that the RS-UE distance decreases. Nevertheless, this probability is only 50% when the RS and the UE are separated approximately 100m.

To understand the impact that the RS's height has on the RS-UE LoS probability, Figure 4.5 presents a scenario equivalent to the one in Figure 4.2, *i.e.*, the RS's height is greater than the height of the roof-top.

In this case, the LoS probability varies with the height of the RS, it is concluded that this dependence is not as significant as in the eNB-RS link. This alteration is related to the changes of the heights in the eNB-RS and the RS-UE links. In one hand, in the eNB-RS link, the heights are not much lower than the roof-tops' heights. On the other hand, in the RS-UE both elements have an height inferior to the roof-top height, being the UE's height a much lower one.

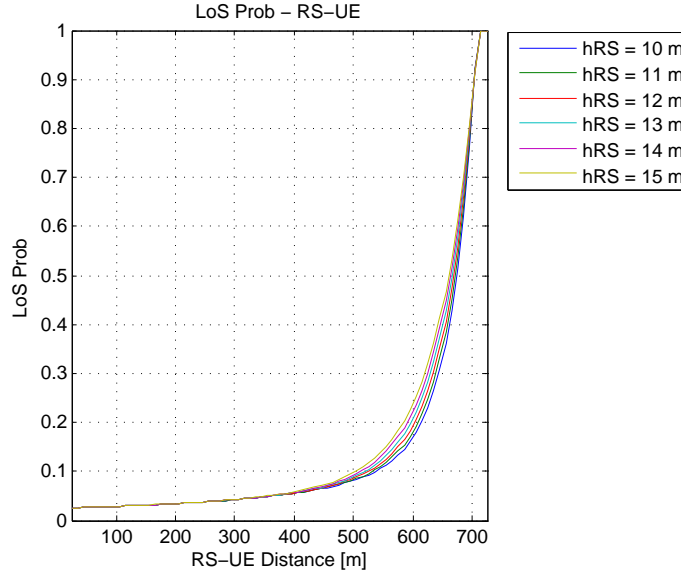


Figure 4.5: LoS Probability for RS-UE link with  $h_{RS}=10$  m.

## 4.2 SNIR vs eNB-RS Distance

In this section, a research of SNIR is performed taking into account that the RS and the UE are in LoS situation with the eNB and the RS, respectively.

In the following, the SNIR depends mostly on two factors: the distance between the transmitter and the receiver and also if they are either in a LoS or in a NLoS situation.

To understand in what way the SNIR of the eNB-RS link is dependent on the eNB-RS distance, in Figure 4.6 is illustrated the SNIR value as a function of eNB-RS distance, in which these two elements are in a LoS and in a NLoS situation.

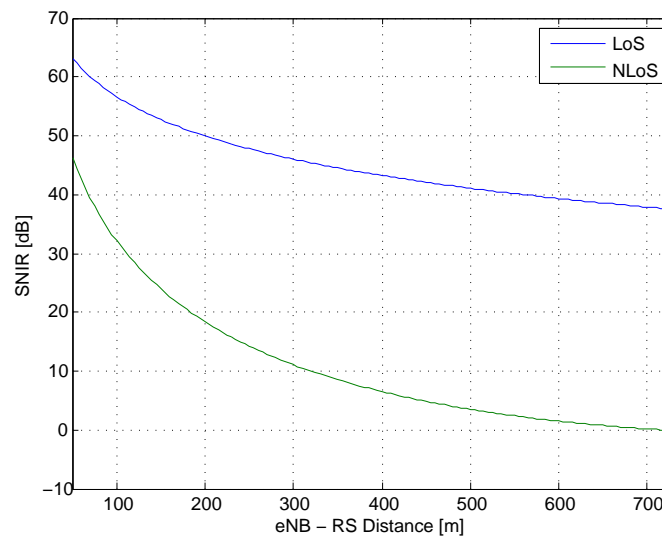


Figure 4.6: RS SNIR in LoS and NLoS situation.

The first conclusion obtained is that the greater the eNB-RS distance, the lower the RS SNIR. This behavior is due to two factors resulting from an increase of the eNB-RS distance: the received power in the RS decreases and the interference power level of adjacent cells, which the RS is subjected, increases. Figure 4.7 illustrates this situation, being  $PL$  and  $PL_i$  the path-loss for the eNB-RS link and path-loss of the six interference RSs, respectively.

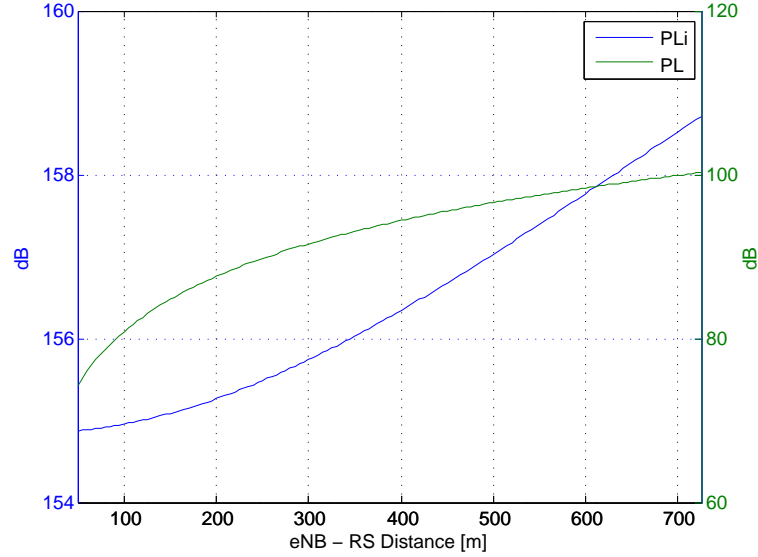


Figure 4.7: RS path-loss and path-loss for RS interference cells.

As can be seen, the path-loss for the eNB-RS link increases as the distance between each other increases. The same happens for the path-loss of the six interference RSs, because the RS is placed towards the cell edge and it is, therefore, more subjected to unwanted higher power levels.

From Figure 4.7 it is also possible to conclude that the eNB-RS path-loss link suffers a greater attenuation than the path loss relating to the interfering cells. On one hand, the eNB-RS link path-loss oscillates about 25 dB, and on the other hand the path-loss of interfering cells varies only about approximately 4 dB. This happens because it was considered that all neighboring cells were in a NLoS situation with the RS. Consequently, the value of SNIR depends much more on the path-loss concerning the eNB-RS link, than on the adjacent cells interference path-loss.

Another conclusion that can be drawn from Figure 4.6 is that in a NLoS situation, the SNIR decline is much higher than in a LoS situation. While in a LoS situation the SNIR value ranges from about 60 dB to 40 dB, in a NLoS situation the dynamic range is higher: from 60 dB to 0 dB.

In order to increase the simulation realism, a LoS Probability Model is used to calculate the SNIR value, since this is an issue that greatly affects the value of this relation. In Figure 4.8 is represented the SNIR as a function of eNB-RS distance, considering the LoS Probability Model for each simulated distance.

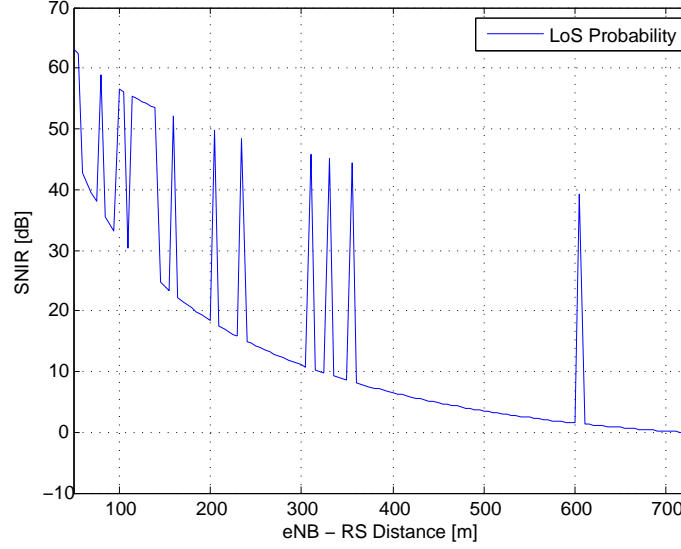


Figure 4.8: RS SNIR with LoS Probability Model.

As expected, the SNIR curve is directly related to the two curves in Figure 4.6, LoS and NLoS. For each value of eNB-RS distance, the SNIR value is calculated taking into account if the RS is in a LoS or in a NLoS situation with the eNB. It is possible to see that, for smaller eNB-RS distances there are more vicissitudes in the SNIR value. For distances greater than half of the cell's radius there are not many oscillations, given that the LoS probability of the eNB-RS is very low, causing the SNIR value to be almost always calculated considering a NLoS situation.

Regarding the UE SNIR, the analysis is similar to the previous one. The UE SNIR as a function of eNB-RS distance is shown in Figure 4.9, in the case of the UE being in a LoS and in a NLoS situation relatively to the RS.

The previous analysis regarding the difference in LoS and NLoS situations is also reasonable for the RS-UE link. The change is that, in this circumstance, the greater the eNB-RS distance, the higher UE SNIR, because the RS is closer to the UE so that the signal strength is higher.

If the LoS Probability Model is considered, the SNIR variation is once again related to the curves of Figure 4.9. The UE SNIR considering the LoS Probability Model is presented in Figure 4.10.

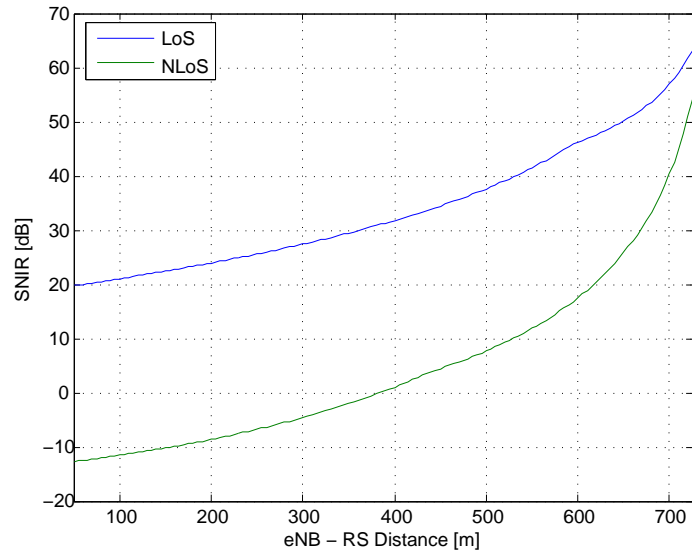


Figure 4.9: UE SNIR in LoS and NLoS situation.

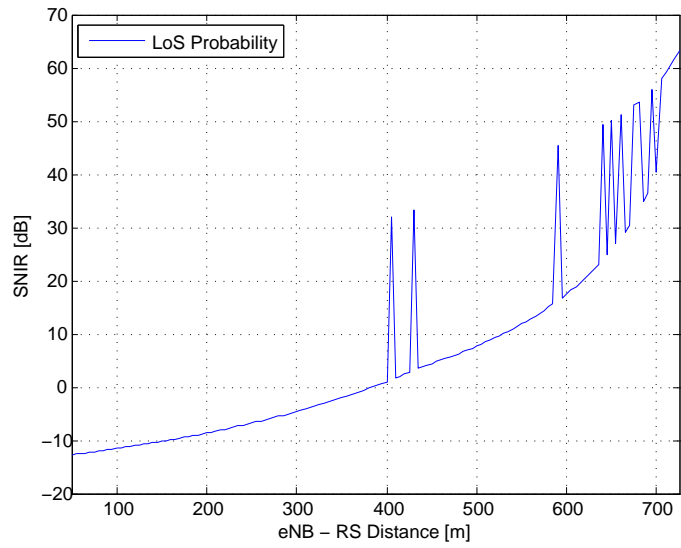


Figure 4.10: UE SNIR with LoS Probability Model.

In this instance, the largest number of SNIR oscillations occurs when the RS is farthest from the eNB. Here, the RS is closer to the UE, making the probability of being in LoS greater, thereby increasing the SNIR value.

In Figure 4.11, the RS-UE link path-loss and the UE path-loss concerning to the neighboring cells are presented.

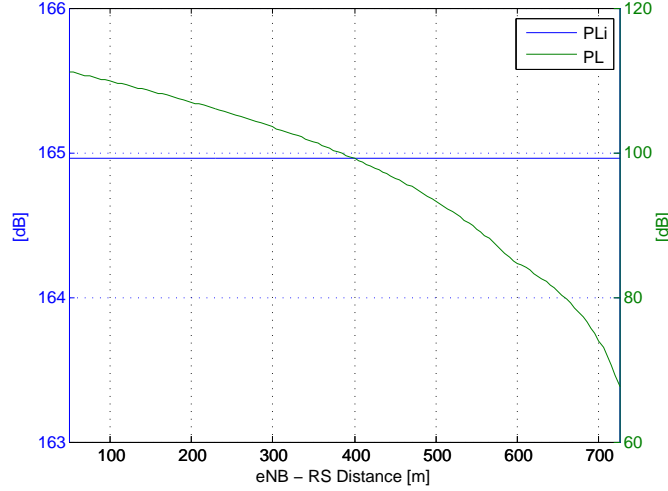


Figure 4.11: UE path-loss and path-loss for UE interference cells.

On one hand, as the simulation is constructed on snapshots where the UE is always positioned at 750 m from the eNB, the level of interference that it is subjected relatively to adjacent cells is constant, not depending on the RS's position. On the other hand, the RS-UE path-loss decreases as the RS moves away from the eNB, since it approaches the UE.

Figure 4.12 evaluates the eNB-RS and RS-UE link path-loss.

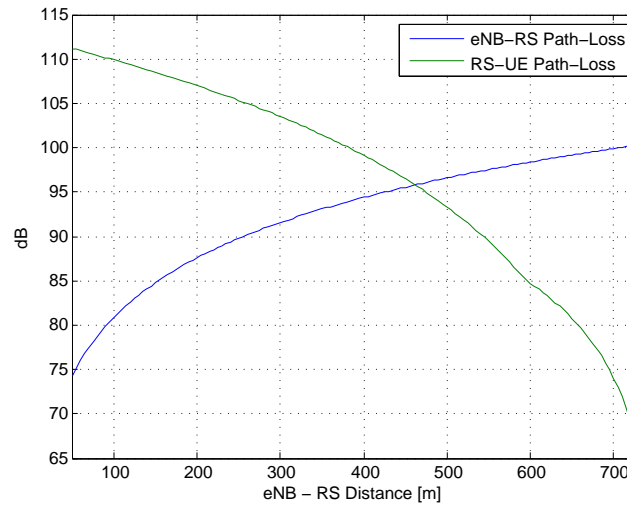


Figure 4.12: eNB-RS and RS-UE path-Loss.



### 4.3 Throughput Performance in the TD and OL-SM MIMO Modes

One of the main advantages of LTE, in comparison with previous technologies, is adapting the transmission according to the radio channel quality. Within this process, an adaptation of the used modulation and channel coding is made, according with the SNIR value received by the RS and eNB, and being sent by the UE and RS, respectively.

In this section it is underlined the importance that the correct CQI utilization has for a determined value of SNIR. In order to understand the CQI performance as a function of SNIR, a eNB-RS link was simulated for SNIR values ranging from  $-30$  dB to  $40$  dB. In the following, the throughput for each value was calculated. The simulation was made for the TD and OL-SM MIMO modes, with the objective of understanding the difference between the two modes.

Figure 4.13 presents the throughput in the eNB-RS link for TD mode, as a function of SNIR.

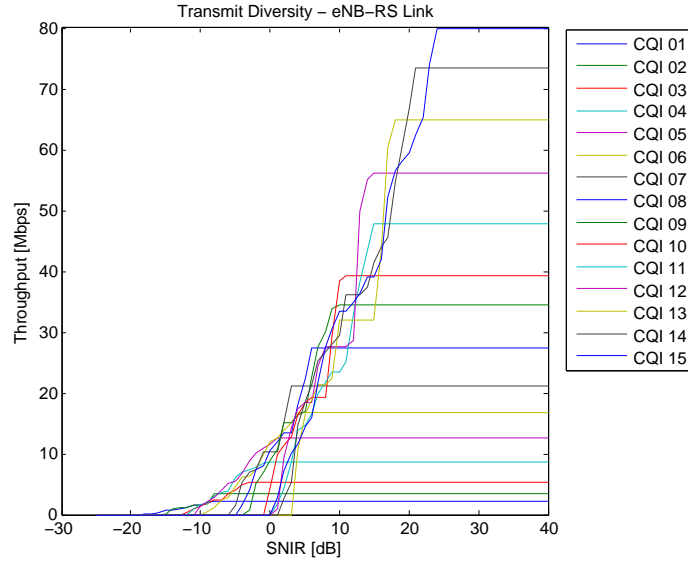


Figure 4.13: Throughput for the eNB-RS radio link in TD mode.

It is shown that higher order modulations, *i.e.*, with higher CQI values, only should be used for high values of SNIR, allowing a successful transmission. In fact, as the modulation order becomes higher, so does the necessary SNIR. It is possible to check that the utilization of a higher order modulation is not synonymous to a higher level of throughput, whatever the SNIR. This situation occurs since higher order modulation usage at low SNIR experiences

transmission errors, increasing retransmissions for a given CQI.

Figure 4.14 presents the previous scenario but using the OL-SM mode. As it was already mentioned, the OL-SM mode allows to obtain values of throughput which is not possible in the TD mode.

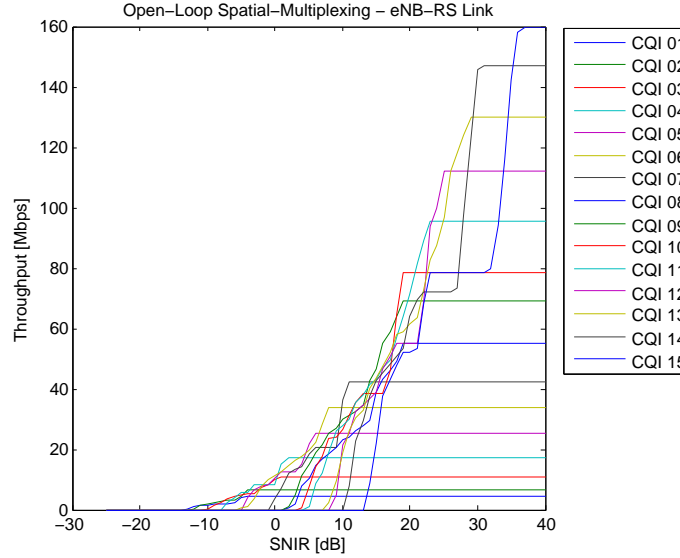


Figure 4.14: Throughput for the eNB-RS radio link in OL-SM mode.

Comparing Figures 4.13 and 4.14, a displacement to the right can be seen in the CQI curves, for the same SNIR values. In other words, the same performance is displaced to higher values of SNIR. So, in the TD mode it is possible to use modulation of a higher order comparing with OL-SM, for the same values of SNIR.

Observing the maximum throughput value obtained in each CQI, it is easily noticed that the OL-SM MIMO mode throughput is almost the double when compared with the TD mode.

The issue is even more deeply discussed if the number of used retransmissions, for the two modes in each CQI and for different values of SNIR, is also analysed.

In Figures 4.15 and 4.16 are illustrated the number of retransmissions used in the TD and OL-SM modes, respectively.

Analyzing Figures 4.15 and 4.16, it is also possible to notice what was described in Section 2.4.4: for the same value of SNIR, the TD MIMO mode needs less retransmissions than in the OL-SM. TD mode should be used when the receiver does not have very high SNIR values. On the other hand, the OL-SM mode is designed for the situations where the propagation's conditions are very good and with low interference. Only in these conditions the OL-SM mode is fully explored.

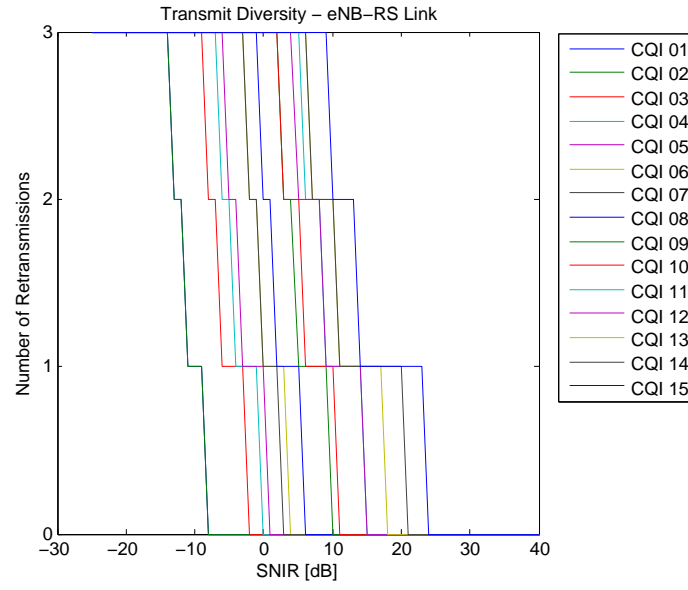


Figure 4.15: Number of retransmissions for the eNB-RS link in TD mode.

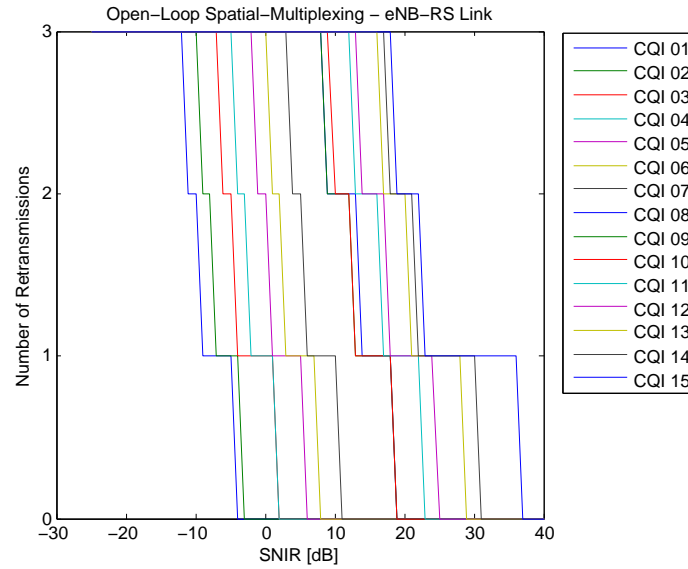


Figure 4.16: Number of retransmissions for the eNB-RS link in OL-SM mode.

Thus, the TD mode should be used, for example, on the cell edge where the SNIR values are lower. On the other hand, OL-SM mode should be utilized near the eNB or in indoor hotspots, where high values of SNIR are guaranteed.

#### 4.4 Performance of AF and SDF Relay Station Types

As explained in Section 2.5.3, in contrast of the SDF RS type, the AF RS type does not have the ability to demodulate and modulate the received data. This technical difference implies that the used CQI in the eNB-RS and the RS-UE links is the same. On the other side, when a SDF RS type is used, the data will be modulated again, in order to adapt the transmission to the radio channel propagation conditions.

In order to compare the performance of these two RSs, several indicators of the transmission's quality were analyzed such as: the used CQI in the eNB-RS and the RS-UE links, the UE BER, the number of retransmitted frames in the RS-UE link and the UE throughput.

Because the RS performance is heavily dependent of the scenario conditions, the comparison between these two RSs types is based on two scenarios with different characteristics. In the first scenario (see Figure 4.17) the RS is in a LoS situation with the eNB at 25 m eNB-RS distance. In the second scenario (see Figure 4.18), the RS is in a LoS situation with eNB at 25 m eNB-RS distance, and the RS and the UE are in LoS situation with the eNB and the RS, respectively, at 325 m eNB-RS distance. For the others snapshots, these elements are in a NLoS situation between each other.

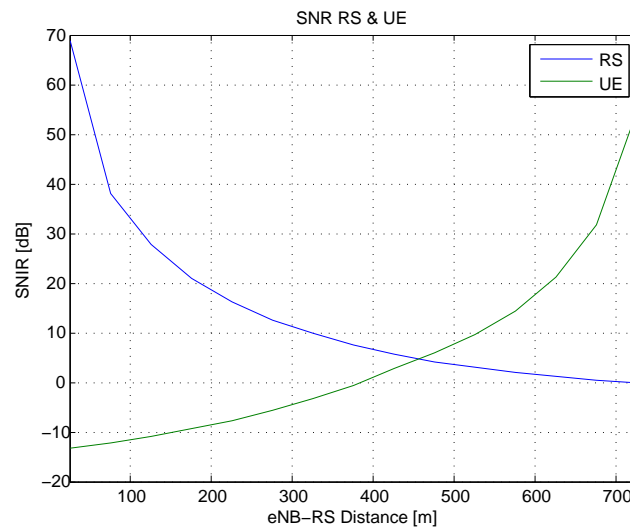


Figure 4.17: RS and UE SNIR in the first scenario.

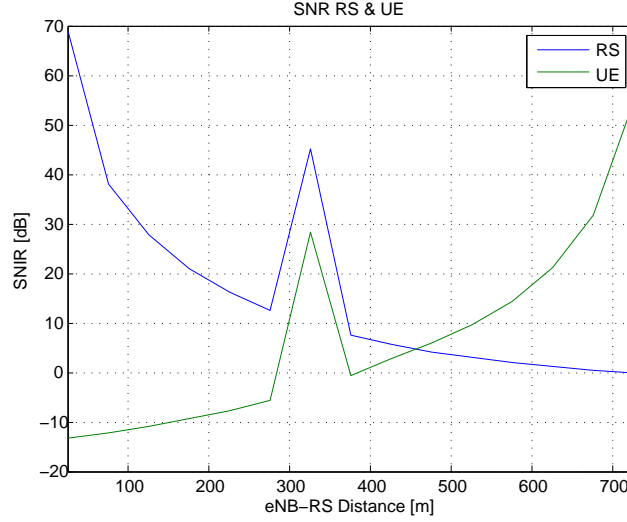


Figure 4.18: RS and UE SNIR in the second scenario.

From Figure 4.17 and Figure 4.18, one can see that the RS SNIR and the UE SNIR have increased approximately 30 dB, in the snapshot which corresponds to the LoS situation.

Figure 4.19 and Figure 4.20 present the used CQI by the RS and the UE when an AF RS type is used, in the first and second scenarios, respectively.

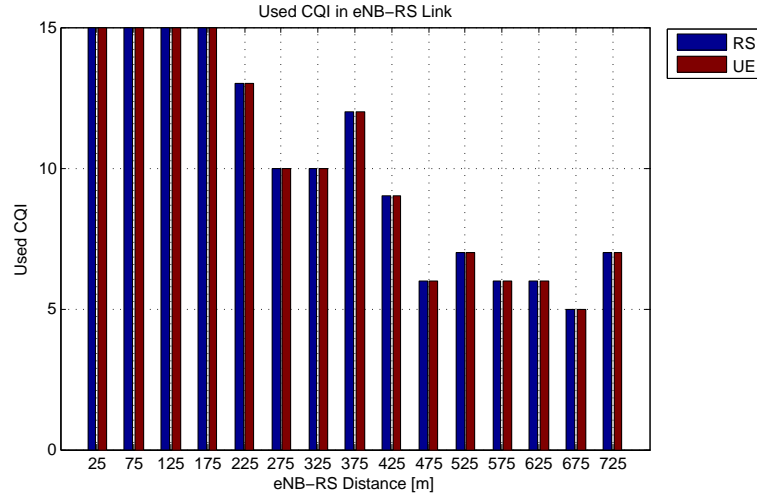


Figure 4.19: Used CQI for AF RS type in the first scenario.

It is seen that the used CQI by the RS and the UE is the same, due to the utilization of an AF RS type. From these Figures, one can also see that as the eNB-RS distance increases, the value of the used CQI decreases, because the RS SNIR also decreases, forcing the adoption of a lower order modulation. Despite of the UE SNIR increase, the used CQI by the RS is the same, by virtue of the UE SNIR not being considered.

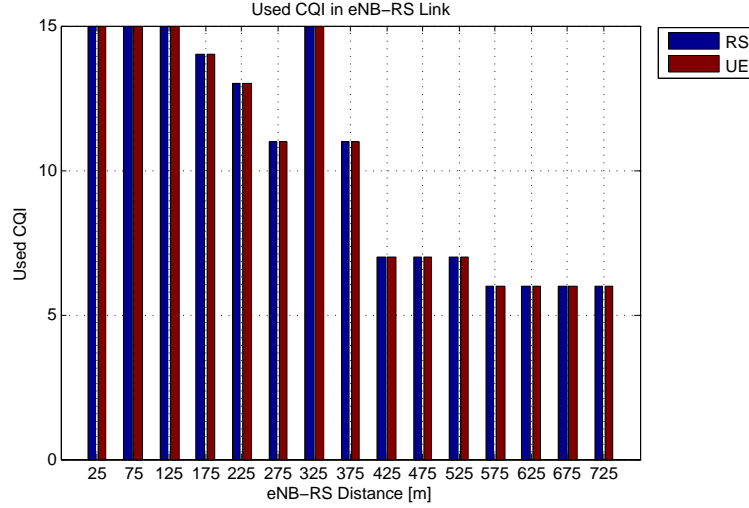


Figure 4.20: Used CQI for AF RS type in the second scenario.

The difference between the two scenarios is that, in the second scenario the RS SNIR at 325 m eNB-RS distance is enough to use a CQI value of 15. As it will be shown, the use of this value has repercussions in the UE BER, the number of retransmitted frames and in the UE throughput.

Similarly to Figures 4.19 and 4.20, in Figures 4.21 and 4.22 is presented the used CQI by the RS and the UE, when a SDF RS type is utilized in the first and second scenarios, respectively.

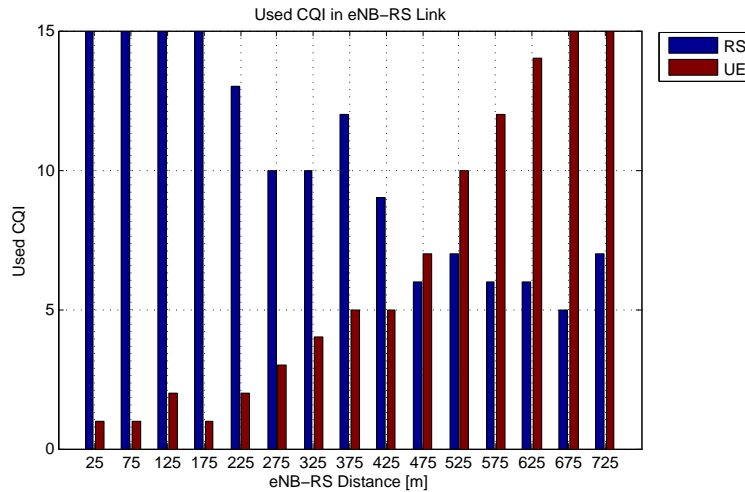


Figure 4.21: Used CQI for SDF RS type in the first scenario.

Due to the CQI value being adapted in the eNB-RS link, independently of the RS type, the used CQI in the eNB-RS link is exactly the same to the one used in the AF RS type simulation. One can see that, unlike to the scenario in Figures 4.20 and 4.19, the used CQI

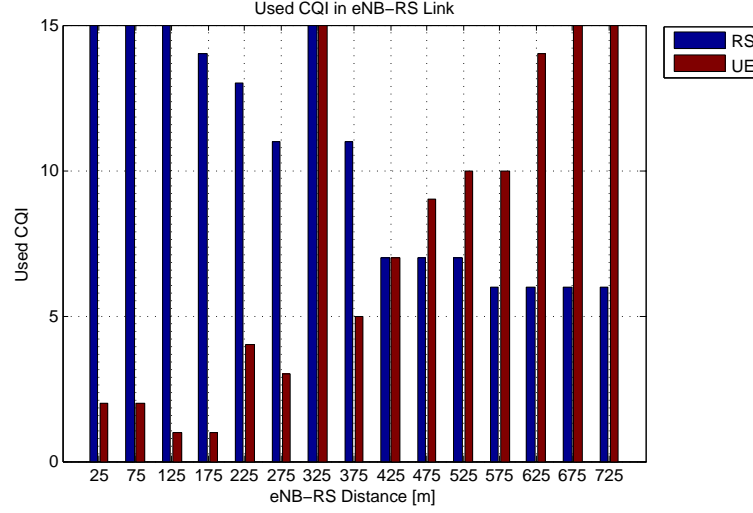


Figure 4.22: Used CQI for SDF RS type in the second scenario.

in the RS-UE link is the one that maximizes the UE throughput. It is possible to observe that as the eNB-RS distance increases, the used CQI by the UE gets higher. This increase is due to the proximity between the RS and the UE, resulting in a higher UE SNIR and, consequently, allowing higher order modulations.

Comparing the two scenarios, due to the fact that the RS and the UE are in LoS situation with the eNB and the RS, respectively, the SNIR is enough for the use of a CQI value equal to 15. It is seen that the used CQI by the UE suffers a considerable increase: in the first scenario the used CQI was 4 and, in the first scenario, it was 15. It is advisable to remember that in this snapshot, the UE SNIR increases approximately 30 dB.

One of the consequences of the CQI adaptation is the decrease of the BER. Therefore, the chosen CQI value will be the one that ensures the highest data rates and an UE BLER lower than 10%, whenever it is possible. Figures 4.23 and 4.24 present the UE BER in a case where an AF and SDF RS is used, in the first and second scenarios, respectively.

In both scenarios, the UE BER, when a SDF RS type is utilized, is always lower than the BER when an AF RS type is used. The SDF RS type does not always ensure an UE BER equal to zero, but it safeguards a much lower error data rate than the AF RS type.

From Figure 4.23, one can also see that for short eNB-RS distances, *i.e.*, long RS-UE distances, the error data rate is lower using a SDF RS type, for the reason that the UE SNIR decrease is balanced with a suitable CQI value to the radio propagation conditions. Nevertheless, for larger eNB-RS distances, *i.e.*, the RS is closer to the UE, the UE BER tends to be equal for the two RSs types. In addition, the AF RS type may also achieve a null error

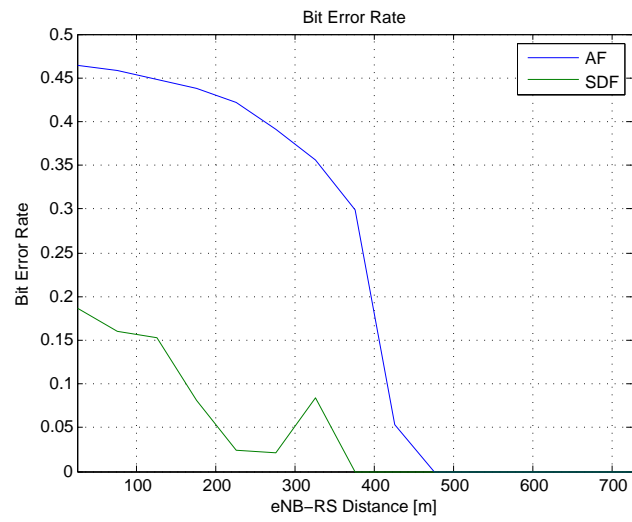


Figure 4.23: UE BER in the first scenario.

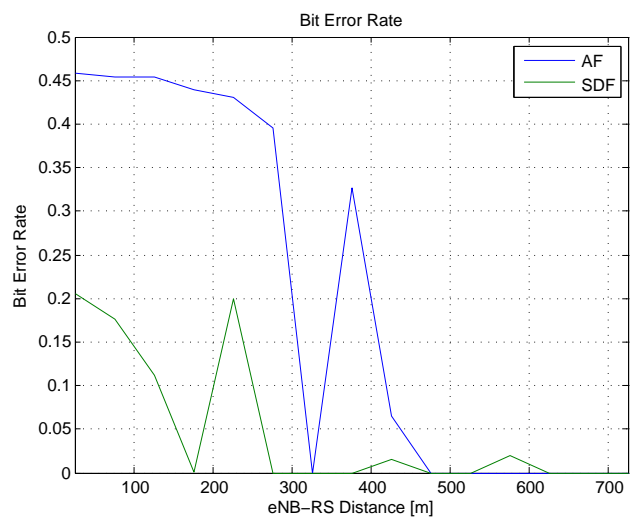


Figure 4.24: UE BER in the second scenario.



data rate as result of the used CQI in the eNB-RS link can also being used in the RS-UE link, due to the UE SNIR increase.

For the snapshot where the RS and the UE are in LoS situation (325 m) with the eNB and the RS, respectively, the UE BER is null, for both RS types, as shown in Figure 4.24. While in the SDF RS type case, the UE BER decrease is not significant, in the AF RS type, there is a decrease of approximately from 0,35 to 0. Rather, it is once again proven that the performance of the RS is extremely conditioned by its location.

One of the ways to test if the used CQI value is suitable for the radio channel conditions, is to analyze the HARQ mechanism's performance. The aim of HARQ is to correct errors, using frame retransmission. Hence, the number of retransmitted frames conduces to concluding if the used CQI is the adequate one. If there is a higher number of retransmitted frames, the used CQI is too high for the conditions that the radio channel presents. On the other side, if there is a high percentage of non-retransmitted frames, the used CQI is the most suitable.

In order to analyze the HARQ mechanism's performance are presented two normalized histograms of the retransmitted frames by the RS. For each snapshot, is shown the percentage of frames that were not retransmitted, and the percentage of frames that were sent one, two or three times by the RS to the UE. The normalized histogram represented in Figure 4.25 concerns the AF RS type in the first scenario.

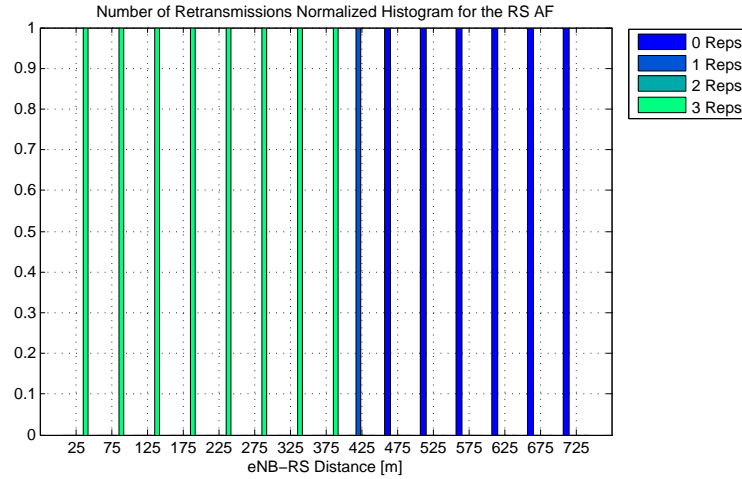


Figure 4.25: Normalized histogram for AF RS type in the first scenario.

It is seen that, when the AF RS type is used, the number of retransmissions is always three for eNB-RS distances until one half of the cell's radius. This means that the CQI is not the appropriated to use by virtue of the UE can not successfully received the data sent by the RS, not even with the HARQ mechanism. From Figure 4.25, one can also see that as the

RS gets away from the eNB, the number of retransmissions has a tendency to decrease, for the reason that the used CQI in the eNB-RS link also decreases and the UE SNIR increases. As a result, the used CQI in the eNB-RS link can be the same than the used CQI in the RS-UE link.

The normalized histogram for RS SDF type in the first scenario, is depicted in Figure 4.26.

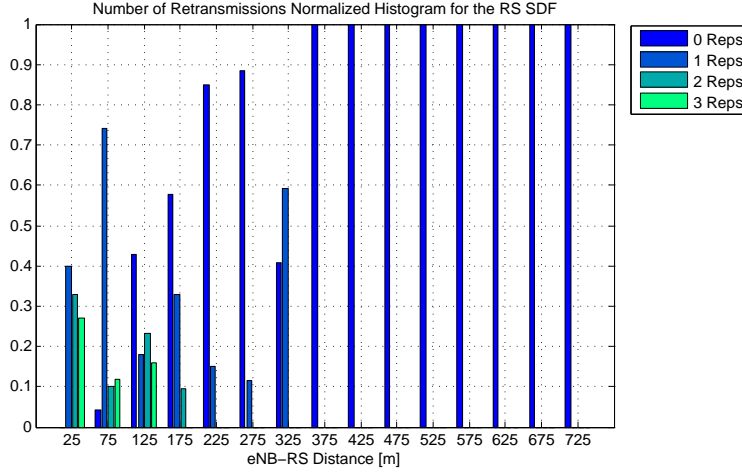


Figure 4.26: Normalized histogram for SDF RS type in the first scenario.

One can see that, unlike to the scenario in Figure 4.25, despite of the still existing frames retransmitted three times, the number of never repeated frames is the greater part. For longer distance between the RS and the UE, where the UE SNIR presents the lowest value, it is seen that all the frames have to be repeated at least once. Therefore, using a SDF RS type and even with a suitable CQI value, there is no guarantee if the UE would not use the HARQ mechanism.

Comparing the two figures, it is possible to conclude that if a SDF RS is used, the UE dismisses the HARQ mechanism for lower SNIR.

Similarly to Figures 4.25 and 4.26, Figures 4.27 and 4.28 present the HARQ mechanism in the second scenario.

Comparing Figure 4.25 with Figure 4.27, in the LoS situation snapshot (325 m), the number of retransmissions decreased from three to zero. Hence, the SNIR increase due to the LoS situation, is enough for the UE to discard the HARQ mechanism.

Rather, for the SDF RS type, the number of retransmissions also decreases, as shown in Figure 4.28. Comparing Figure 4.26 with Figure 4.28, in the LoS snapshot, the percentage of frames that were successfully received on the first attempt increased from 40% to 100%.

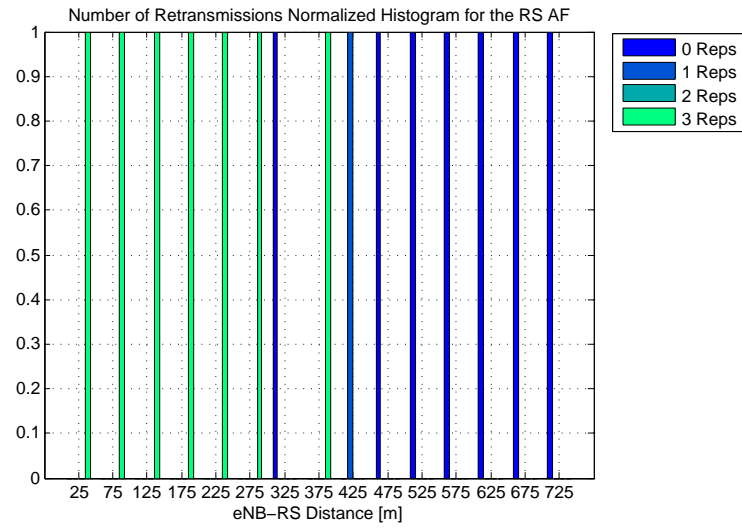


Figure 4.27: Normalized histogram for AF RS type in the second scenario.

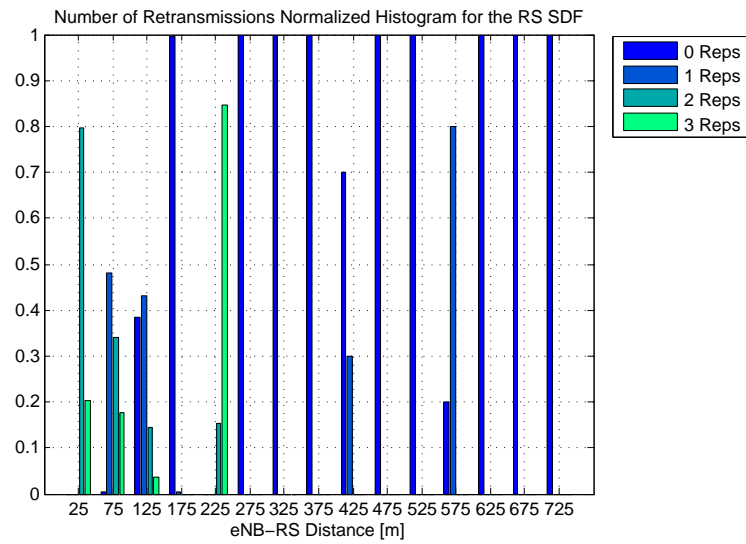


Figure 4.28: Normalized histogram for SDF RS type in the second scenario.

Figure 4.28 shows that at 225 m all the frames were repeated, at least two times. Analyzing also the UE BER value of Figure 4.24, it can be concluded that the used CQI was not the most correct. From Figure 4.22, it is seen that, in this snapshot, the used CQI by the UE is higher than the used CQI in the next snapshot, where the UE SNIR is higher. This imperfection is a result of an incorrect choice of the CQI value by the simulator. It is important to underline that the CQI choice is made considering the results presented in Section 4.3.

Finally, in Figure 4.29 it is shown the UE throughput as a function of the eNB-RS distance, in the first scenario. From Figure 4.29 one can also see the UE throughput when a RS is not used.

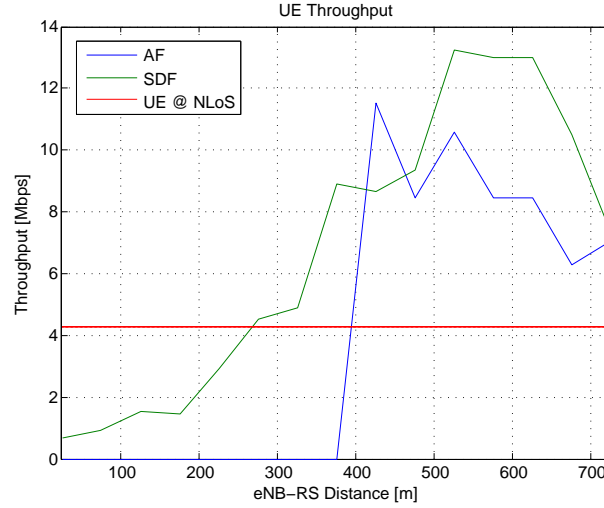


Figure 4.29: UE throughput in the first scenario.

As it would be expected, when the SDF RS type was tested, the UE throughput is superior than in the AF RS Type. Furthermore, in the AF RS type context, the UE throughput only has a value different from 0 Mbps, when the RS is positioned at eNB-RS distances higher than one half of the cell's radius. This is due to the fact that from this distances, the used CQI in the eNB-RS link tends to decrease, while the UE SNIR increases as result of the RS being closer to the UE. Consequently, the radio propagation conditions are reasonable for an UE throughput different than 0 Mbps.

In the last two snapshots (675 and 725 m), the UE throughput decreases considerably. This is related to the decrease of the used CQI in the eNB-RS link and the increase of the number of retransmitted frames in this link. It is important to underline that in the final snapshot, 40% of the frames which were sent by eNB to RS were retransmitted one time and 60% two times. For this reason, it is not advisable to install the RS near to the cell edge,

due to the considerable eNB-RS quality decrease.

Figure 4.30 illustrates the UE throughput in the second scenario.

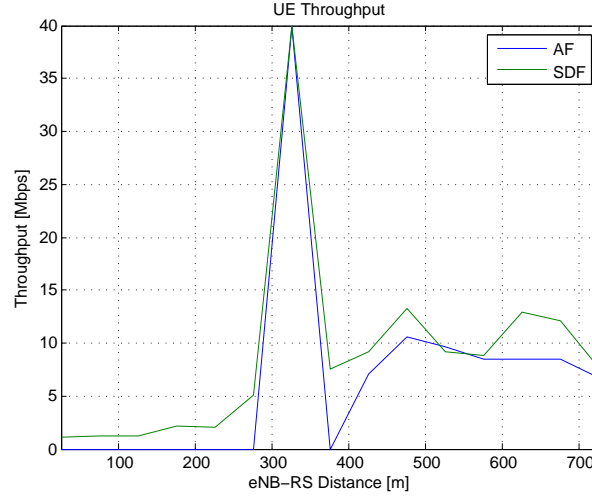


Figure 4.30: UE throughput in the second scenario.

It is seen that in the LoS situation snapshot, the two RSs types achieve the same UE throughput. Relatively to the AF type, the UE throughput is 0 *Mbps* until that snapshot, being 0 *Mbps* again in the next one, where a NLoS situation is again considered. This means that the circumstance of the RS being closer to the UE, is not a necessary condition to a maximized UE throughput. It is important to underline that the SNIR increased more even with a LoS situation than to shorter eNB-RS distances. From Figure 4.30, one can also see that in the LoS situation snapshot, the UE throughput is higher than in the closer RS-UE distance snapshot.

Despite the diminution of approximately 30 *Mbps* between the LoS snapshot and the next snapshot, one can see from the Figure 4.30 that the SDF RS type always promises data rates different than 0 *Mbps*, as seen in the previous scenario.

Concluding, the SDF RS type has always a better performance than the AF RS type, because it adapts the transmission according to the RS-UE radio channel quality.

Using a RS SDF type, a better UE throughput is ensured for distances where, using an AF type RS, the UE throughput would be 0 *Mbps*. Therefore, it may be considered the utilization of the AF RS type, when the eNB-RS link quality is not much higher when compared to the RS-UE link. By reason of the UE SNIR being equal or superior to the RS SNIR, the used CQI in the eNB-RS link may also be used in the RS-UE link. This solution must be used when the priority is to increase coverage, instead of offering high data rates, to a specific area of the cell. This way, with a less complex equipment, and, therefore, with a

minor delay, it is possible to ensure a better UE throughput.

In one hand, for the AF RS type, the ideal position is at one half of the cell's radius, because, only from this distance, it can guarantee that the data rates are equal or higher to the one that UE would have if it has connected directly to the eNB. In the other hand, the ideal position for a SDF RS type is from one third of the cell's radius.

The ideal position for the RS is the one where the RS is in LoS situation with the eNB and, if possible, with the UE, because these are in the conditions that maximize, considerably, the UE throughput. Hence, it is advisable for the RS positioning to be near traffic hotspots, in order to step up the performance for the highest number of users.

## 4.5 Relay Positioning Impact for TD and OL-SM MIMO Modes

The aim of the final simulation is to understand how the chosen MIMO mode affects the UE throughput, in the case of transmission is made in TD and OL-SM mode, in the eNB-RS and the RS-UE links.

As these two modes are heavily dependent on the radio propagation conditions, this section presents two simulation scenarios, which were simultaneously analyzed. The presented simulation scenarios are the same that are described in Section 4.4.

Figure 4.31 and Figure 4.32 present the used CQI value as a function of the eNB-RS distance in the eNB-RS and the RS-UE links, respectively, for TD and OL-SM modes in the first scenario.

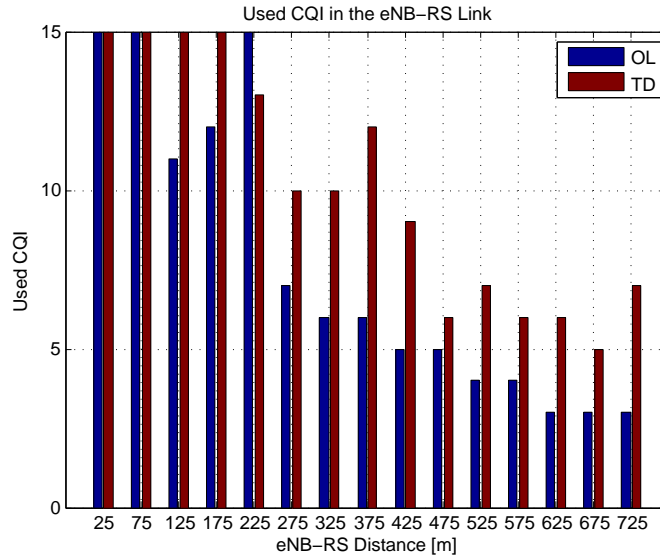


Figure 4.31: Used CQI in the eNB-RS link in the first scenario.

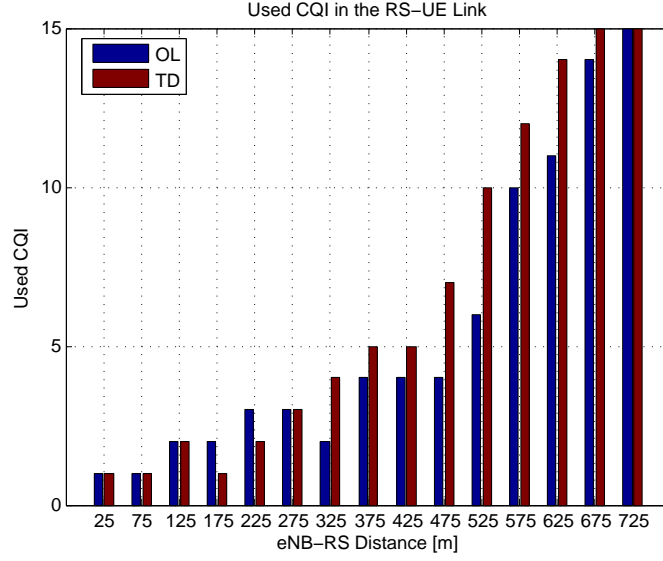


Figure 4.32: Used CQI in the RS-UE link in the first scenario.

Analyzing Figure 4.31, it is clear that how bigger the distance that separates the eNB from RS gets, the lower will be the indicated CQI value for the transmission. This behavior is checked in the TD mode as in the OL-SM mode, and is justified by the decrease of SNIR as the RS moves apart from the eNB. Besides the fact that the received power is lower, the interference with neighbor cells will be higher, degrading the quality of the signal.

In Figure 4.32, where it is illustrated the used CQI in the RS-UE link, the behavior is the inverse of the one described above. As the RS is placed at a higher distance from the eNB, its SNIR decreases but, at the same time, the RS gets closer to the UE, upgrading the RS-UE link quality, as expected. Consequently, an improvement in this relation makes it possible to use increasing values of CQI.

Analyzing both figures, the used CQI value is higher in the TD mode than in the OL-SM mode. Once again, it is concluded that in the TD mode it is possible to use a higher order modulation than in the OL-SM mode, practically for all snapshots.

In Figures 4.33 and 4.34 are illustrated the used CQI in the eNB-RS and the RS-UE links, respectively, in the second scenario.

In this scenario, because the three nodes are in LoS situation at 325 m eNB-RS distance, there is a peak in the used CQI value, since there was an increase of the SNIR. As it will be seen, this situation has an impact in the UE throughput.

In Figures 4.35 and 4.36 is illustrated the UE BER in the first and second scenarios, respectively, for the case where the TD and the OL-SM modes are used.

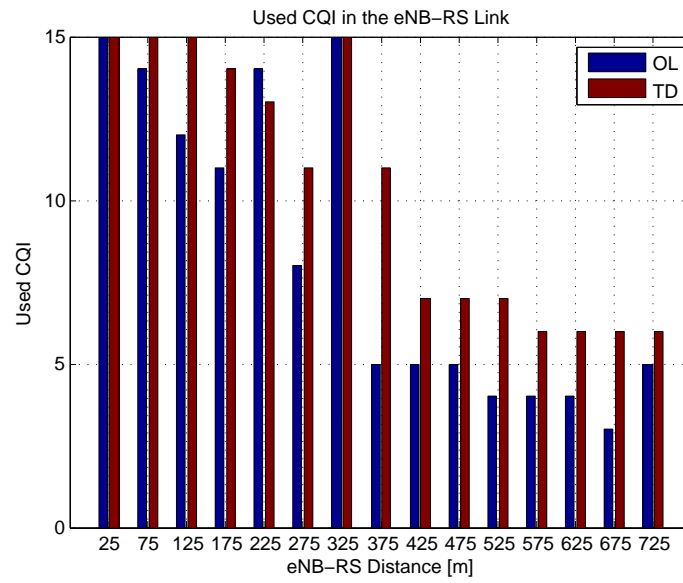


Figure 4.33: Used CQI in the eNB-RS link in the second scenario.

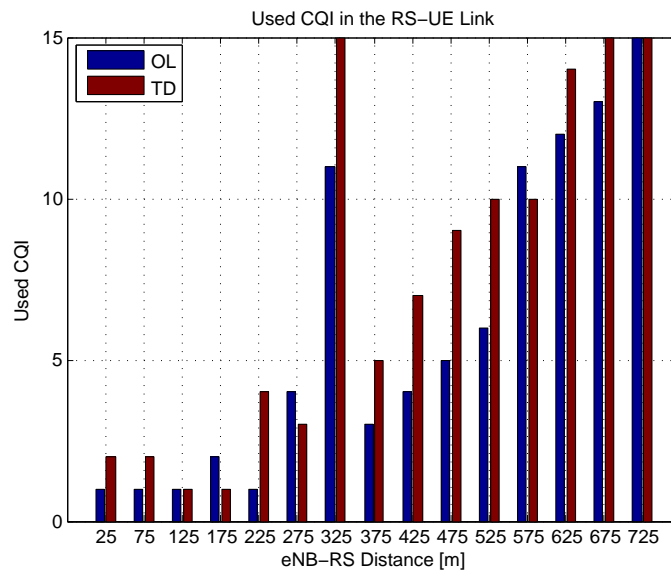


Figure 4.34: Used CQI in the RS-UE link in the second scenario.



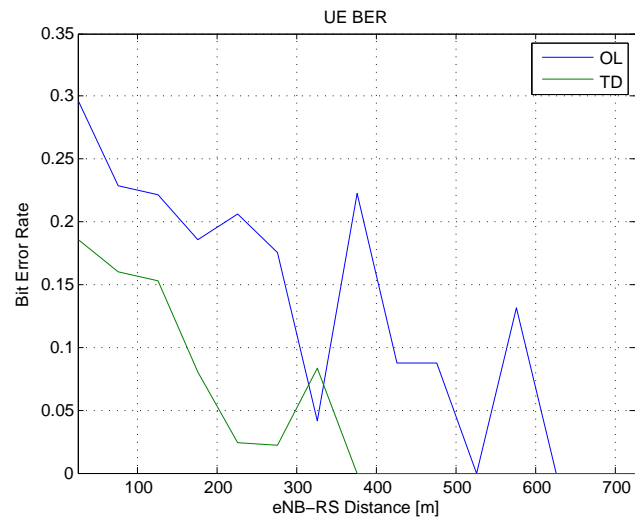


Figure 4.35: UE BER in the first scenario.

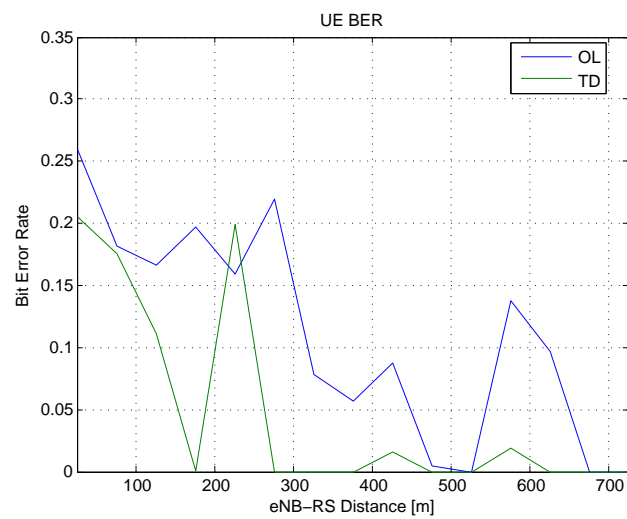


Figure 4.36: UE BER in the second scenario.

In both cases it is possible to see that the TD mode reaches lower BER values than the OL-SM mode, even often using higher order modulations. In one hand, the TD mode achieves BER values equal to zero for eNB-RS distances higher than one half of the cell's radius. In the other hand, the OL-SM mode only reaches this value for higher eNB-RS distances, *i.e.*, when the RS is closer to the UE.

These results are due to the fact that the TD mode uses the MIMO technique to take advantage of the transmission and/or reception diversity, and not to increase the UE throughput. Meaning that, while in the TD mode the aim of using multiple antennas scheme is to decrease the error rate, by sending the redundant information, the OL-SM mode uses the multiple streams to send different information, increasing the throughput.

Comparing the two scenarios, it is shown that the LoS situation at 325 m only has repercussions in the TD mode. In this case, it stands out that the UE BER decreases considerably in this snapshot. On the other side, in the OL-SM mode, the UE BER value does not suffer a considerable change. This difference of behavior is related to the high value of CQI utilized in both modes. From 4.33, one can also see that in the snapshot for the 325 m eNB-RS distance, the used CQI in the TD and the OL-SM MIMO modes, is equal to 15, *i.e.*, the highest order modulation possible. Whereas the TD mode can achieve an UE BER equal to zero, the OL-SM mode can not reach this value, as a result of this mode requiring a higher SNIR than the TD mode. For the OL-SM to reach an UE BER equal to zero, it is necessary to use a lower CQI or a higher SNIR.

In the following, the use of the HARQ mechanism will be analyzed. In Figures 4.37 and 4.38 is presented the normalized histogram for the retransmitted frames from RS to UE in OL-SM and TD modes, respectively, in the first scenario.

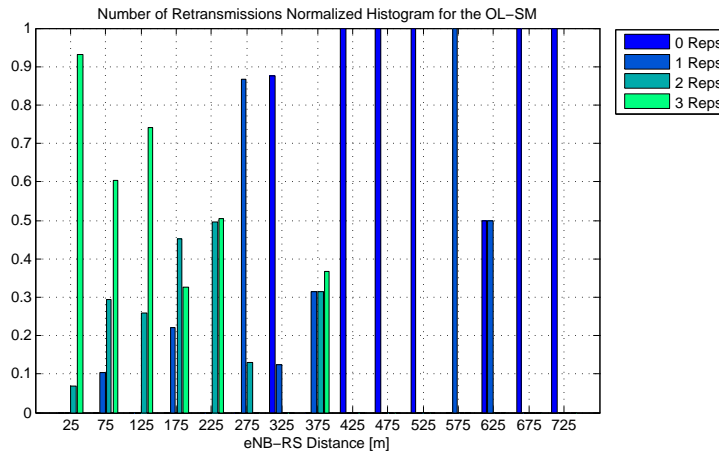


Figure 4.37: Normalized histogram for OL-SM in the first scenario.

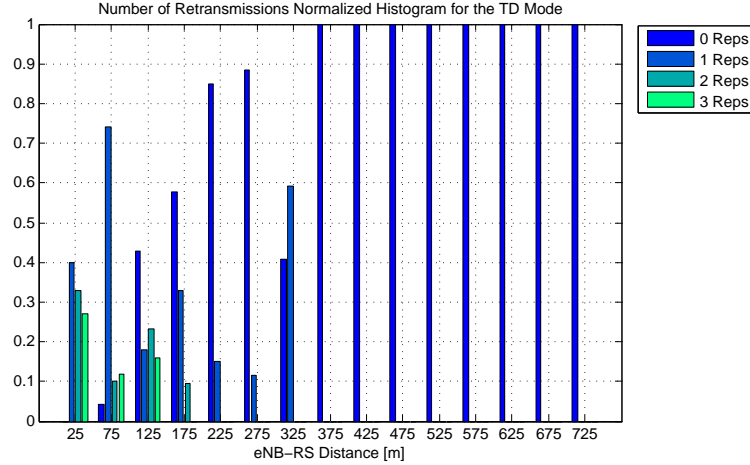


Figure 4.38: Normalized histogram for TD mode in the first scenario.

The first conclusion to be drawn is that the OL-SM mode needs a higher number of retransmissions than the TD mode. This fact is directly related to the purpose of the use of the MIMO technique by the TD, as explained earlier.

From Figure 4.37, one can also observe that for a 225 m eNB-RS distance, the number of retransmitted frames is higher than in the previous snapshot(175 m). Additionally, from Figures 4.31 and 4.32, it is seen that the used CQI in both links is higher in OL-SM mode than in TD mode. Therefore, it is possible to conclude that the used CQI requires a higher retransmissions number than the used CQI in the 175 m snapshot.

Making an overall review of the presented snapshots, it is possible to conclude that, the TD mode presents a higher number of frames which have not been retransmitted, when compared to the OL-SM mode.

Using the OL-SM mode, to eNB-RS distances up to one half of the cell's radius, most of the frames (90% in the first snapshot) had to be repeated two or three times. Additionally, in the TD mode, the number of frames that the RS must send to the UE is considerably lower. For eNB-RS distances higher than to one half of the cell's radius, the number of repetitions tends to be null in both modes, because of the UE SNIR increases.

In Figures 4.39 and 4.40 is presented the normalized histogram of the retransmissions number, in the second scenario, for the OL-SM and TD modes, respectively.

Comparing Figure 4.37 and 4.38 with Figures 4.39 and 4.40, respectively, it is possible to see that the number of repetitions is considerably lower but only in the TD mode. On one hand, in the TD mode, the number of repetitions decreased to zero. On the other hand, in the OL-SM mode, the number of retransmissions did not suffer a great alteration due to the

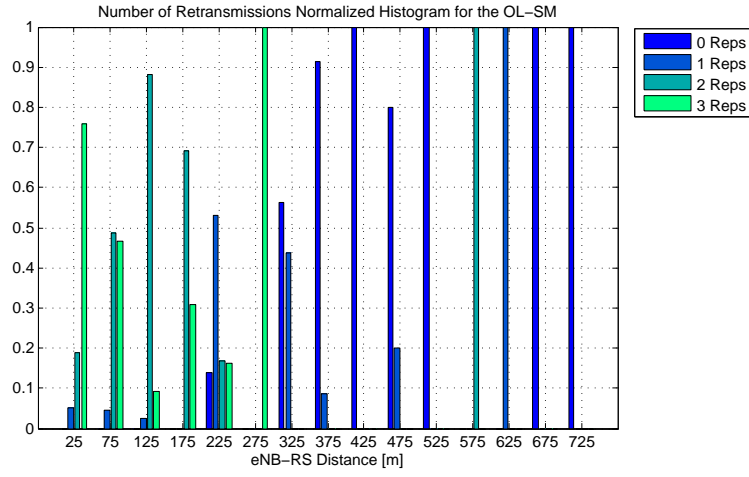


Figure 4.39: Normalized histogram for OL-SM in the second scenario.

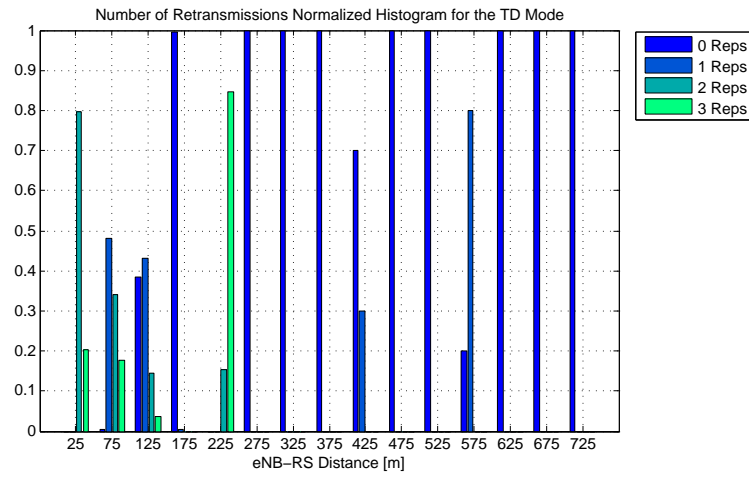


Figure 4.40: Normalized histogram for TD mode in the second scenario.

previous justification relatively to the UE BER value - the value of SNIR is not enough for such a high increase in the CQI value, without the use of retransmissions. If the SNIR value was higher, the number of repetitions in the OL-SM mode would also decrease despite of the used CQI value.

As explained in Section 4.3, the fact that a higher value of CQI is used does not mean a higher value of throughput. There are cases where the OL-SM mode, despite using a lower order modulation, can offer higher data rates than the TD mode. This happens because the double of information is sent in the OL-SM mode, in comparison with the TD mode. In Figure 4.29 and 4.30 is illustrated the UE throughput for the first and second scenarios, respectively, as a function of the RS placement.

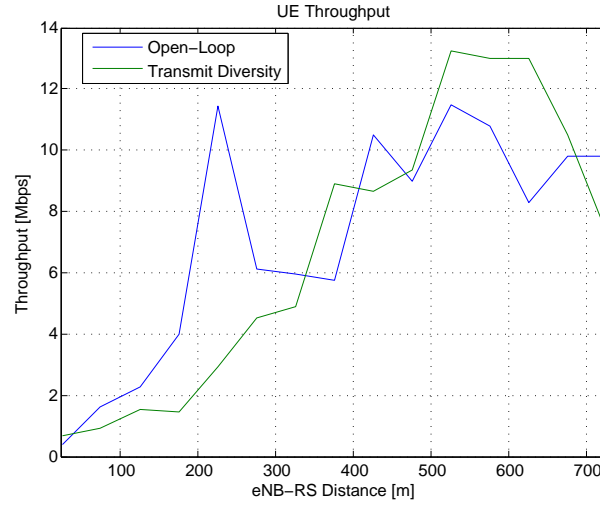


Figure 4.41: UE throughput in the first scenario.

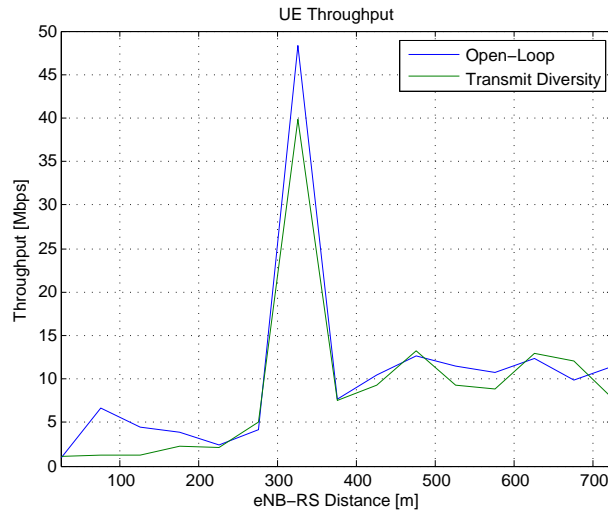


Figure 4.42: UE throughput in the second scenario.

The situation previously described can be checked from Figure 4.41 at the 325 *m* and 425 *m*, where the OL-SM manages to provide a much higher throughput value than the TD mode, even using a lower CQI value.

It is also evident that, as the RS steps away from the eNB, the UE throughput, in the TD mode, tends to be higher than the throughput in OL-SM mode, leading to the conclusion that, at the cell edge, the TD mode should be the one to use.

In the second scenario, it is clear that, when the conditions are favorable, the OL-SM mode should be the one to use instead of the TD mode. In the snapshot where the RS and the UE are in LoS with the eNB and the RS, respectively, the OL-SM mode reaches a higher UE throughput than the TD mode. In this scenario, is not obvious if in cell edge condition the TD mode is more suitable. Despite of the used CQI in the OL-SM mode being lower to the one used in the TD mode, the data rate is approximately the same because in the OL-SM mode the double of the information is sent.

In conclusion, despite of having a higher UE BER, a lower used CQI value and a higher number of retransmissions, the OL-SM mode can sometimes offer peak data rates that the TD mode does not ever achieve. Considering the LTE dynamic transition between TD and OL-SM modes, the overall UE throughput should be similar to the maximum function between the two curves. Therefore, when the radio propagation conditions are sufficiently good, it is advisable to make the change from TD to OL-SM mode, in order to maximize the UE throughput and to take advantage of the MIMO technique.

## Chapter 5

# Conclusions and Future Work

### 5.1 Performed Work

The presented work on this thesis has the aim to quantify the associated gain as result of the insertion of a RS in a LTE wireless network.

In order to do so, a RS module was developed over an existing simulator, and simulations for the eNB-RS-UE and eNB-UE links were made. The developed RS module may work configured in two different approaches: AF and SDF. While the AF RS type only amplifies and forwards the received data, the SDF RS type was built with more capacity and performance skills, making it able to adapt the transmission to the radio channel propagation conditions.

In order to test the MIMO performance, two MIMO modes were implemented: the TD and the OL-SM mode. In this way, the simulator can be configured to work in several possible combinations, simply by configuring the type of the RS to test and the MIMO mode to use. It is important to underline that the MIMO mode utilized in the eNB-RS link may be different than the one utilized in the RS-UE link.

In parallel, the system was developed so that the use of the HARQ mechanism was considered. Although this technique was already developed in the used simulator, it suffered intense simulation improvements, in order to enable the RS utilization.

Among the many adaptations that were made in the used simulator, the way that the results are presented stands out the most. In order to make the simulations, the simulator utilizes the SNIR as a measure to check the quality of the channel. Therefore, to answer the question “What is the ideal position to place the RS?”, was necessary to develop a relation between the distance and the SNIR. In the following, a mechanism was implemented to adapt the CQI, being this one of the main advantages of LTE technology,

To make the simulation more realistic, a LoS Probability Model was adopted. Hence, depending on the distance that separates the network nodes, the simulations were made taking into account the probability of these being in a LoS situation.

In Section 4.1 was studied the implemented LoS Probability Model. It was then concluded that, when the RS is at higher or equal height than the eNB, the probability of being in LoS with the eNB is 100%. As for the case in which the RS is placed lower than the eNB, the probability of being in a LoS situation decreases as the distance increases. In addition, if the option is to put the RS, for example, in a facade of a building, with the aim to create an hotspot for a users' group, it is advisable for the RS and the eNB not to be very distant. Relatively to the RS-UE link, this is not so dependent on the RS's height. The obtained conclusion was that the probability of the UE being in LoS with the RS, is only 50% when they are separated by 100 *m*.

The relation between the SNIR and the distance was the investigated subject in Section 4.2. The first conclusion was that, the bigger the distance that separates the eNB from the RS, the greater is the difference in the SNIR value between a LoS and NLoS situation. Another of the aspects that was possible to quantify was the eNB-RS link path-loss and the interference level that the RS suffers due to the neighbor cells: the eNB-RS path-loss is more dependent on the distance than the path-loss related to the RS interferences. When the LoS Probability Model, developed earlier, was used, it was seen that the SNIR varies much more for shorter distances. This is due to the value of the probability being the one that makes a constant change from LoS to NLoS situation, and vice-versa. This behavior was also verified in the UE's test. When the RS was closer to the UE, there was a higher number of oscillations of the UE SNIR.

In Section 4.3 was studied the performance of the TD and OL-SM MIMO modes. To proceed to data analysis, several modulations were tested, in a range of SNIR values, utilizing the HARQ mechanism. It was then concluded that the utilization of a higher order modulation is not synonymous to a higher level of throughput, whatever the SNIR. This situation occurs since higher order modulation usage at low SNIR experiences transmission errors, increasing retransmissions for a given CQI. In other words, the same performance is displaced to higher values of SNIR. So, in the TD mode it is possible to use modulation of a higher order comparing with OL-SM, for the same values of SNIR. Concerning the UE throughput, it was seen that the OL-SM mode can reach data rates that are never achieved in the TD mode. Considering the HARQ mechanism, in the OL-SM mode are necessary more



retransmissions than in the TD mode.

The comparison between the AF and the SDF RS types, was discussed in Section 4.4. The main conclusion is that the SDF always has a better performance than the AF RS type, since it has the ability to adapt the transmission to the radio channel conditions. Nevertheless, the AF RS type may be used when the quality of the RS-UE link is higher or equal to the one of the eNB-RS link, achieving an improvement of the UE throughput even with a less complex RS and consequently, a cheaper solution for operators. When both relays are in LoS conditions, it was noticed that their performance is the same. Using an AF RS type, the UE BER values are null when this is departed from the eNB at a superior distance to two thirds of the cell's radius. As for the SDF RS type, starting from distances of one third of the cell's radius it can ensure a UE BER value equal to zero. Relatively to the HARQ mechanism, the number of retransmissions is much higher when it is used a AF RS type than a SDF RS type.

Finally, in Section 4.5 was analyzed the impact of the utilization of the TD and OL-SM modes in a SDF RS type. Even when in the OL mode was used a lower CQI, the UE throughput was superior than in the TD mode. When the LoS situation was tested, the SNIR was not enough to use the higher order modulation in the OL-SM mode. Nevertheless, the OL-SM mode can reach UE throughput values far superior than the TD mode. Considering the worst case scenario where the UE is placed at cell edge, the LTE TD mode should be responsible for maximizing performance, since the UE is under low SNIR conditions. For lower interference conditions (high SNIR), OL-SM potential should be fully explored. The best performance will be the one that switches between both modes, in order to take advantage of the OL-SM mode to reach high peak data rates, when the conditions do allow it.

## 5.2 Future Work

There are a few attractive topics that may be explored, in future researches, to make the system simulation more realistic and complete. The following improvements are note worthy:

- Adapt the RS module so it may also work as a RS Type II;
- Introduce UE mobility in Fixed Relaying Testing;
- Develop and implement CoMP techniques;
- Produce and implement a MRS module;

- Implement remaining MIMO modes, with a special emphasis to the CL-SM mode and Beamforming;
- Adapt the simulator for the utilization of real maps, drawing specific conclusions of a given scenario;
- Utilization of the Bandwidth Aggregation Technique.

# Bibliography

- [1] ITU, “ITU World Radiocommunication Seminar highlights future communication technologies,” December 2010.
- [2] A. Martins, P. Vieira, and A. Rodrigues, “Throughput Enhancement using Fixed Relaying in LTE Networks,” *Conference on Electronics, Telecommunications and Computers (CETC 2011)*, November 2011.
- [3] A. Martins, P. Vieira, and A. Rodrigues, “Transmit Diversity versus Open Loop Spatial Multiplexing MIMO Performance for LTE Fixed Relaying,” *The 2012 IEEE 75th Vehicular Technology Conference, (VTC2012-Spring), Yokohama, Japan*, May 2012.
- [4] A. Martins, P. Vieira, and A. Rodrigues, “Análise de Desempenho utilizando Diversidade de Transmissão e Multiplexagem Espacial em Malha Aberta para Redes LTE com Repetidores Fixos,” *5º Congresso URSI/Anacom*, 2011.
- [5] R. R. Americas, “Transition to 4G: 3GPP Broadband Evolution to IMT-Advanced,” September 2010.
- [6] Cisco, “Visual Networking Index: Global Mobile Data Traffic Forecast Update, 2009-2015,” February 2011.
- [7] Cisco, “Visual Networking Index: Global Mobile Data Traffic Forecast Update, 2009-2014.” White Paper, February 2010.
- [8] U. Forum, “Mobile Broadband Evolution: The Roadmap From HSPA to LTE.” White Paper, February 2009.
- [9] 3GPP, “Requirements for Evolved UTRA (E-UTRA) and Evolved UTRAN (E-UTRAN),” TR 25.913, 3rd Generation Partnership Project (3GPP), Mar. 2006.

- [10] C.-X. Wang, X. Hong, X. Ge, X. Cheng, G. Zhang, and J. Thompson, "Cooperative MIMO Channel Models: A survey," *Communications Magazine, IEEE*, vol. 48, no. 2, pp. 80–87, 2010.
- [11] S. Sesia, I. Toufik, and M. Baker, *LTE - The UMTS Long Term Evolution: From Theory To Practice*. Wiley, 2009.
- [12] P. Vieira and A. Rodrigues, "An Insight Into Cooperative MIMO Communications in Wireless Networks," *The 13th International Symposium on Wireless Personal Multimedia Communications*, p. 5, 2010.
- [13] F. KHAN, *LTE for 4G Mobile Broadband*. Cambridge University Press, 2009.
- [14] V. Eerola, "LTE Network Architecture Evolution."
- [15] H. Holma and A. Toskala, *LTE for UMTS - OFDMA and SC-FDMA Based Radio Access*. Wiley, 2009.
- [16] Ericsson, "LTE - An Introduction." White Paper, June 2009.
- [17] A. Technologies, "3GPP Long Term Evolution: System Overview, Product Development, and Test Challenges." Application Note, June 2009.
- [18] T. Innovations, "The Seven Modes of MIMO in LTE." White Paper.
- [19] J. Lee, J.-K. Han, and J. Zhang, "MIMO Technologies in 3GPP LTE and LTE-Advanced," *EURASIP Journal on Wireless Communications and Networking*, vol. 2009, p. 10, 2009.
- [20] M. Kottkamp, "Rohde & Schwarz LTE-Advanced Technology Introduction," 2010.
- [21] M. Iwamura, K. Etemad, M.-H. Fong, R. Nory, and R. Love, "Carrier Aggregation Framework in 3GPP LTE-Advanced [WiMAX/LTE Update]," *Communications Magazine, IEEE*, vol. 48, no. 8, pp. 60–67, 2010.
- [22] NTT DOCOMO, INC., "Carrier aggregation deployment scenarios." 3GPP TSG-RAN WG2, January 2010.
- [23] G. Americas, "Release 9, release 10 and beyond: HSPA+, LTE/SAE and LTE-Advanced," in *3GPP Mobile Broadband Innovation Path To 4G*, February 2010.

- [24] D. Jiang, Q. Wang, J. Liu, G. Liu, and C. Cui, "Uplink Coordinated Multi-Point Reception for LTE-Advanced Systems," in *Proc. 5th Int. Conf. Wireless Communications, Networking and Mobile Computing WiCom '09*, pp. 1–4, 2009.
- [25] Q. Wang, D. Jiang, G. Liu, and Z. Yan, "Coordinated Multiple Points Transmission for LTE-Advanced Systems," in *Proc. 5th Int. Conf. Wireless Communications, Networking and Mobile Computing WiCom '09*, pp. 1–4, 2009.
- [26] 3GPP, "RP-091434, Relays for LTE," RP 091434, 3rd Generation Partnership Project (3GPP), 2009.
- [27] 3GPP, "Spacial channel model for Multiple Input Multiple Output (MIMO) simulations," TR 25.996, 3rd Generation Partnership Project (3GPP), June 2007.
- [28] P. Kyösti, J. Meinilä, L. Hentilä, X. Zhao, T. Jämsä, C. Schneider, M. Narandzić, M. Milojević, A. Hong, J. Ylitalo, V.-M. Holappa, M. Alatossava, R. Bultitude, Y. de Jong, and T. Rautiainen, "WINNER II Channel Models. Part I. Channel Models," tech. rep., EC FP6, Sept. 2007.
- [29] C. Mehlführer, M. Wrulich, J. C. Ikuno, D. Bosanska, and M. Rupp, "Simulating the Long Term Evolution Physical Layer," in *Proc. of the 17th European Signal Processing Conference (EUSIPCO 2009)*, (Glasgow, Scotland), Aug. 2009.
- [30] L. Hentilä, P. Kyösti, M. Käske, M. Narandzic, and M. Alatossava., "MATLAB implementation of the WINNER Phase II Channel Model ver1.1 [online]," (Glasgow, Scotland), Dec. 2007.
- [31] P. Kyösti, J. Meinilä, L. Hentilä, X. Zhao, T. Jämsä, C. Schneider, M. Narandzić, M. Milojević, A. Hong, J. Ylitalo, V.-M. Holappa, M. Alatossava, R. Bultitude, Y. de Jong, and T. Rautiainen, "WINNER II Channel Models. Part II. Radio Channel Measurement and Analysis Results," tech. rep., EC FP6, Sept. 2007.